



SUPPLEMENTARY APPENDICES

Research Report 217

Long-Term Exposure to Outdoor Ultrafine Particles and Black Carbon and Effects on Mortality in Montreal and Toronto, Canada

Scott Weichenthal et al.

Appendix A: Supplementary Tables A.1–A.16 and Figures A.1–A.59 Appendix B: Monitoring and Backcasting Details

The Appendices were reviewed for spelling, grammar, and cross-references to the main report. They have not been formatted or fully edited by HEI. This document was reviewed by the HEI Improved Exposure Assessment Studies Review Panel.

Correspondence may be addressed to Dr. Scott Weichenthal, Department of Epidemiology, Biostatistics, and Occupational Health, McGill University, 1110 Pines Avenue West, Montreal, Quebec, Canada, H3A 1A2; email: scott.weichenthal@mcgill.ca.

Although this document was produced with partial funding by the United States Environmental Protection Agency under Assistance Award CR–83998101 to the Health Effects Institute, it has not been subjected to the Agency’s peer and administrative review and, therefore, may not necessarily reflect the views of the Agency; no official endorsement by it should be inferred. The contents of this document have not been reviewed by private party institutions, including those that support the Health Effects Institute; therefore, it may not reflect the views or policies of these parties; no endorsement by them should be inferred.

© 2024 Health Effects Institute, 75 Federal Street, Suite 1400, Boston, MA 02110

CONTENTS

| | |
|------------------------------------------------------------------------------------------------------------------------------------------------------------------------------------------------------------|----|
| APPENDIX A: Supplementary Tables A.1–A.16 and Figures A.1–A.59..... | 5 |
| APPENDIX A TABLES..... | 5 |
| Table A.1. Study Area Characteristics..... | 5 |
| Table A.2. Fixed-Site Monitoring Results..... | 5 |
| Table A.3. Instrument Limits of Detection..... | 5 |
| Table A.4. Locations Used for Hourly Ambient Weather Conditions..... | 6 |
| Table A.5. Land Use and Traffic Parameters Examined for LUR Model Development..... | 6 |
| Table A.6. Comparison of Descriptive Statistics for Road Segments Visited Various Number of Times During Monitoring Campaign..... | 7 |
| Table A.7. Comparison of Land Use and Traffic Parameters for Road Segments Visited Various Number of Times During Monitoring Campaign..... | 7 |
| Table A.8. Model RMSE in Test Set..... | 8 |
| Table A.9. Pearson Correlation Between LUR and CNN Model Predictions in Test Set..... | 8 |
| Table A.10. Comparison of Model Performance When Trained on City-Specific Data versus Multi-city Data..... | 8 |
| Table A.11. Comparison of LUR Model Performance with and without Temporal Adjustment..... | 9 |
| Table A.12. Comparison of CNN Model Performance with and without Temporal Adjustment in Validation Set..... | 9 |
| Table A.13. Median Difference Between LUR and CNN Predicted Values in Test Set..... | 10 |
| Table A.14. Median Difference Between LUR and CNN Predicted Values in Test Set for Road Segments When Observed Aggregated UFP Number Concentration Was Greater than 45,000 particles/cm ³ | 10 |
| Table A.15. Slope and Intercept of Predictions versus Observed Values in Test Set..... | 11 |
| Table A.16. Hazard Ratios for Interquartile Increases in O _x Exposures and Mortality..... | 11 |
| APPENDIX A FIGURES..... | 12 |
| Figure A.1. Mobile monitoring routes in Montreal (A) and Toronto (B)...... | 12 |
| Figure A.2. Maps of the training, validation, and test sets in Toronto and Montreal..... | 12 |
| Figure A.3. Directed acyclic graphs for the relationships between outdoor UFP number concentrations (A) and black carbon (B) and mortality..... | 13 |
| Figure A.4. Spatial coverage of the Montreal UFP number concentrations monitoring data when restricting the minimum number of visits per road segment..... | 14 |
| Figure A.5. Spatial coverage of the Toronto UFP number monitoring data when restricting the minimum number of visits per road segment..... | 15 |
| Figure A.6. Spearman’s correlations between land use and traffic parameters included in the Montreal LUR for UFP number concentrations..... | 16 |
| Figure A.7. Spearman’s correlations between land use and traffic parameters included in the Montreal LUR model for UFP size..... | 17 |

| | |
|--------------------------------------------------------------------------------------------------------------------------------------------------------------------------------------------------------------------------------------------|----|
| Figure A.8. Spearman’s correlations between land use and traffic parameters included in the Montreal LUR for BC..... | 18 |
| Figure A.9. Spearman’s correlations between land use and traffic parameters included in the Toronto LUR for UFP number concentrations. | 19 |
| Figure A.10. Spearman’s correlations between land use and traffic parameters included in the Toronto LUR model for UFP size..... | 20 |
| Figure A.11. Spearman’s correlations between land use and traffic parameters included in the Toronto LUR for BC..... | 21 |
| Figure A.12. Maps of spatial variation in median meteorological conditions during monitoring for Montreal (A: temperature; B: relative humidity; C: wind speed) and Toronto (i: temperature; ii: relative humidity; iii: wind speed). | 22 |
| Figure A.13. Relationships between meteorological variables and changes in pollutant levels in each of the Montreal LUR models. | 23 |
| Figure A.14. Relationships between meteorological variables and changes in pollutant levels in each of the Toronto LUR models. | 24 |
| Figure A.15. Comparing test set LUR mean UFP size predictions to CNN predictions in Montreal and Toronto (A) with a histogram of observed values for reference (B)..... | 25 |
| Figure A.16. Comparing test set LUR BC predictions to CNN predictions in Montreal and Toronto (A) with a histogram of observed values for reference (B). | 26 |
| Figure A.17. Comparing LUR and CNN predictions of UFP number concentrations from the city-specific model and the multi-city models. | 27 |
| Figure A.18. Comparing UFP number concentrations model predictions from the city-specific models to the multi-city models..... | 28 |
| Figure A.19. Observed UFP number concentrations over 40,000 particles/cm ³ in Toronto are all situated on highways..... | 29 |
| Figure A.20. Observed UFP number concentrations over 40,000 particles/cm ³ in Montreal are all situated on highways..... | 29 |
| Figure A.21. Visualizing intermediate activations of filters of the Conv2D layer in the CNN models trained on Toronto data and trained on Montreal and Toronto data. | 30 |
| Figure A.22. Scatter plots of observed and predicted UFP number concentrations in the test set. | 31 |
| Figure A.23. Scatter plots of observed and predicted mean UFP size in the test set. | 32 |
| Figure A.24. Scatter plots of observed and predicted BC in the test set..... | 33 |
| Figure A.25. Identifying the clusters of Toronto LUR UFP number concentration predictions in the test set..... | 34 |
| Figure A.26. Inspecting the Toronto LUR UFP number concentration prediction clusters in the test, train and validate sets..... | 34 |
| Figure A.27. Identifying the locations of the LUR UFP number concentration prediction clusters... | 35 |
| Figure A.28. Inspecting distributions of land use and traffic parameters stratified by LUR UFP number concentration prediction cluster..... | 36 |
| Figure A.29. Average daily traffic NO _x response curves in the Toronto BC and UFP number concentration LUR models. | 37 |

| | |
|---------------------------------------------------------------------------------------------------------------------------------------------------------------------------|----|
| Figure A.30. Spatial distribution of UFP number concentrations model errors (scaled) in all data for the LUR, CNN, and combined models in Toronto and Montreal..... | 38 |
| Figure A.31. Spatial distribution of UFP size model errors (scaled) in all data for the LUR, CNN, and combined models in Toronto and Montreal. | 39 |
| Figure A.32. Spatial distribution of BC model errors (scaled) in all data for the LUR, CNN, and combined models in Toronto and Montreal. | 40 |
| Figure A.33. Surfaces of scaled differences between predicted UFP number concentrations from LUR and CNN models in Toronto and Montreal..... | 41 |
| Figure A.34. Surfaces of scaled differences between predicted UFP size from LUR and CNN models in Toronto and Montreal. | 41 |
| Figure A.35. Surfaces of scaled differences between predicted BC concentrations from LUR and CNN models in Toronto and Montreal. | 42 |
| Figure A.36. Sensitivity analysis for UFP number concentrations prediction surfaces from LUR models trained without latitude and longitude for Toronto and Montreal. | 42 |
| Figure A.37. Sensitivity analysis for UFP size prediction surfaces from LUR models trained without latitude and longitude for Toronto and Montreal. | 43 |
| Figure A.38. Sensitivity analysis for BC prediction surfaces from LUR models trained without latitude and longitude for Toronto and Montreal. | 43 |
| Figure A.39. CNN predictions for UFP number concentrations in Montreal for original and modified images. | 44 |
| Figure A.40. CNN predictions for BC in Montreal for original and modified images. | 45 |
| Figure A.41. CNN predictions for UFP number concentrations in Toronto for original and modified images. | 46 |
| Figure A.42. CNN predictions for BC in Toronto for original and modified images..... | 47 |
| Figure A.43. Changes in CNN predictions for UFP number concentrations when using images of Sunnybrook Park in Toronto downloaded in December 2021 versus July 2022. | 48 |
| Figure A.44. Changes in CNN predictions for BC when using images of Sunnybrook Park in Toronto downloaded in December 2021 versus July 2022. | 49 |
| Figure A.45. Mobility-weighted combined models for UFP number concentrations in Toronto and Montreal using neighborhood-level survey data from various years. | 50 |
| Figure A.46. Mobility-weighted combined models for UFP size in Toronto and Montreal using neighborhood-level survey data from various years. | 51 |
| Figure A.47. Mobility-weighted combined models for BC in Toronto and Montreal using neighborhood-level survey data from various years. | 52 |
| Figure A.48. Change in Toronto combined model UFP number concentrations predictions after applying 2006 and 2016 mobility weights. | 53 |
| Figure A.49. Change in Toronto combined model BC concentration predictions after applying 2006 and 2016 mobility weights. | 53 |
| Figure A.50. Change in Montreal combined model UFP number concentration predictions after applying 2003 and 2018 mobility weights. | 54 |
| Figure A.51. Change in Montreal combined model BC predictions after applying 2003 and 2018 mobility weights..... | 54 |

| | |
|----------------------------------------------------------------------------------------------------------------------------------------------------------------|----|
| Figure A.52. Toronto combined model UFP number concentrations surfaces backcasted to various years. | 55 |
| Figure A.53. Toronto combined model UFP size surfaces backcasted to various years. | 56 |
| Figure A.54. Toronto combined model BC surfaces backcasted to various years..... | 57 |
| Figure A.55. Montreal combined model UFP number concentration surfaces backcasted to various years. | 58 |
| Figure A.56. Montreal combined model UFP size surfaces backcasted to various years..... | 59 |
| Figure A.57. Montreal combined model BC surfaces backcasted to various years..... | 60 |
| Figure A.58. Concentration-response curves of outdoor BC and mortality outcomes. | 61 |
| Figure A.59. Concentration-response curves for outdoor UFP number concentrations, UFP size, and mortality outcomes for the LUR and CNN models separately. | 62 |
| APPENDIX B: MONITORING AND BACKCASTING DETAILS..... | 63 |
| 1. MONITORING LESSONS LEARNED..... | 63 |
| 2. ROUTE SELECTION FOR MOBILE MONITORING..... | 65 |
| 3. QUALITY CONTROL PROCEDURES FOR DATA COLLECTION..... | 66 |
| 4. HISTORIC TRAFFIC DATA..... | 68 |
| 5. FIXED-SITE MONITORING..... | 71 |
| REFERENCES | 72 |
| ABBREVIATIONS AND OTHER TERMS | 72 |

APPENDIX A: Supplementary Tables A.1–A.16 and Figures A.1–A.59

APPENDIX A TABLES

Table A.1. Study Area Characteristics

| Study Area | Population | Area | Maximum Elevation | January/July Mean Low/High | Mean Annual Precipitation | Mean Relative Humidity |
|------------|-------------|---------------------|-------------------|----------------------------|---------------------------|------------------------|
| Montreal | 1.9 million | 472 km ² | 233 m | -14°C/+26°C | 1,000 mm | 60% |
| Toronto | 2.9 million | 630 km ² | 209 m | -7°C/+27°C | 831 mm | 61% |

Table A.2. Fixed-Site Monitoring Results

| City and Pollutant | n | Mean (SD) | Percentile | | |
|-----------------------------------------|----|---------------|------------|-------|-------|
| | | | 5th | 50th | 95th |
| Montreal^a | | | | | |
| UFP number (particles/cm ³) | 18 | 5,391 (899) | 4,358 | 5,442 | 6,609 |
| UFP size (nm) | 18 | 49.6 (6.4) | 39.9 | 50 | 57.5 |
| NO ₂ (ppb) | 64 | 3.0 (1.3) | 1.2 | 2.8 | 7.9 |
| O ₃ (ppb) | 68 | 34.3 (3.4) | 29.9 | 33.9 | 41.5 |
| Toronto | | | | | |
| UFP number (particles/cm ³) | 21 | 4,887 (1,602) | 2,626 | 4,705 | 7,099 |
| UFP size (nm) | 21 | 49.0 (5.3) | 38.3 | 50.8 | 55.8 |
| BC (ng/m ³) | 53 | 3662 (1015) | 2,069 | 3,532 | 5,579 |
| NO ₂ (ppb) | 57 | 6.7 (2.4) | 3.5 | 6.3 | 10.5 |
| O ₃ (ppb) | 56 | 30.1 (3.7) | 25.6 | 29.5 | 37.3 |

BC = black carbon; NO₂ = nitrogen dioxide; O₃ = ozone; SD = standard deviation; UFP = ultrafine particles.

^aFixed-site black carbon data were not collected in Montreal because of instrument failure.

Table A.3. Instrument Limits of Detection

| Instrument (Manufacturer) | Measure | Detection Range | Reported Accuracy | Time Resolution |
|---------------------------|------------|------------------------------------------------------------|-------------------|-----------------|
| DiSCmini (Testo) | UFP number | 10 ³ –10 ⁶ particles/cm ³ | ±30% | 1 sec |
| | UFP size | 10–300 nm | ±30% | 1 sec |
| Partector 2 (Naneos) | UFP number | 0–10 ⁶ particles/cm ³ | ±30% | 1 sec |
| | UFP size | 10–300 nm | ±30% | 1 sec |
| MA350 (microAeth) | BC | 30–10 ⁶ ng/m ³ | ±100 ng | 1 sec |

BC = black carbon; UFP = ultrafine particles.

Table A.4. Locations Used for Hourly Ambient Weather Conditions

| Study Area | Station Code | Station Name | Longitude | Latitude |
|----------------------|--------------|----------------------------|-----------|----------|
| Montreal | CYUL | Pierre Elliot Trudeau Intl | -73.7414 | 45.4683 |
| Toronto ^a | CYYZ | Lester B Pearson Intl | -79.6306 | 43.6772 |
| Toronto ^a | CYTZ | Toronto City Center | -79.3950 | 43.6286 |

^aThe mean value from the two Toronto stations was used.

Table A.5. Land Use and Traffic Parameters Examined for LUR Model Development

| Variable | Source (Year) |
|-----------------------------------------------------------------------|---------------------------------------------------|
| Average daily traffic NO _x emissions within buffer (grams) | EMME + MOVES (2020) |
| Average daily traffic volume within buffer (#) | EMME (2020) |
| Building land use area within buffer (m ²) | DMTI (2013) |
| Length of bus routes within buffer (m) | City of Montreal (2016) City of Toronto (2020) |
| Number of bus stops within buffer (#) | City of Montreal (2016) City of Toronto (2020) |
| Commercial land use area within buffer (m ²) | DMTI (2013) |
| Governmental land use area within buffer (m ²) | DMTI (2013) |
| Length of highways within buffer (m) | DMTI (2013) |
| Industrial land use area within buffer (m ²) | DMTI (2013) |
| Length of major roads within buffer (m) | DMTI (2013) |
| Number of intersections within buffer (#) | City of Montreal (2020) City of Toronto (2020) |
| Number of NPRI NO _x sources within buffer (#) | NPRI (2014) |
| Number of NPRI PM sources within buffer (#) | NPRI (2014) |
| Open area within buffer (m ²) | DMTI (2013) |
| Park area within buffer (m ²) | DMTI (2013) |
| Population living within buffer (# people) | Statistics Canada (2011) |
| Length of railroad within buffer (m) | DMTI (2013) |
| Residential land use area within buffer (m ²) | DMTI (2013) |
| Number of restaurants within buffer (#) | Google (2018) |
| Length of roads within buffer (m) | DMTI (2013) |
| Total traffic NO _x emissions within buffer (grams) | EMME + MOVES (2020) |
| Total traffic count within buffer (#) | EMME (2020) |
| Waterbody area within buffer (m ²) | DMTI (2013) |
| Distance to nearest airport (m) | DMTI (2013) |
| Distance to nearest bus stop (m) | City of Montreal (2016) City of Toronto (2020) |
| Distance to nearest highway (m) | DMTI (2013) |
| Distance to nearest major road (m) | DMTI (2013) |
| Distance to nearest NPRI NO _x source (m) | NPRI (2014) |
| Distance to nearest NPRI PM source (m) | NPRI (2014) |
| Distance to nearest port (m) | World Port Index (2019) |
| Distance to nearest rail (m) | DMTI (2013) |
| Distance to nearest shore (m) | Statistics Canada (2011) |

LUR = land use regression; MOVES = Motor Vehicle Emission Simulator; NO_x = nitrogen oxides; NPRI = National Pollutant Release Inventory; PM = particulate matter.

Table A.6. Comparison of Descriptive Statistics for Road Segments Visited Various Number of Times During Monitoring Campaign^a

| City | Visits per Road Segment (<i>n</i>) | UFP Number (particles/cm ³) | | UFP Size (nm) | | BC (ng/m ³) | |
|----------|--------------------------------------|-----------------------------------------|---------------------|----------------|---------------------|-------------------------|---------------------|
| | | Median (IQR) | 5th–95th percentile | Median (IQR) | 5th–95th percentile | Median (IQR) | 5th–95th percentile |
| Toronto | <i>n</i> ≥ 10 | 15,831 (12,255) | 7,265– 38,695 | 33.8 (5.8) | 25.6–44.0 | 1,099 (933) | 569–2,738 |
| | <i>n</i> ≥ 6 | 15,791 (12,798) | 7,231– 48,952 | 33.8 (7.1) | 23.3–44.0 | 1,155 (1,034) | 441–3,145 |
| | 6 > <i>n</i> > 1 | 17,849 (22,385) | 5,017– 79,049 | 33.9 (11.3) | 20.3–50.6 | 1,339 (1,352) | 198–4,885 |
| | <i>n</i> = 1 | 16,621 (21,524) | 3,261– 92,723 | 34 (17.4) | 18.0–55.4 | 1,082 (1,353) | 15–3,963 |
| Montreal | <i>n</i> ≥ 10 | 16,030 (14,551) | 5,220– 46,609 | 29.1 (9.1) | 19.8–43.0 | 1,189 (1,127) | 291–2,861 |
| | <i>n</i> ≥ 6 | 15,141 (13,693) | 4,913– 46,709 | 29.6 (10.0) | 19.0–45.1 | 1,083 (1,106) | 257–2,871 |
| | 6 > <i>n</i> > 1 | 12,034 (11,667) | 2,923– 47,130 | 31.5 (15.0) | 17.0–54.0 | 854 (942) | 101–3,116 |
| | <i>n</i> = 1 | 8,181 (10,603) | 1,713– 39,895 | 34.3 (25.2) | 16.0–65.0 | 675 (1,091) | 15–3,024 |

BC = black carbon; IQR = interquartile range; UFP = ultrafine particles.

^aAll models were developed using data from road segments visited six or more times (*n* ≥ 6).

Table A.7. Comparison of Land Use and Traffic Parameters for Road Segments Visited Various Number of Times During Monitoring Campaign^a

| City | Visits per Road Segment (<i>n</i>) | Median Traffic or Land Use Within 100 m | | | | | | Median Distance to Feature | |
|----------|--------------------------------------|-----------------------------------------|-----------------|--------------------|-----------------------------|------------------------------------|---------------------------------------|-----------------------------------|-------------|
| | | NO _x emissions (g) | Road length (m) | Highway length (m) | Open area (m ²) | Residential area (m ²) | Number of bus stops (m ²) | NPRI PM _{2.5} source (m) | Highway (m) |
| Toronto | <i>n</i> ≥ 10 | 86 | 668 | 339 | 8,120 | 11,051 | 0.93 | 2,024 | 966 |
| | <i>n</i> ≥ 6 | 79 | 690 | 342 | 8,138 | 12,300 | 0.95 | 1,995 | 871 |
| | 6 > <i>n</i> > 1 | 78 | 725 | 380 | 8,983 | 13,173 | 0.98 | 2,032 | 1,005 |
| | <i>n</i> = 1 | 49 | 607 | 225 | 5,811 | 15,670 | 1.03 | 2,261 | 1,262 |
| Montreal | <i>n</i> ≥ 10 | 111 | 886 | 414 | 10,399 | 12,173 | 1.1 | 1,600 | 403 |
| | <i>n</i> ≥ 6 | 95 | 851 | 377 | 9,787 | 12,307 | 1.09 | 1,532 | 515 |
| | 6 > <i>n</i> > 1 | 47 | 755 | 240 | 6,882 | 14,258 | 1.45 | 1,285 | 527 |
| | <i>n</i> = 1 | 21 | 632 | 83 | 3,728 | 18,739 | 1.4 | 1,751 | 891 |

NO_x = nitrogen oxides; NPRI = National Pollutant Release Inventory; PM_{2.5} = particulate matter ≤ 2.5 μm in aerodynamic diameter.

^aAll models were developed using data from road segments visited six or more times (*n* ≥ 6). The land use and traffic parameters in this table were selected because they had the strongest associations with UFP and BC (i.e., the lowest MSE in univariable regressions).

Table A.8. Model RMSE in Test Set^a

| City | Pollutant | RMSE in Test Set | | |
|----------|-----------------------------------------|------------------|-------|----------|
| | | LUR | CNN | Combined |
| Montreal | UFP number (particles/cm ³) | 0.450 | 0.495 | 0.442 |
| | UFP size (nm) | 6.245 | 6.631 | 6.165 |
| | BC (ng/m ³) | 0.458 | 0.514 | 0.457 |
| Toronto | UFP number (particles/cm ³) | 0.367 | 0.394 | 0.358 |
| | UFP size (nm) | 4.054 | 4.622 | 4.050 |
| | BC (ng/m ³) | 0.360 | 0.387 | 0.346 |

BC = black carbon; CNN = convolutional neural network; LUR = land use regression; RMSE = root mean square error; UFP = ultrafine particles.

^aUFP number concentration and BC were log-transformed for model development.

Table A.9. Pearson Correlation Between LUR and CNN Model Predictions in Test Set

| City | Pollutant | Pearsons <i>r</i> |
|----------|-----------------------------------------|-------------------|
| Montreal | UFP number (particles/cm ³) | 0.80 |
| | UFP size (nm) | 0.83 |
| | BC (ng/m ³) | 0.77 |
| Toronto | UFP number (particles/cm ³) | 0.86 |
| | UFP size (nm) | 0.82 |
| | BC (ng/m ³) | 0.83 |

BC = black carbon; CNN = convolutional neural network; LUR = land use regression; UFP = ultrafine particles.

Table A.10. Comparison of Model Performance When Trained on City-Specific Data versus Multi-city Data^a

| City | Pollutant | <i>R</i> ² in Test Set | | | | | |
|----------|-----------------------------------------|-----------------------------------|------------|---------------|------------|---------------|------------|
| | | LUR | | CNN | | Combined | |
| | | City-specific | Multi-city | City-specific | Multi-city | City-specific | Multi-city |
| Montreal | UFP number (particles/cm ³) | 0.59 | 0.54 | 0.49 | 0.47 | 0.60 | 0.55 |
| | UFP size (nm) | 0.48 | 0.44 | 0.41 | 0.38 | 0.49 | 0.46 |
| | BC (ng/m ³) | 0.58 | 0.58 | 0.50 | 0.49 | 0.60 | 0.58 |
| Toronto | UFP number (particles/cm ³) | 0.71 | 0.62 | 0.66 | 0.63 | 0.73 | 0.69 |
| | UFP size (nm) | 0.56 | 0.38 | 0.43 | 0.39 | 0.55 | 0.43 |
| | BC (ng/m ³) | 0.60 | 0.49 | 0.53 | 0.51 | 0.61 | 0.59 |

BC = black carbon; CNN = convolutional neural network; LUR = land use regression; UFP = ultrafine particles.

^aOne model was trained on data pooled from both cities.

Table A.11. Comparison of LUR Model Performance with and without Temporal Adjustment^a

| City | Pollutant | LUR Model R^2 in Test Set | | |
|----------|-----------------------------------------|--------------------------------------------------------|--------------------------------------------------------------|-----------------------------------------------|
| | | Temporal adjustment in training set (primary analysis) | Temporal adjustment in validation set (sensitivity analysis) | No temporal adjustment (sensitivity analysis) |
| Montreal | UFP number (particles/cm ³) | 0.60 | 0.59 | 0.57 |
| | UFP size (nm) | 0.48 | 0.46 | 0.41 |
| | BC (ng/m ³) | 0.58 | 0.58 | 0.56 |
| Toronto | UFP number (particles/cm ³) | 0.71 | 0.70 | 0.70 |
| | UFP size (nm) | 0.56 | 0.50 | 0.51 |
| | BC (ng/m ³) | 0.60 | 0.57 | 0.55 |

BC = black carbon; LUR = land use regression; UFP = ultrafine particles.

^aTemporal adjustment was conducted in the training data set during training and in the validation set after training (as was done with the CNN models). Comparison showed only a small change in model performance, which suggests that there was only a small degree of weather-related temporal variation in the aggregated monitoring data.

Table A.12. Comparison of CNN Model Performance with and without Temporal Adjustment in Validation Set^a

| City | Pollutant | CNN Model R^2 in Test Set | |
|----------|-----------------------------------------|----------------------------------------------------------|-----------------------------------------------|
| | | Temporal adjustment in validation set (primary analysis) | No temporal adjustment (sensitivity analysis) |
| Montreal | UFP number (particles/cm ³) | 0.49 | 0.45 |
| | UFP size (nm) | 0.41 | 0.36 |
| | BC (ng/m ³) | 0.50 | 0.47 |
| Toronto | UFP number (particles/cm ³) | 0.66 | 0.68 |
| | UFP size (nm) | 0.43 | 0.43 |
| | BC (ng/m ³) | 0.53 | 0.51 |

BC = black carbon; CNN = convolutional neural network; UFP = ultrafine particles.

^aComparison showed only a small change in model performance, which suggests that there was only a small degree of weather-related temporal variation in the aggregated monitoring data.

Table A.13. Median Difference Between LUR and CNN Predicted Values in Test Set

| Pollutant | Montreal | Toronto |
|-----------------------------------------|------------------------------|----------------------------------|
| | Mean difference (95% CI) | Mean difference (95% CI) |
| UFP number (particles/cm ³) | 271.24 (-5,469.1, 12,175.44) | (-17,070.19, -2,231.83 6,113.85) |
| UFP size (nm) | -0.41 (-6.29, 6.31) | 0.79 (-3.49, 5.44) |
| BC (ng/m ³) | 22.07 (-369.19, 976.72) | -51.12 (-745.15, 781.05) |

BC = black carbon; CI = confidence interval; CNN = convolutional neural network; LUR = land use regression; UFP = ultrafine particles.

Table A.14. Median Difference Between LUR and CNN Predicted Values in Test Set for Road Segments When Observed Aggregated UFP Number Concentration Was Greater than 45,000 particles/cm³

| Pollutant | Median Difference (5th, 95th percentile) | |
|-----------------------------------------|------------------------------------------|-------------------------|
| | Montreal | Toronto |
| UFP number (particles/cm ³) | 8,724 (-3,368, 25,943) | -5871 (-29,269, 10,550) |
| UFP size (nm) | -4.71 (-11.02, 1.16) | 1.23 (-3.45, 4.76) |
| BC (ng/m ³) | 323 (-263, 1,248) | -157 (-929, 788) |

BC = black carbon; CNN = convolutional neural network; LUR = land use regression; UFP = ultrafine particles.

Table A.15. Slope and Intercept of Predictions versus Observed Values in Test Set

| Pollutant | Model | Parameter | Montreal | Toronto |
|--------------------------------------------|----------|-----------|----------------------|---------------------|
| | | | Estimate (95% CI) | Estimate (95% CI) |
| UFP number (particles/cm ³) | LUR | Intercept | 0.73 (0.30, 1.15) | -0.29 (-0.69, 0.12) |
| | | Slope | 0.92 (0.88, 0.96) | 1.03 (0.99, 1.08) |
| | CNN | Intercept | -0.87 (-1.48, -0.25) | 0.21 (-0.22, 0.63) |
| | | Slope | 1.09 (1.03, 1.16) | 0.97 (0.93, 1.01) |
| | Combined | Intercept | -0.40 (-0.87, 0.08) | 0.65 (0.3, 1.00) |
| | | Slope | 1.04 (0.99, 1.09) | 0.93 (0.89, 0.96) |
| UFP size (nm) | LUR | Intercept | 3.23 (1.48, 4.98) | 0.64 (-1.22, 2.50) |
| | | Slope | 0.90 (0.85, 0.96) | 0.98 (0.93, 1.03) |
| | CNN | Intercept | -6.79 (-9.47, -4.12) | 4.92 (2.82, 7.02) |
| | | Slope | 1.21 (1.13, 1.29) | 0.88 (0.81, 0.94) |
| | Combined | Intercept | -5.14 (-7.33, -2.96) | 1.73 (-0.11, 3.57) |
| | | Slope | 1.15 (1.09, 1.22) | 0.96 (0.91, 1.02) |
| BC (ng/m ³) | LUR | Intercept | 0.51 (0.20, 0.82) | 0.61 (0.25, 0.96) |
| | | Slope | 0.93 (0.89, 0.98) | 0.92 (0.87, 0.97) |
| | CNN | Intercept | -0.47 (-0.90, -0.05) | 0.57 (0.16, 0.98) |
| | | Slope | 1.08 (1.02, 1.14) | 0.92 (0.87, 0.98) |
| | Combined | Intercept | -0.44 (-0.78, -0.09) | 0.77 (0.44, 1.10) |
| | | Slope | 1.07 (1.02, 1.12) | 0.90 (0.85, 0.94) |

BC = black carbon; CI = confidence interval; CNN = convolutional neural network; LUR = land use regression; UFP = ultrafine particles.

Table A.16. Hazard Ratios for Interquartile Increases in O_x Exposures and Mortality^a

| Cause of Mortality | Hazard Ratio (95% CI) |
|------------------------|----------------------------------|
| | O _x (per 4.51 ppb) |
| Nonaccidental | 1.025 (1.015, 1.035) |
| Cardiovascular | 1.049 (1.029, 1.069) |
| Cardiometabolic | 1.048 (1.029, 1.067) |
| Ischemic heart disease | 1.083 (1.056, 1.111) |
| Cerebrovascular | 1.028 (0.985, 1.073) |
| Respiratory | 1.048 (1.013, 1.084) |
| Lung cancer | 0.976 (0.945, 1.008) |

CI = confidence interval; O_x = ozone.

^aAll models included sociodemographic variables and residential exposure to PM_{2.5}, BC, UFP number concentration, and UFP size.

APPENDIX A FIGURES

Figure A.1. Mobile monitoring routes in Montreal (A) and Toronto (B).

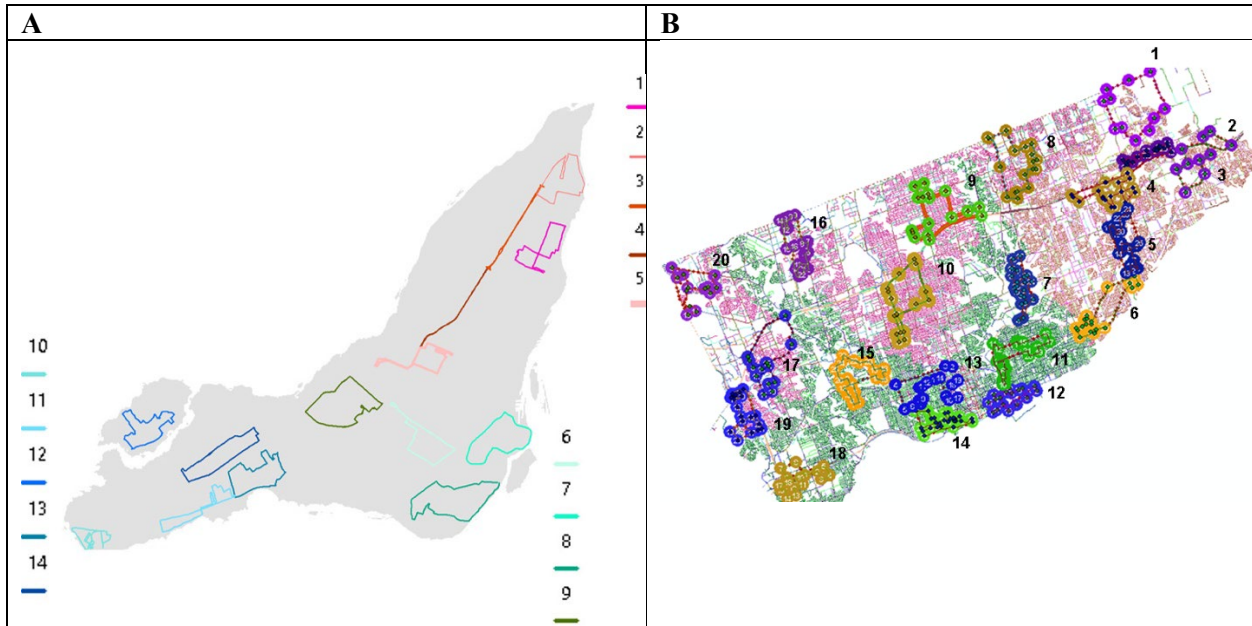


Figure A.2. Maps of the training, validation, and test sets in Toronto and Montreal.

Model development data were split by geohash code (precision 6) to increase the spatial independence of the test set.

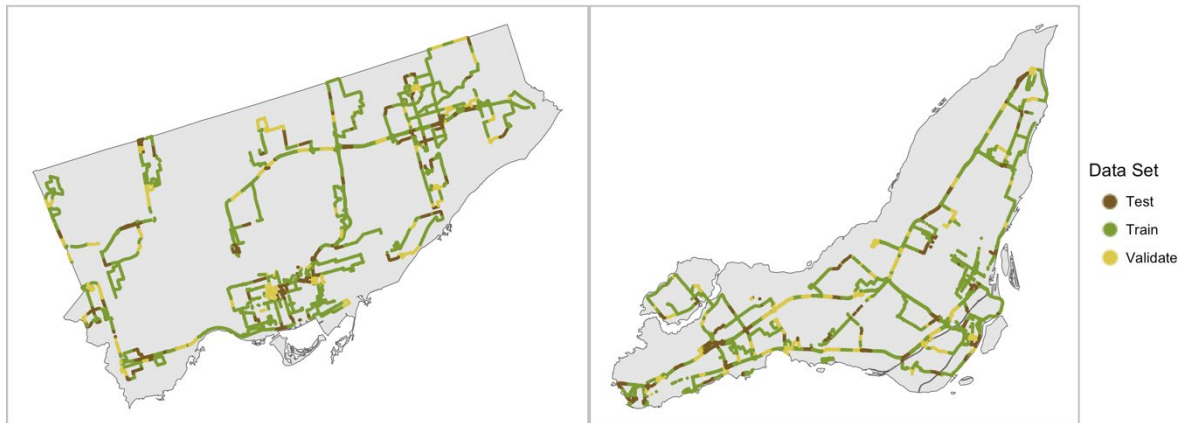
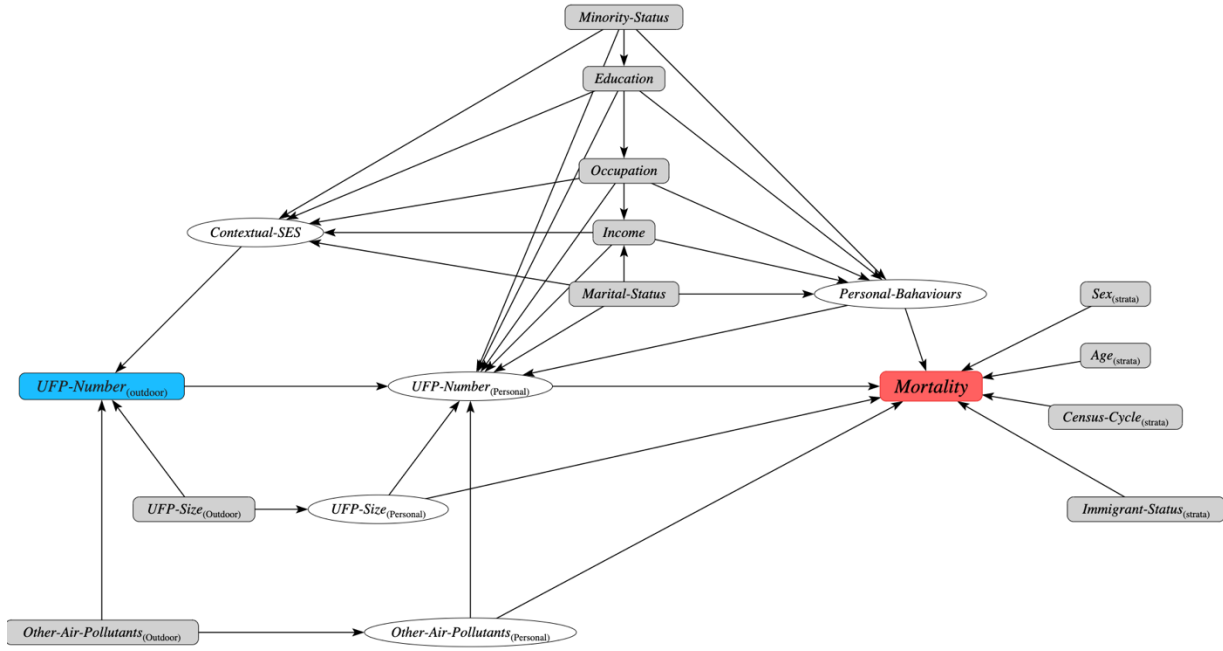


Figure A.3. Directed acyclic graphs for the relationships between outdoor UFP number concentrations (A) and black carbon (B) and mortality.
 Shaded boxes indicate variables included as covariates or strata variables in the analysis. SES = socioeconomic status; UFP = ultrafine particles.

A



B

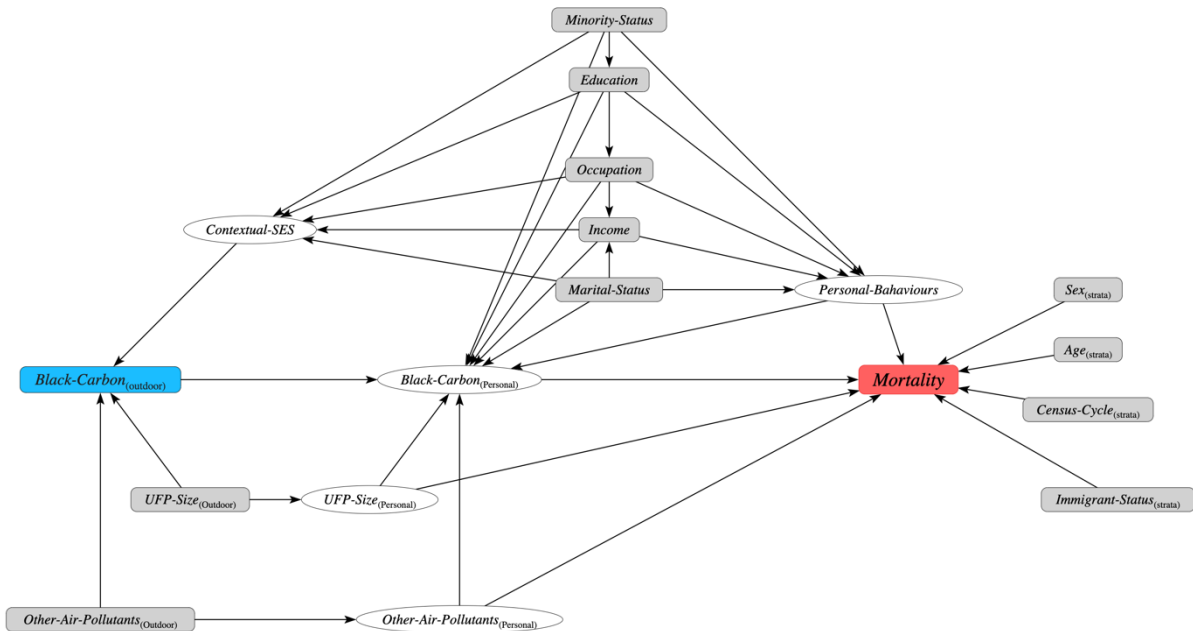


Figure A.4. Spatial coverage of the Montreal UFP number concentrations monitoring data when restricting the minimum number of visits per road segment.
UFP = ultrafine particles.

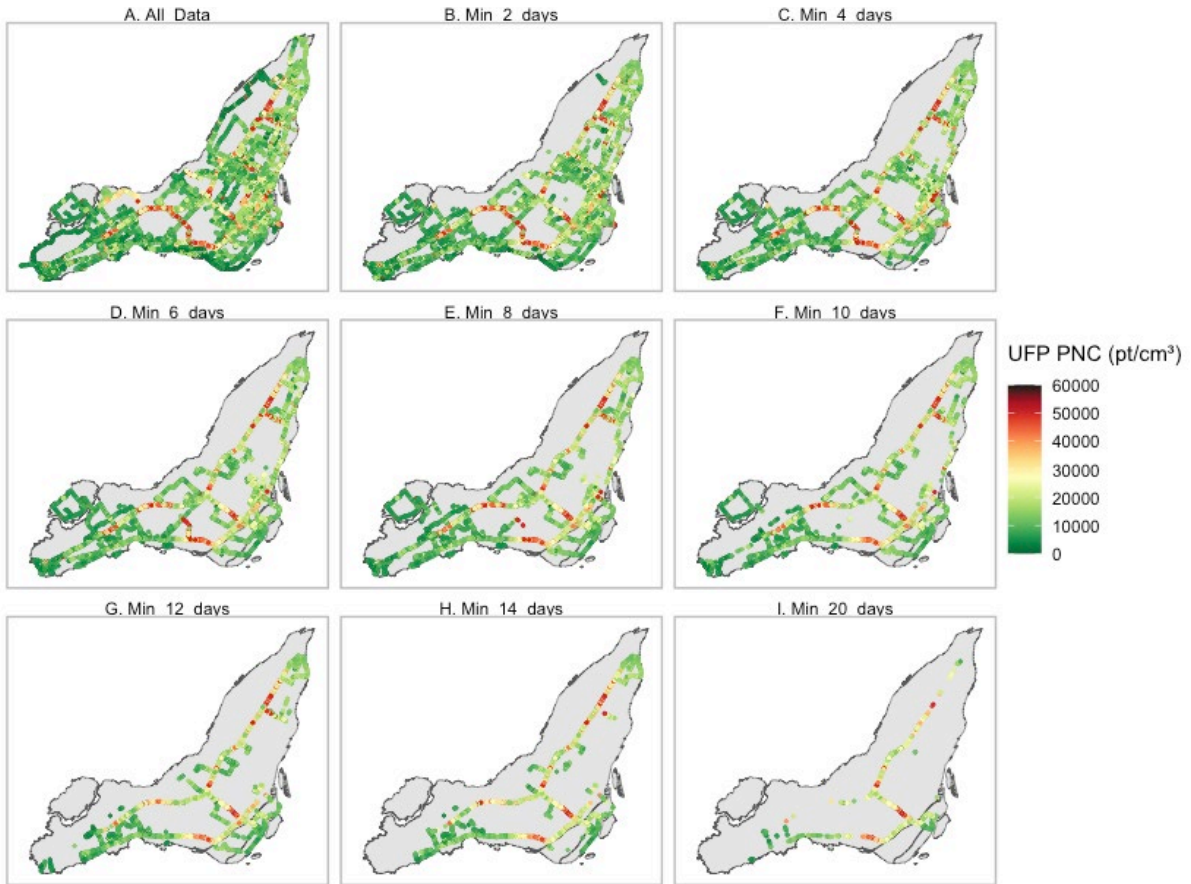


Figure A.5. Spatial coverage of the Toronto UFP number monitoring data when restricting the minimum number of visits per road segment.

UFP = ultrafine particles.



Figure A.6. Spearman's correlations between land use and traffic parameters included in the Montreal LUR for UFP number concentrations.

A criterion for variable selection was a Spearman's $r < 0.7$ with other variables in the model. LUR = land use regression; NO_x = nitrogen oxides; NPRI = National Pollutant Release Inventory; PM = particulate matter; UFP = ultrafine particles.

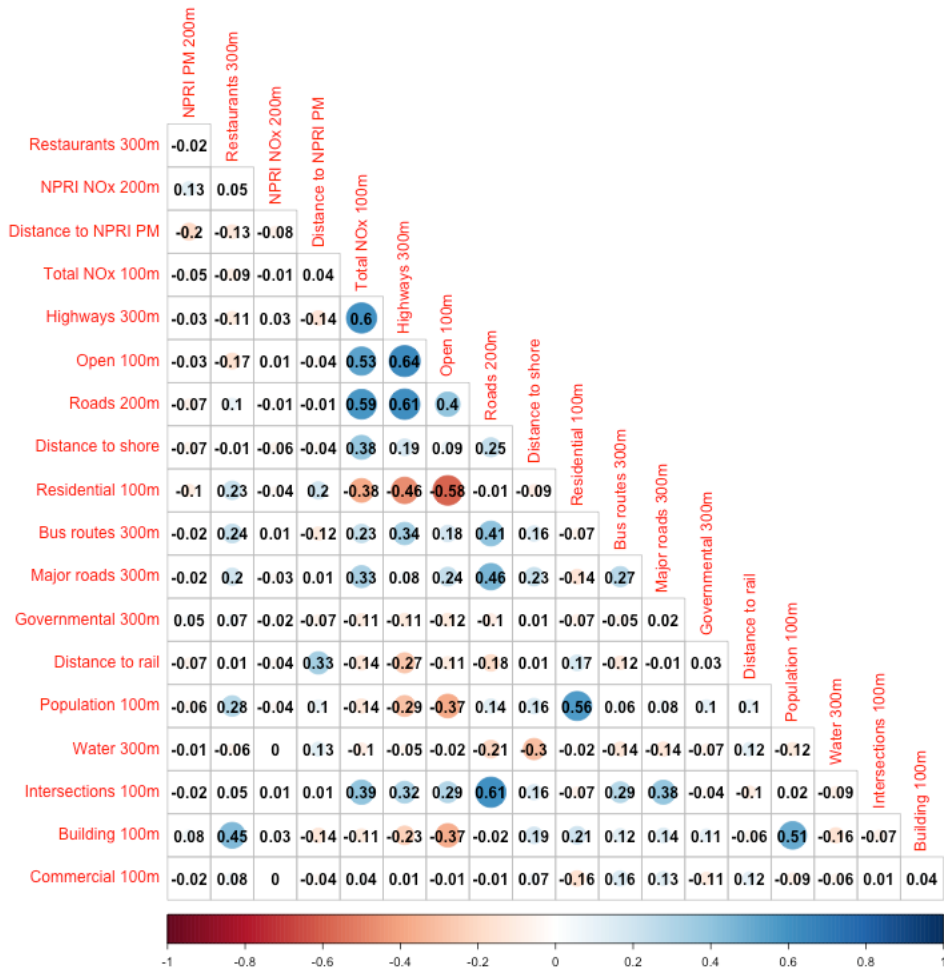


Figure A.7. Spearman’s correlations between land use and traffic parameters included in the Montreal LUR model for UFP size.

A criterion for variable selection was a Spearman’s $r < 0.7$ with other variables in the model. LUR = land use regression; NO_x = nitrogen oxides; NPRI = National Pollutant Release Inventory; PM = particulate matter; UFP = ultrafine particles.

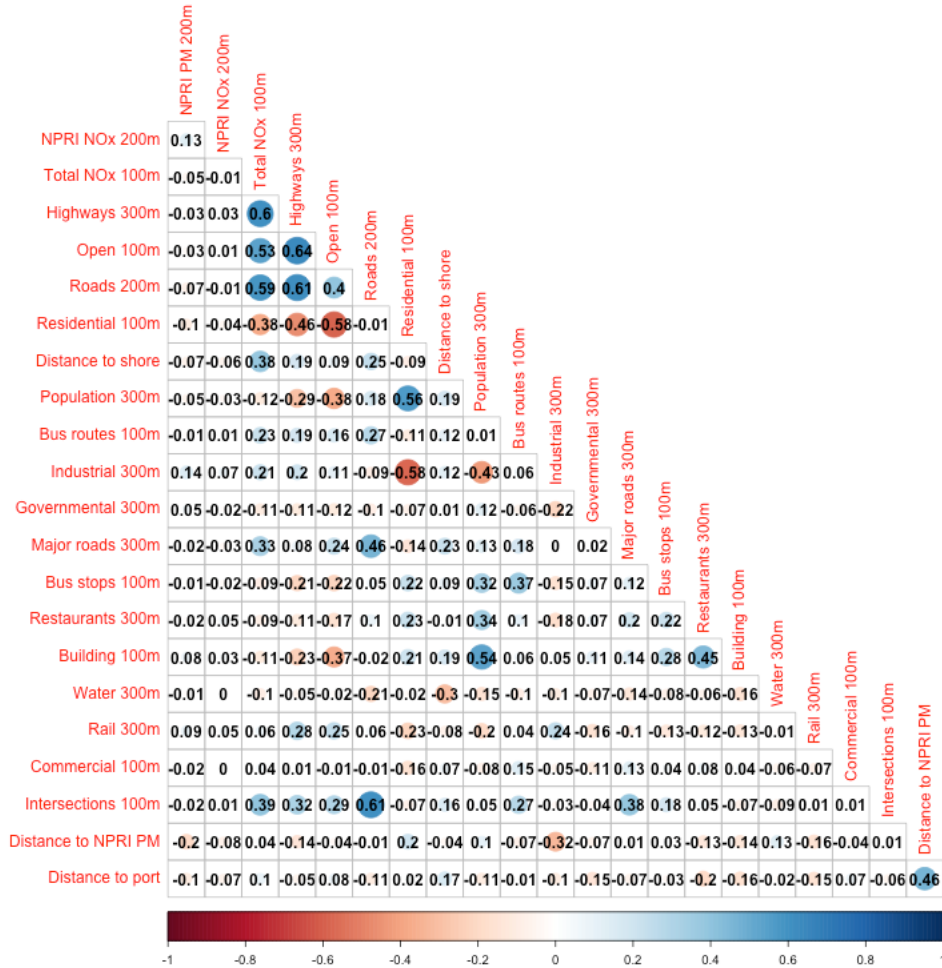


Figure A.8. Spearman's correlations between land use and traffic parameters included in the Montreal LUR for BC.

A criterion for variable selection was a Spearman's $r < 0.7$ with other variables in the model. BC = black carbon; LUR = land use regression; NO_x = nitrogen oxides; NPRI = National Pollutant Release Inventory; PM = particulate matter.

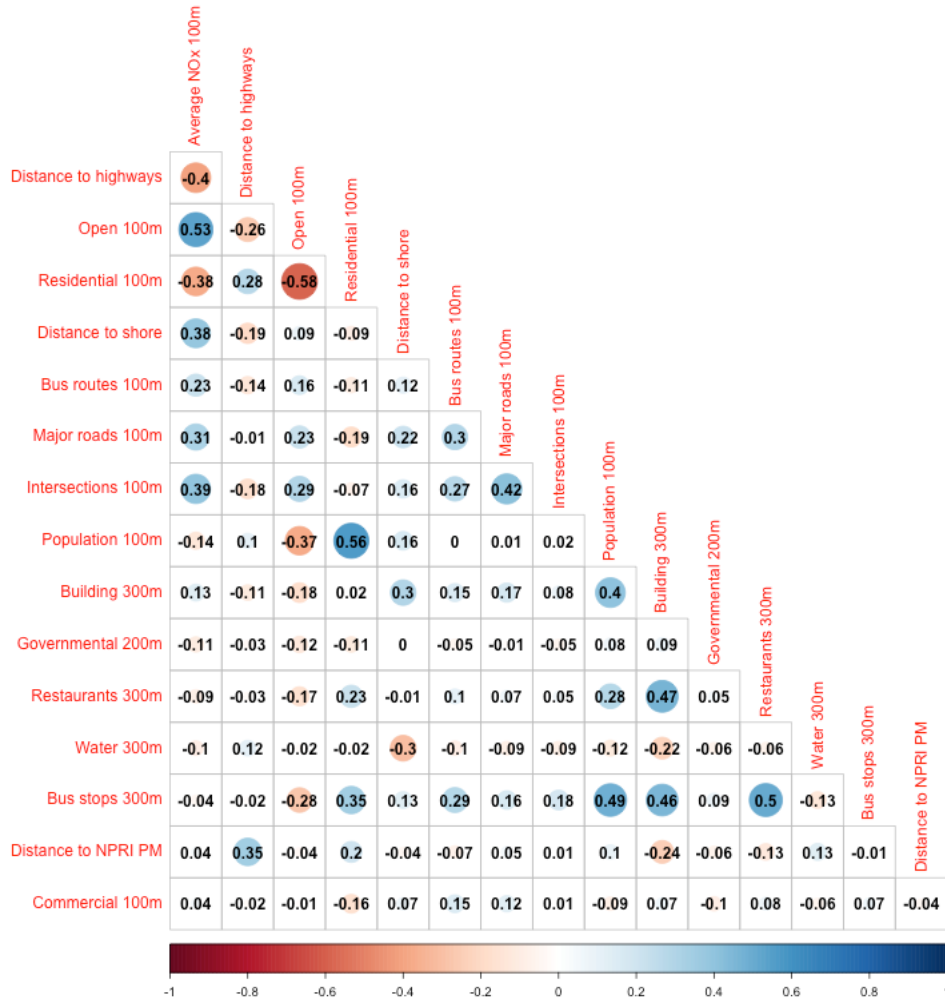


Figure A.9. Spearman’s correlations between land use and traffic parameters included in the Toronto LUR for UFP number concentrations.

A criterion for variable selection was a Spearman’s $r < 0.7$ with other variables in the model. LUR = land use regression; NO_x = nitrogen oxides; NPRI = National Pollutant Release Inventory; PM = particulate matter; UFP = ultrafine particles.

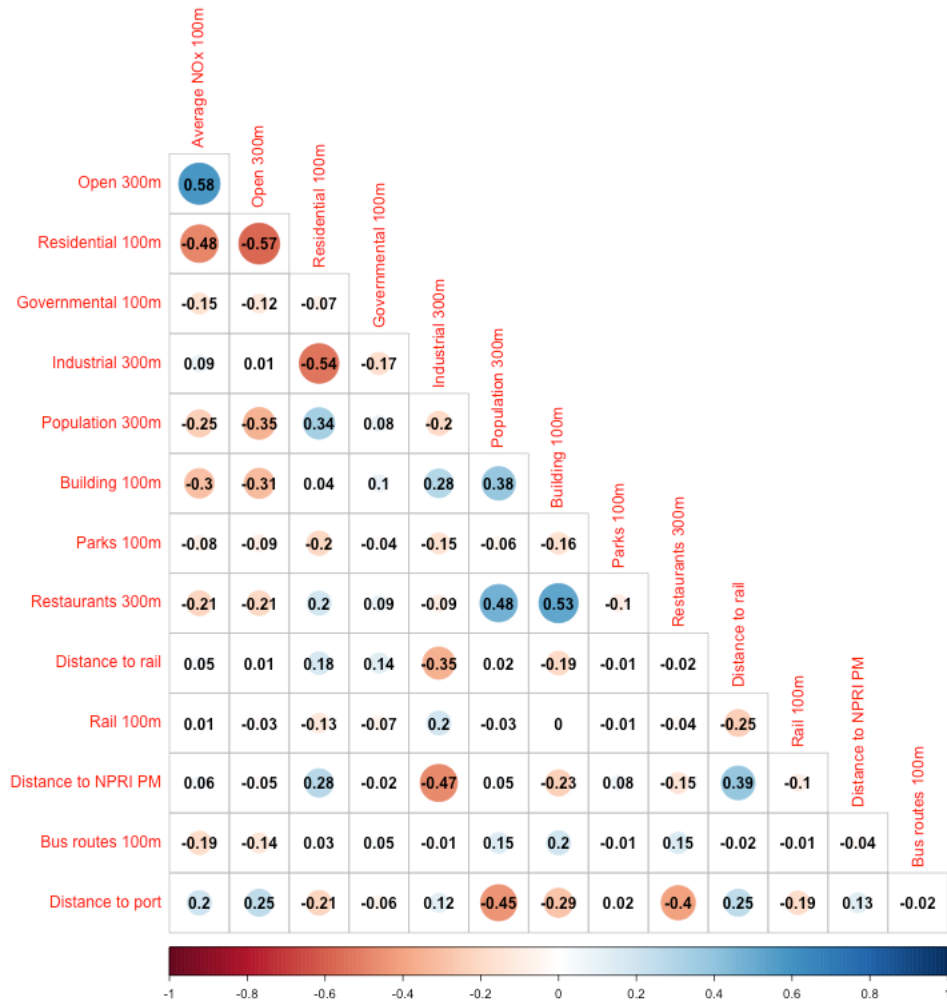


Figure A.10. Spearman’s correlations between land use and traffic parameters included in the Toronto LUR model for UFP size.

A criterion for variable selection was a Spearman’s $r < 0.7$ with other variables in the model. LUR = land use regression; NO_x = nitrogen oxides; NPRI = National Pollutant Release Inventory; PM = particulate matter; UFP = ultrafine particles.

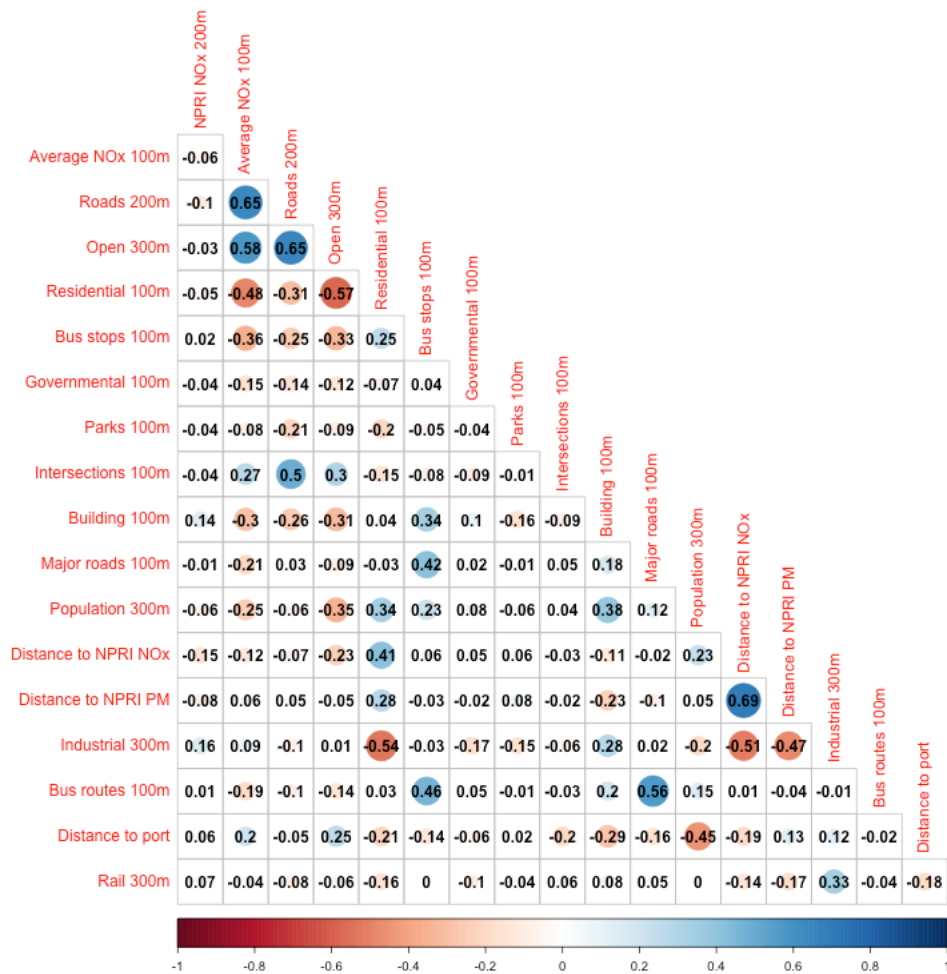


Figure A.11. Spearman’s correlations between land use and traffic parameters included in the Toronto LUR for BC.

A criterion for variable selection was a Spearman’s $r < 0.7$ with other variables in the model. LUR = land use regression; NO_x = nitrogen oxides; NPRI = National Pollutant Release Inventory; PM = particulate matter.

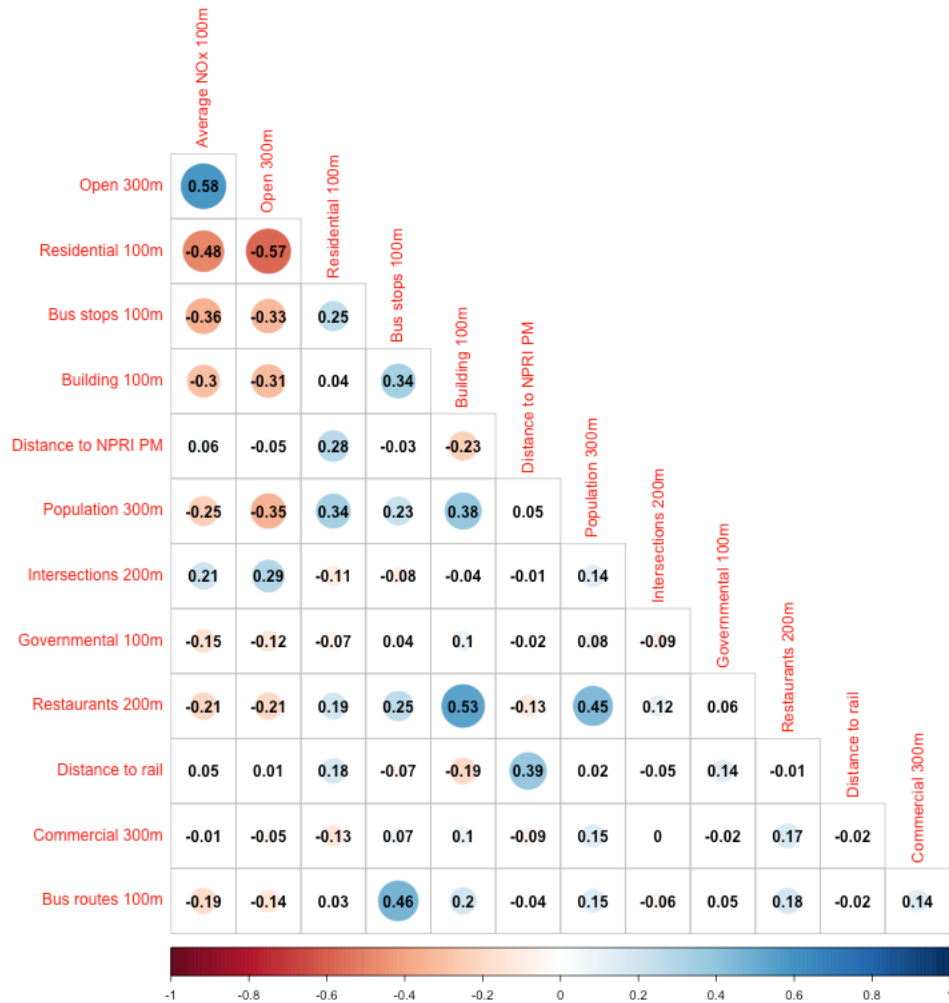


Figure A.12. Maps of spatial variation in median meteorological conditions during monitoring for Montreal (A: temperature; B: relative humidity; C: wind speed) and Toronto (i: temperature; ii: relative humidity; iii: wind speed).

The monitoring campaign was designed to have a temporal balance between monitoring routes, but there were chance imbalances that can be seen in the spatial variation in meteorological conditions during monitoring. To account for the imbalances, models included temporal adjustments.

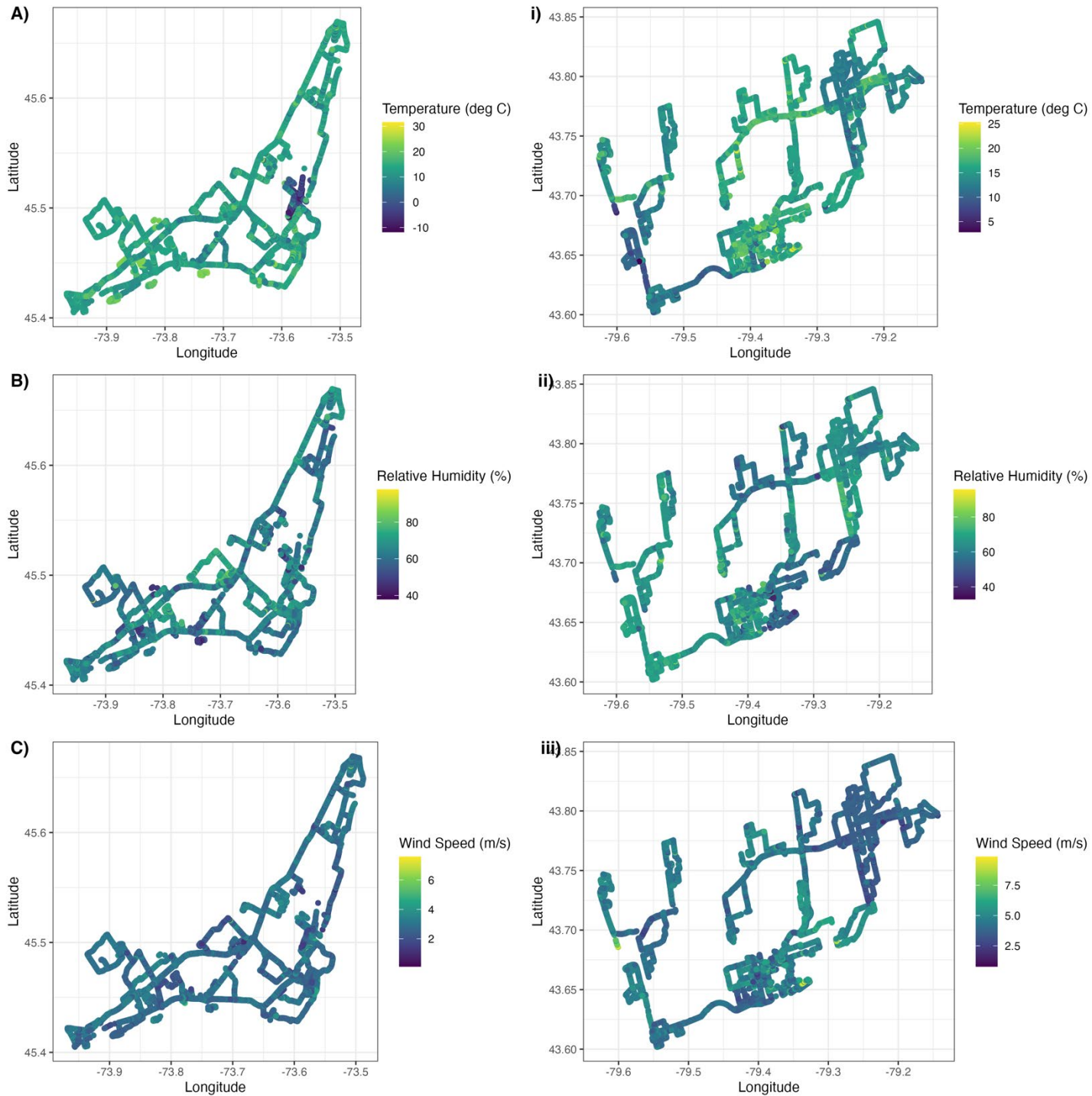


Figure A.13. Relationships between meteorological variables and changes in pollutant levels in each of the Montreal LUR models.

UFP number concentrations and BC were log-transformed for model training; UFP size was not. Each plot includes a rug to show the distribution of the median meteorological values for the training sites. BC = black carbon; LUR = land use regression; UFP = ultrafine particles.

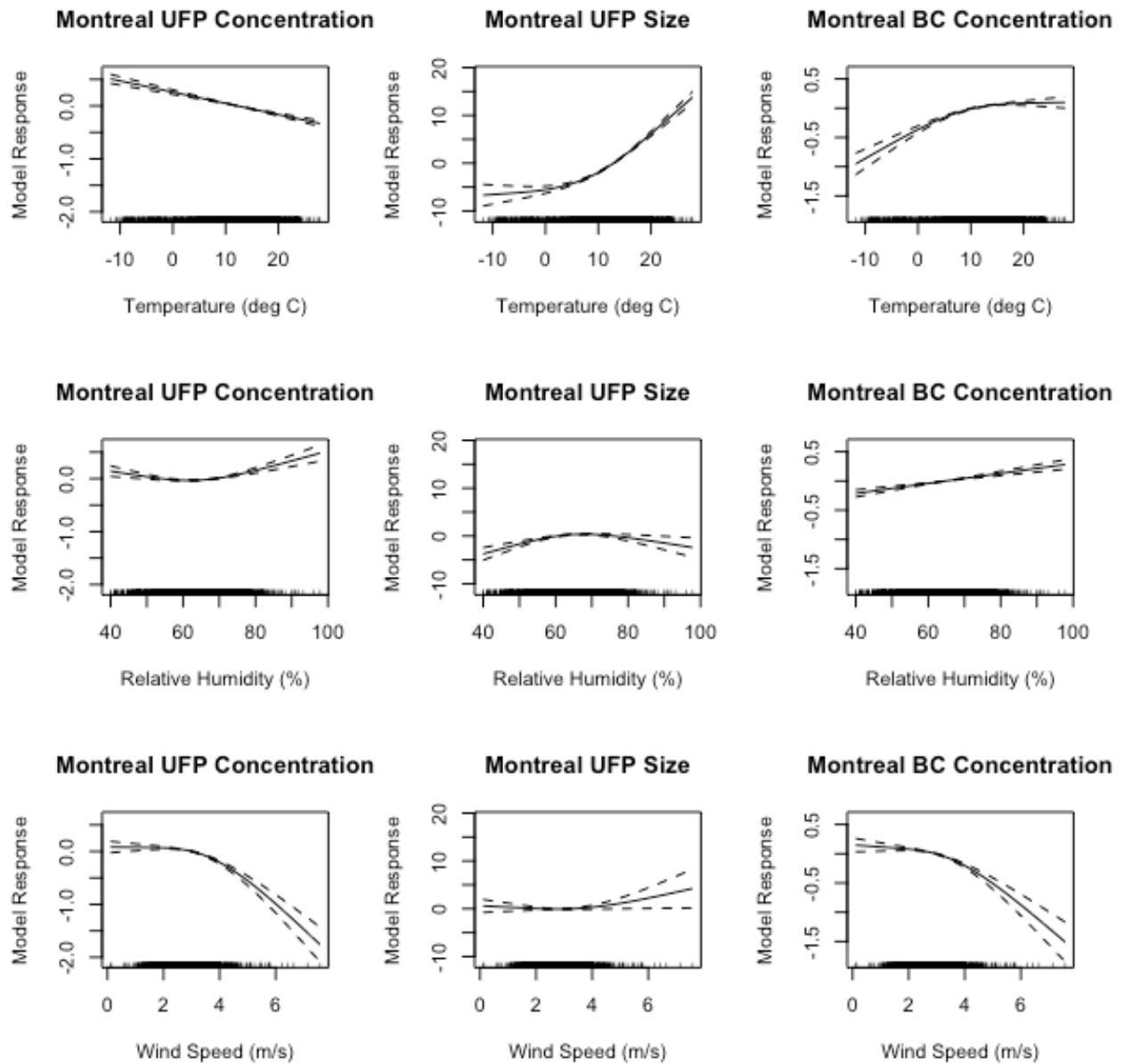


Figure A.14. Relationships between meteorological variables and changes in pollutant levels in each of the Toronto LUR models.

UFP number concentrations and BC were log-transformed for model training; UFP size was not. Each plot includes a rug to show the distribution of the median meteorological values for the training sites. BC = black carbon; LUR = land use regression; UFP = ultrafine particles.

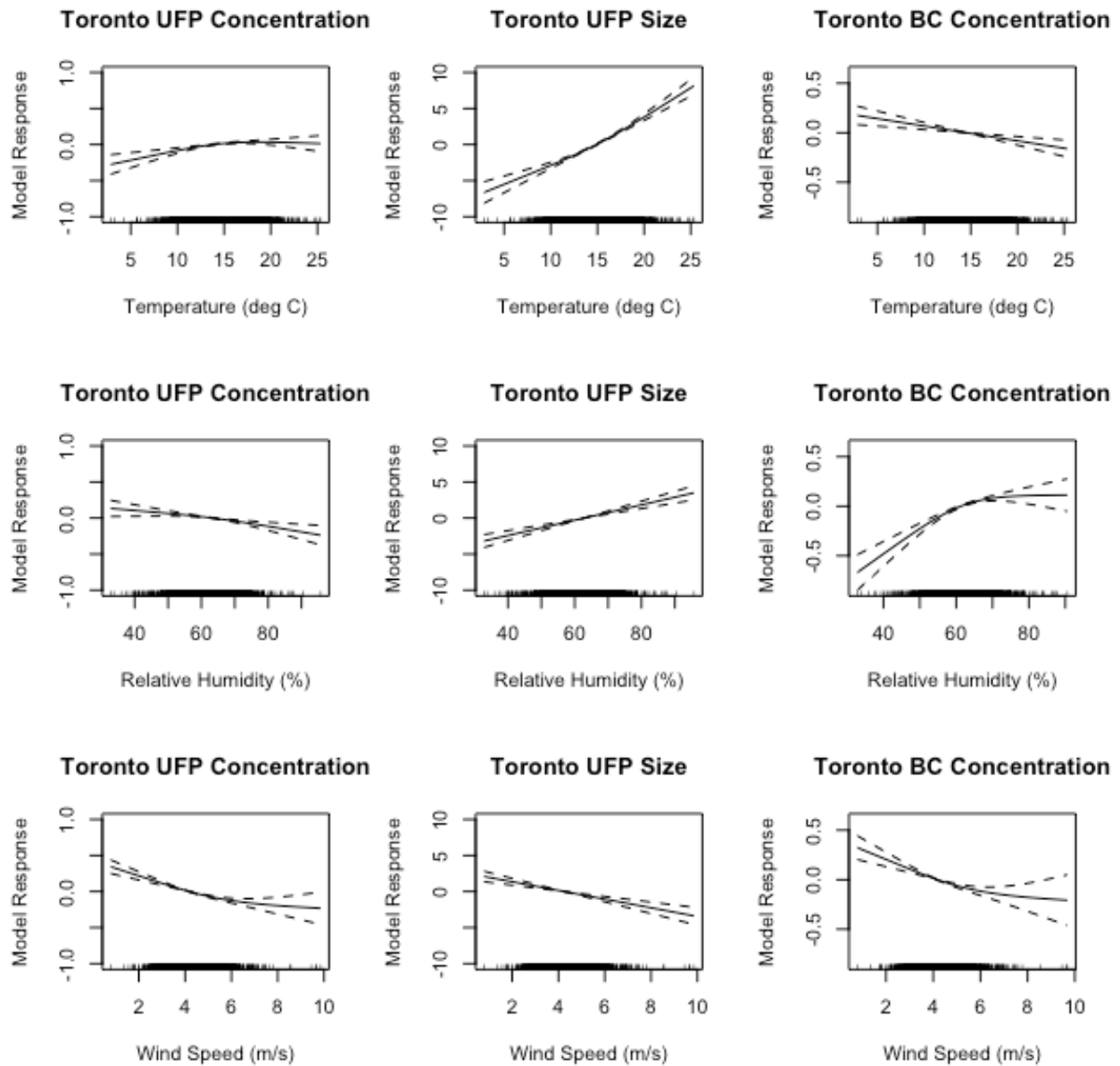


Figure A.15. Comparing test set LUR mean UFP size predictions to CNN predictions in Montreal and Toronto (A) with a histogram of observed values for reference (B).

The median difference in predicted mean UFP size between the Montreal LUR and Montreal CNN was -0.4 nm (5th–95th quantile: -6.29 to 6.31). For Toronto, the median difference was 0.8 nm (5th–95th quantile: -3.49 to 5.44). Pearson correlation coefficient of the LUR and CNN model predictions was 0.83 for Montreal and 0.82 for Toronto. CNN = convolutional neural network; LUR = land use regression; UFP = ultrafine particles.

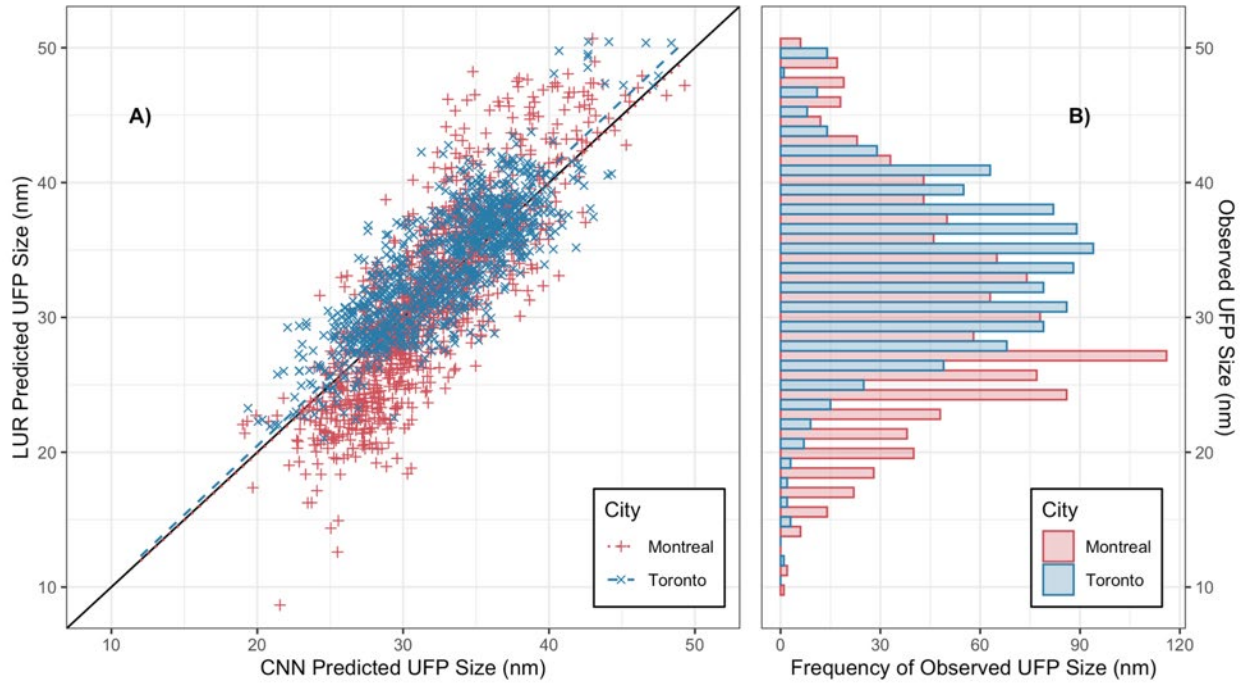


Figure A.16. Comparing test set LUR BC predictions to CNN predictions in Montreal and Toronto (A) with a histogram of observed values for reference (B).

Similar to the UFP number concentration models, for the highest BC concentrations (e.g., near 2,500 ng/m^3), the Montreal CNN predictions appeared to be systematically lower than the Montreal LUR predictions. Unlike the UFP number concentration models, there was no similar contrast for Toronto. The mean difference in predicted BC concentration between the Montreal LUR and Montreal CNN was 22 ng/m^3 (5th–95th quantile: $-369, 977$). For Toronto, the mean difference was $-51 \text{ ng}/\text{m}^3$ (5th–95th quantile: $-745, 781$). The Pearson correlation coefficient of the LUR and CNN model predictions was 0.77 for Montreal and 0.83 for Toronto. BC = black carbon; CNN = convolutional neural network; LUR = land use regression; UFP = ultrafine particles.

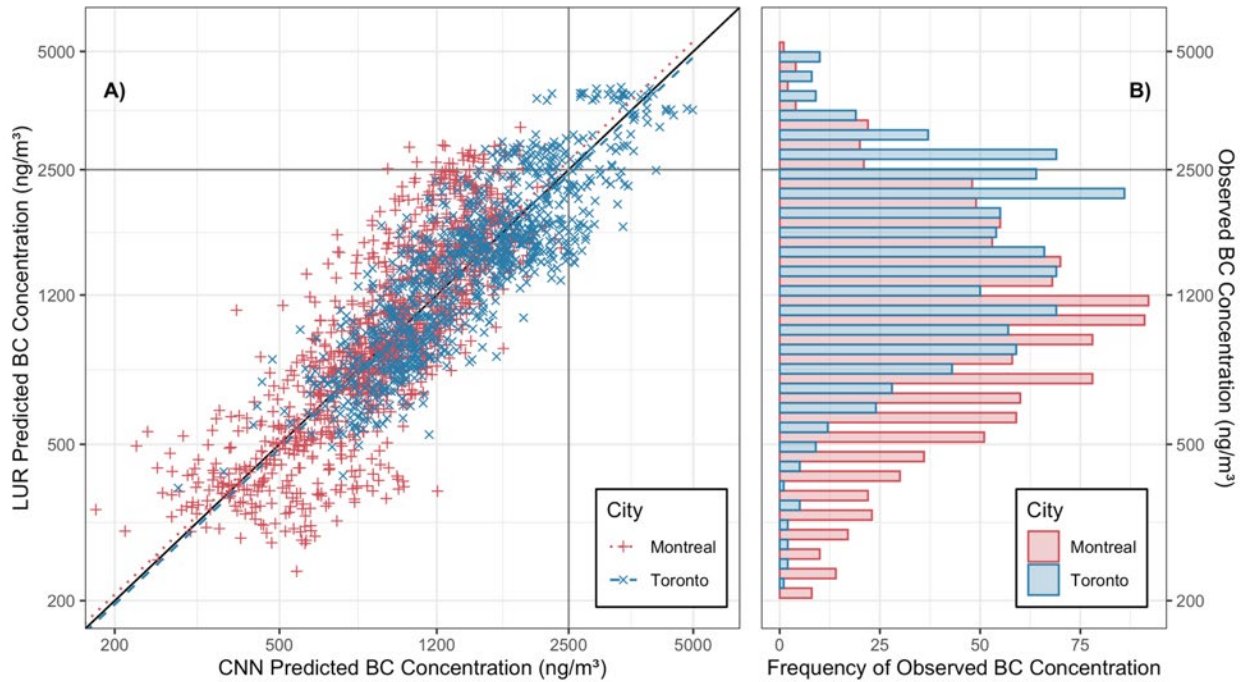


Figure A.17. Comparing LUR and CNN predictions of UFP number concentrations from the city-specific model and the multi-city models.

The multi-city CNN model (trained on Toronto and Montreal; blue in panel B) generates fewer very high predictions in Toronto compared to the city-specific CNN model trained in Toronto (blue in panel A). Conversely, the multi-city CNN model (red in panel B) generates more very high predictions in Montreal than the city-specific model trained on Montreal (red in panel A). The CNN model trained on only Toronto data seems to be better at generating very high UFP number concentration predictions. The multi-city CNN model trained on Toronto and Montreal data seems to generate slightly lower predictions and the CNN model trained on only Montreal data generates even lower predictions. CNN = convolutional neural network; LUR = land use regression; UFP = ultrafine particles.

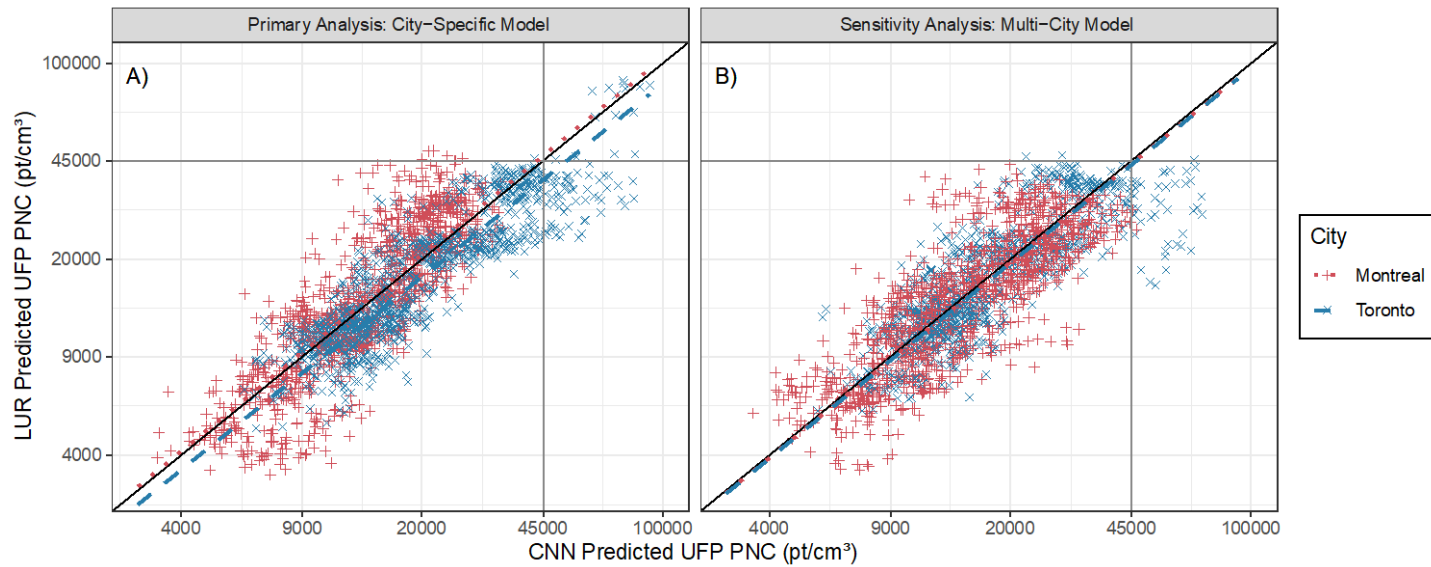


Figure A.18. Comparing UFP number concentrations model predictions from the city-specific models to the multi-city models.

The Montreal CNN (panel A) generates higher predictions when trained on both Toronto and Montreal data (i.e., the multi-city model). The Toronto CNN (panel C) generates higher predictions when trained on only Toronto data (i.e., the city-specific model). CNN = convolutional neural network; LUR = land use regression; UFP = ultrafine particles.

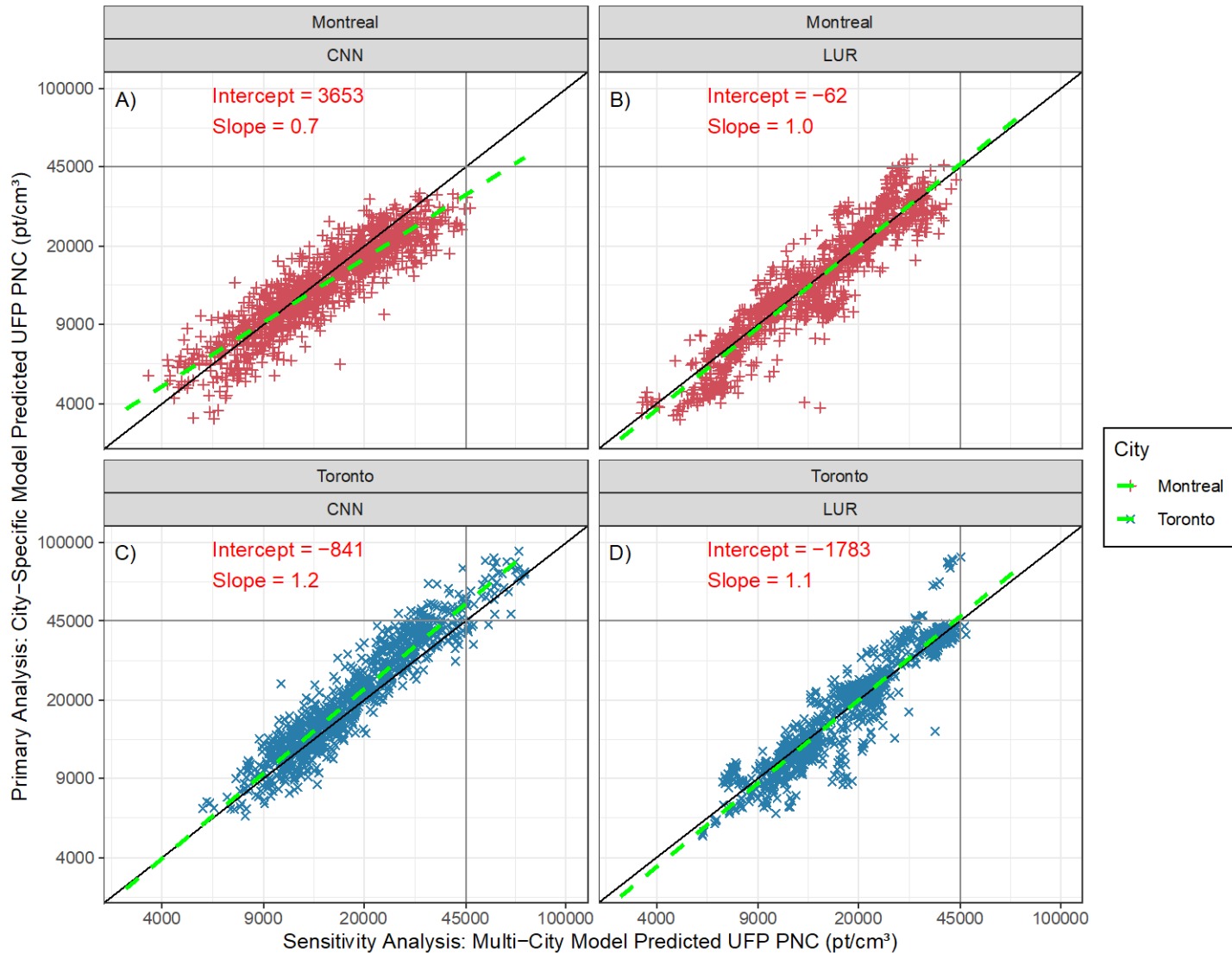


Figure A.19. Observed UFP number concentrations over 40,000 particles/cm³ in Toronto are all situated on highways.

In Toronto, the city-specific CNN model trained on Toronto data generally generated higher predictions than the multi-city CNN model trained on both Montreal and Toronto data. CNN = convolutional neural network; UFP = ultrafine particles.

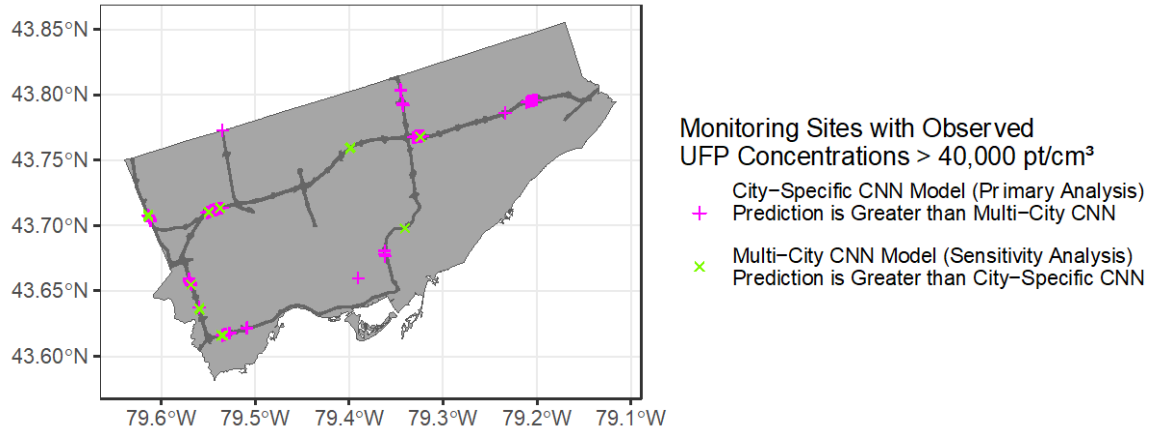


Figure A.20. Observed UFP number concentrations over 40,000 particles/cm³ in Montreal are all situated on highways.

In Montreal, the city-specific CNN model trained on Montreal data generally generated lower predictions than the multi-city CNN model trained on both Montreal and Toronto data. CNN = convolutional neural network; UFP = ultrafine particles.

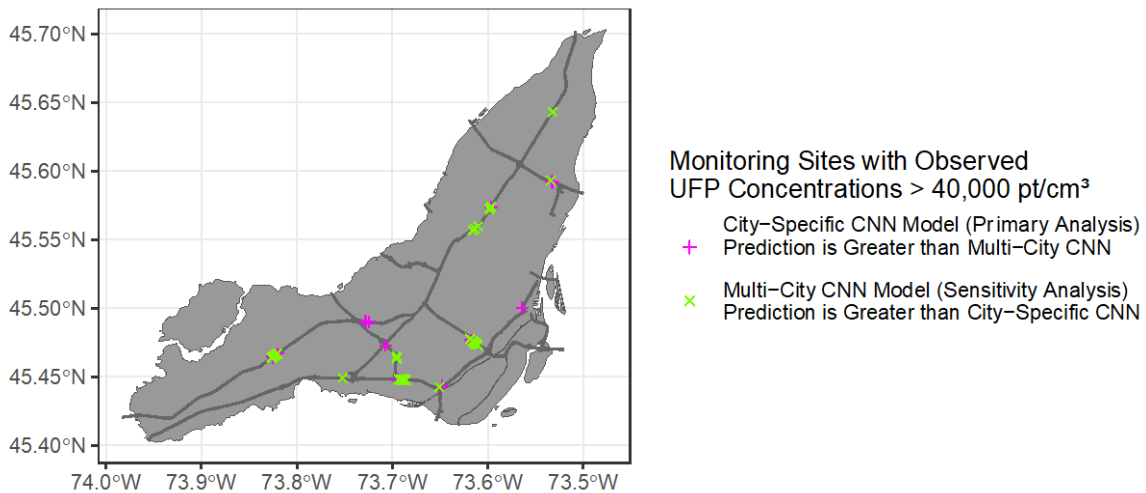


Figure A.21. Visualizing intermediate activations of filters of the Conv2D layer in the CNN models trained on Toronto data and trained on Montreal and Toronto data.

Filters were visualized while the model generated a prediction on a single picture in Toronto. This kind of visualization can provide clues about what features are important for generating a prediction. The majority of the filters of the two models were virtually identical, but one was slightly different and has been enlarged in the figure. Notice the dark pavement in the upper part of the original picture. Panel A shows the city-specific model giving greater importance (i.e., lighter color) to the dark pavement than the multi-city model in panel B. A possible explanation is that the dark pavement was freshly laid asphalt on this major highway running through Toronto. When the model was trained on Toronto data only, the CNN model may have learned to associate dark pavement with very high UFP number concentrations. Conversely, when the model was trained on Montreal and Toronto data, there may have been relatively little fresh asphalt on Montreal highways and thus weaker associations between very high UFP number concentrations and dark pavement in the training dataset. CNN = convolutional neural network; UFP = ultrafine particles.

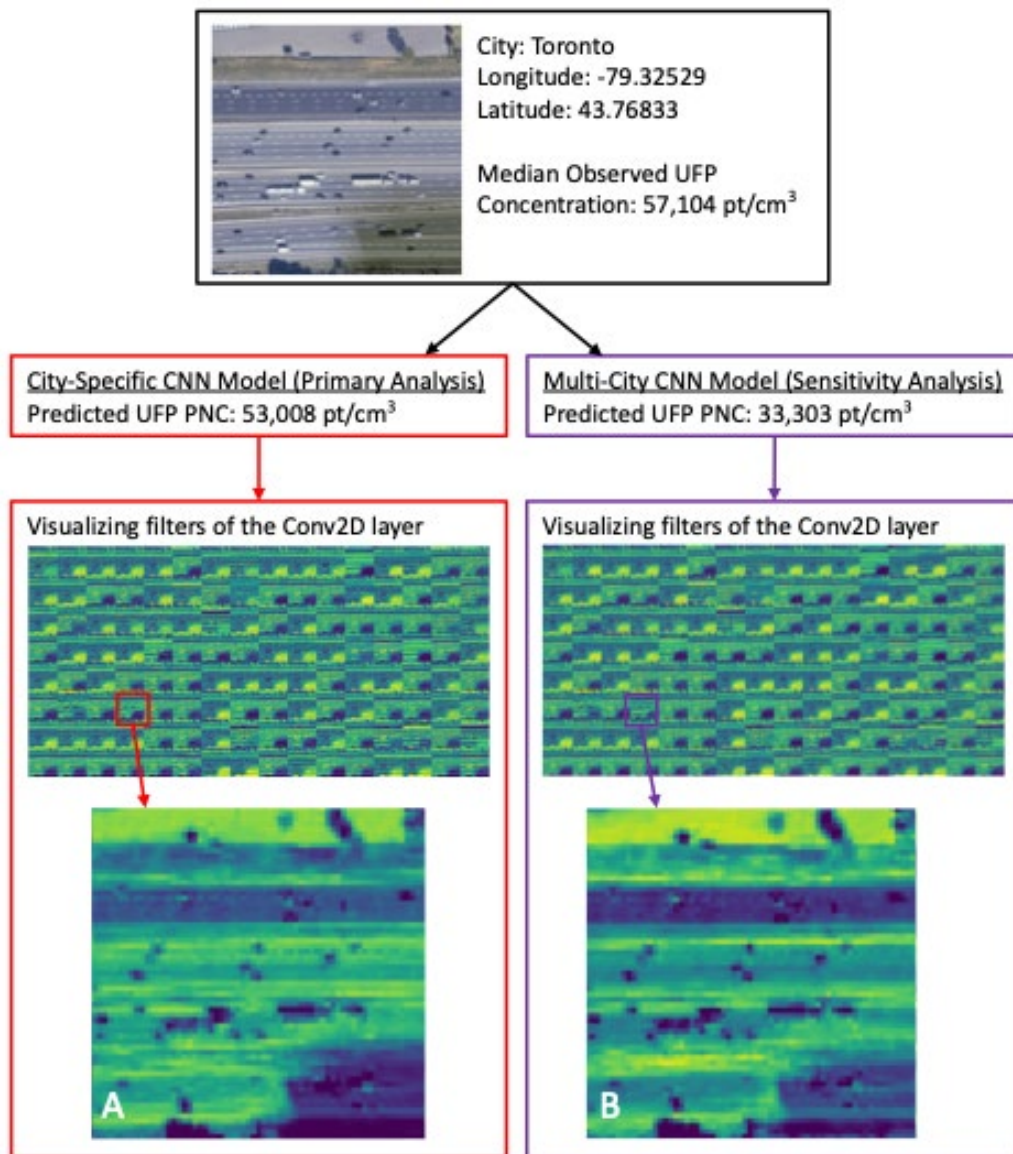


Figure A.22. Scatter plots of observed and predicted UFP number concentrations in the test set. CNN = convolutional neural network; LUR = land use regression; UFP = ultrafine particles.

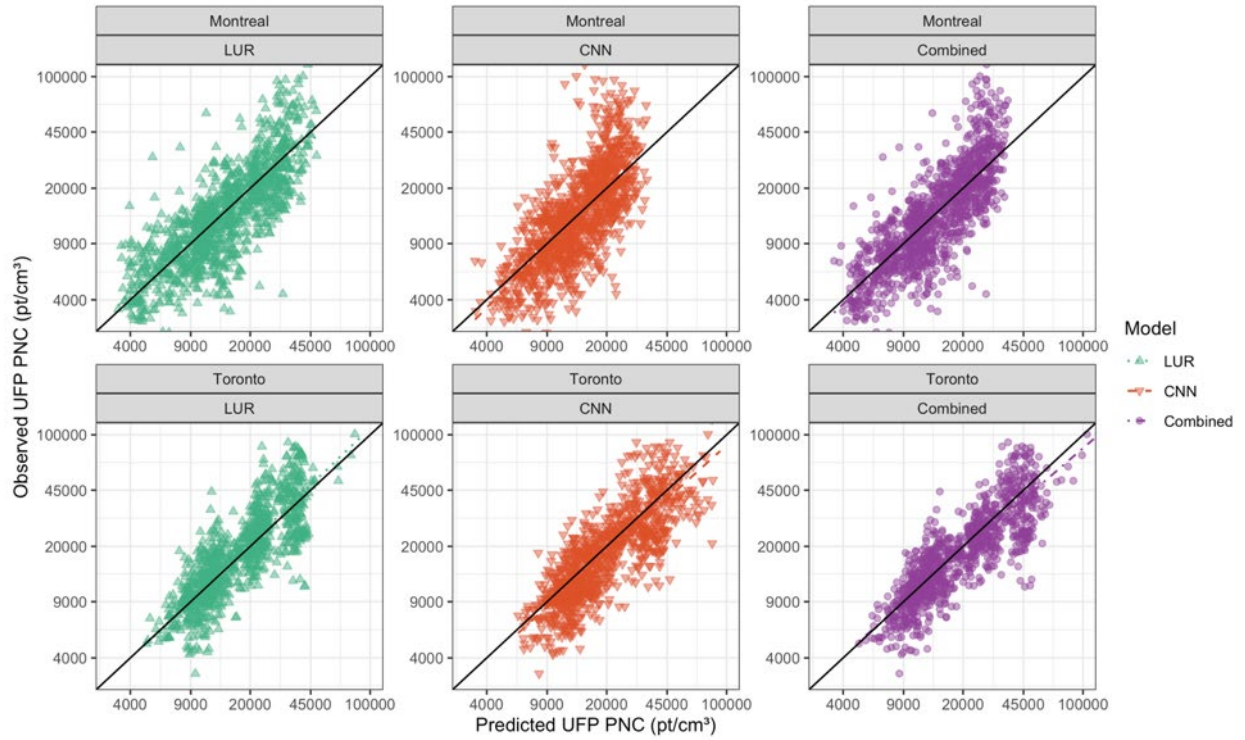


Figure A.23. Scatter plots of observed and predicted mean UFP size in the test set.
CNN = convolutional neural network; LUR = land use regression; UFP = ultrafine particles.

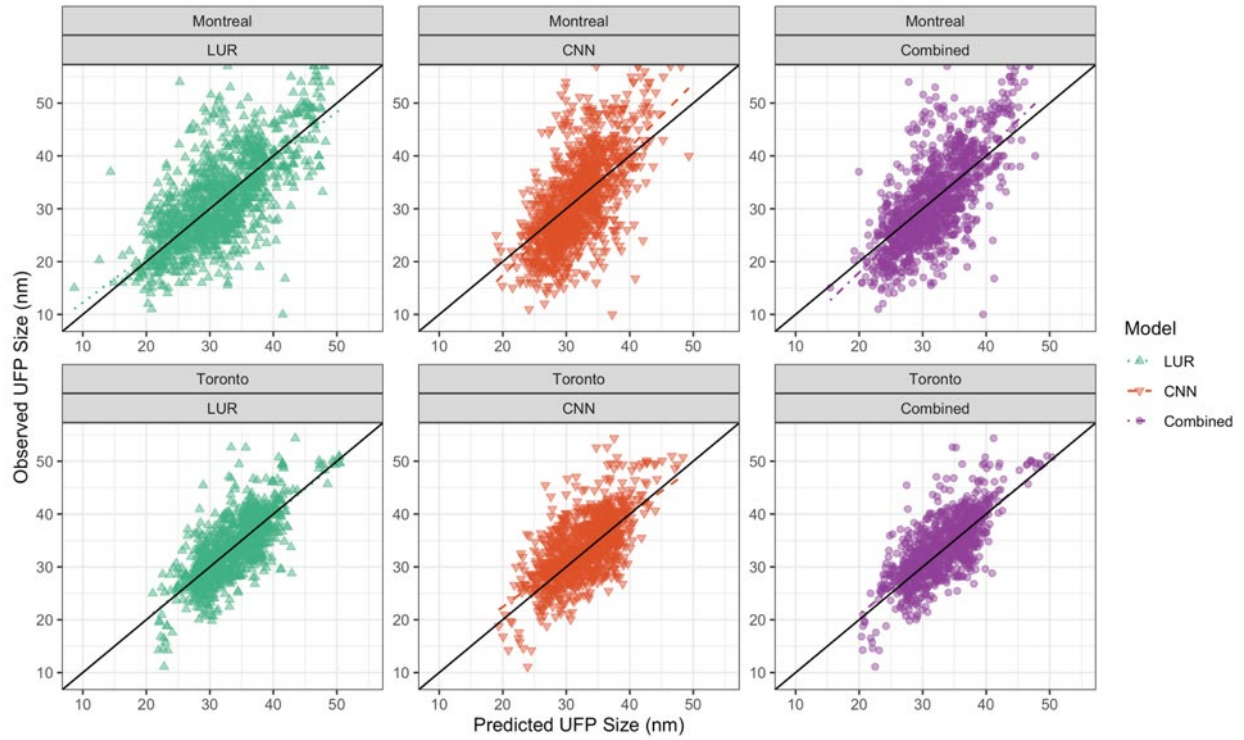


Figure A.24. Scatter plots of observed and predicted BC in the test set.
BC = black carbon; CNN = convolutional neural network; LUR = land use regression.

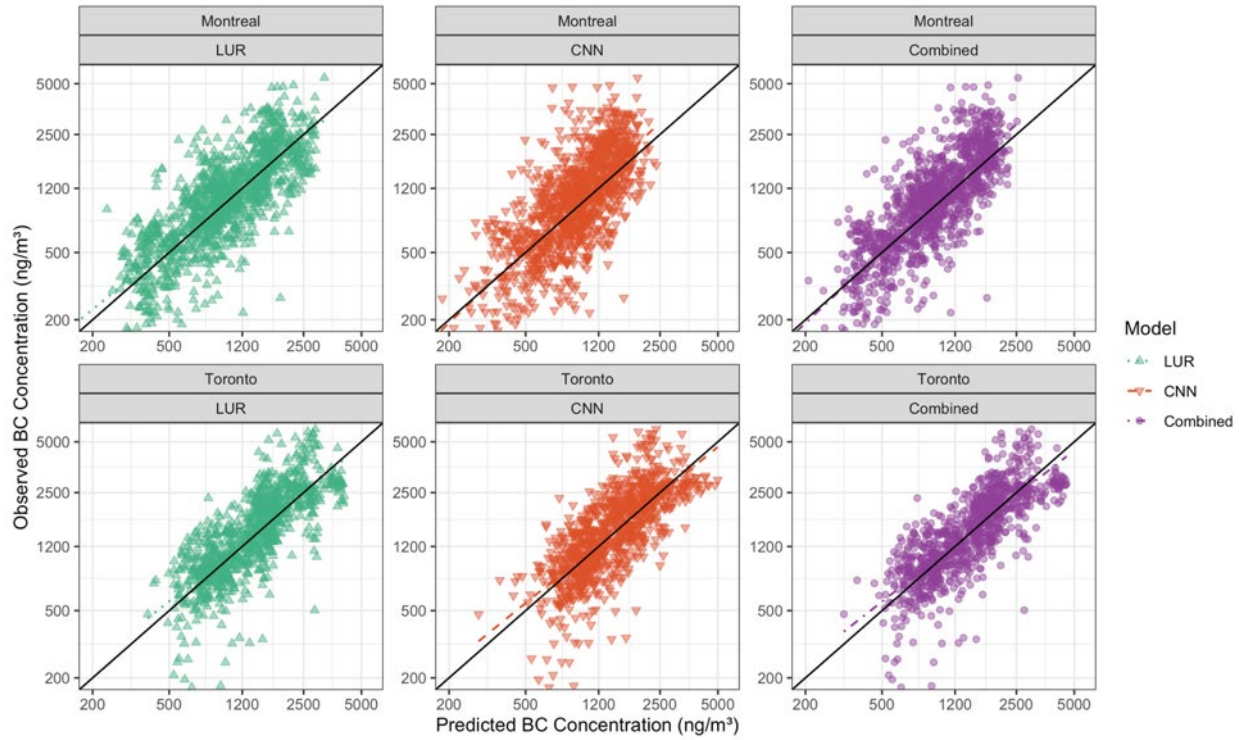


Figure A.25. Identifying the clusters of Toronto LUR UFP number concentration predictions in the test set. The colors indicate the LUR prediction clusters.

There was less distinct clustering in the CNN predictions, and the LUR prediction clusters are somewhat mixed in the CNN predictions. CNN = convolutional neural network; LUR = land use regression; UFP = ultrafine particles.

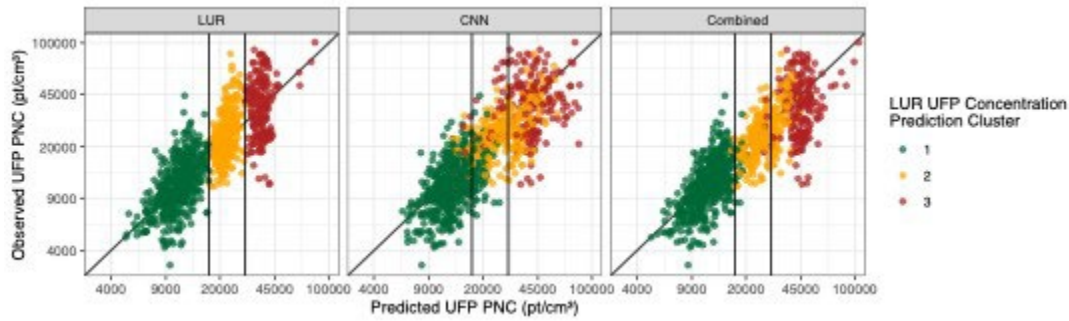


Figure A.26. Inspecting the Toronto LUR UFP number concentration prediction clusters in the test, train and validate sets.

The pronounced clustering with empty space between the clusters observed in the test set was not observed in the training set. The validate set appeared to have two instead of three clusters. This suggests that the clustering may be partially due to chance of the random data split as well as the spatial structure imposed on the data split. LUR = land use regression; UFP = ultrafine particles.

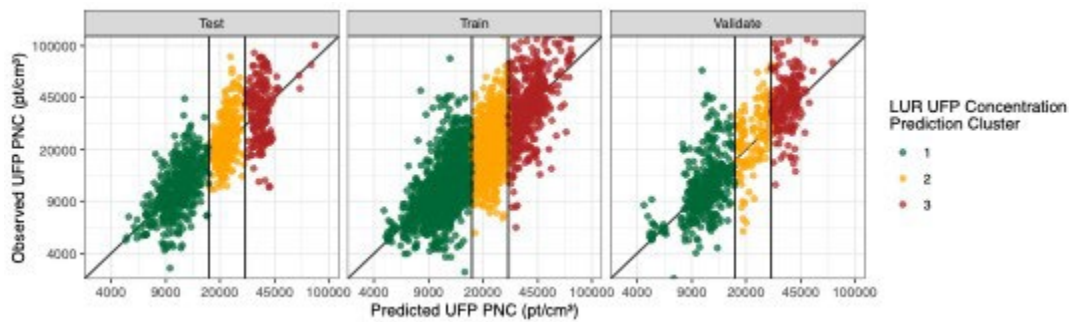


Figure A.27. Identifying the locations of the LUR UFP number concentration prediction clusters. The cluster colors are the same as in Figure A.26. The red clusters appear on major highways, especially near intersecting highways. The yellow cluster appears on or near highways and the green cluster is mostly off. LUR = land use regression; UFP = ultrafine particles.

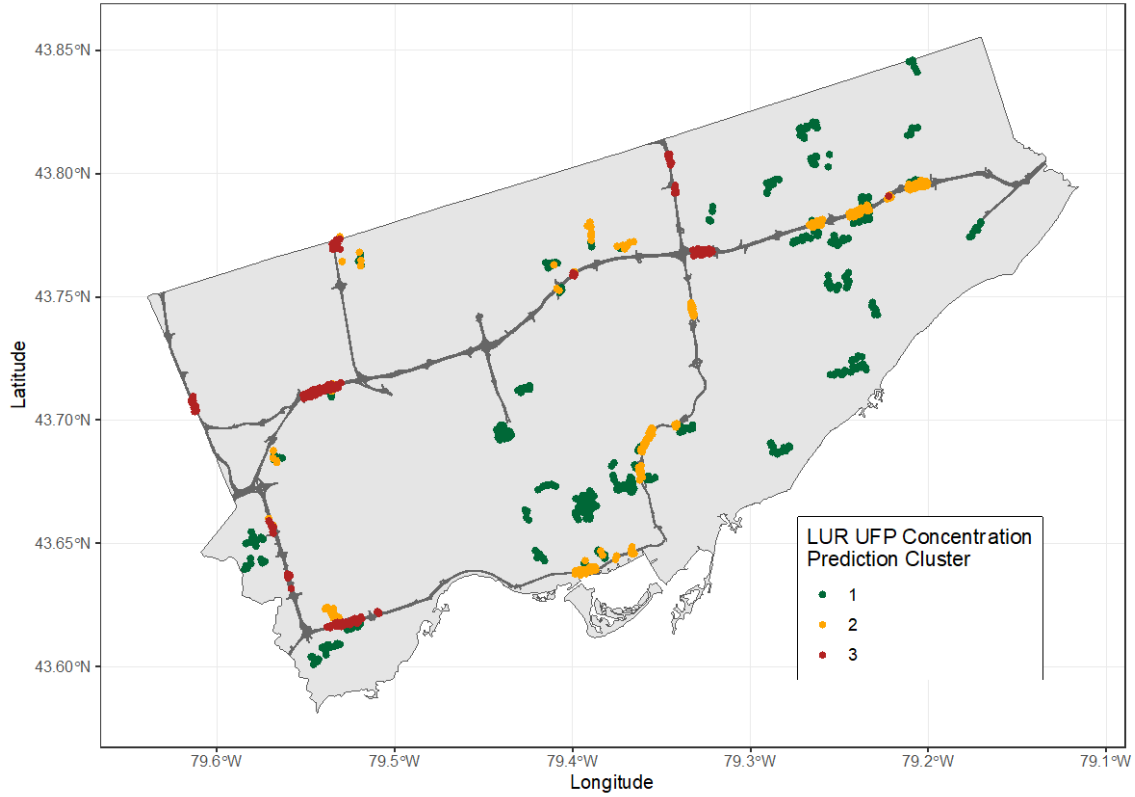


Figure A.28. Inspecting distributions of land use and traffic parameters stratified by LUR UFP number concentration prediction cluster.

These are the land use and traffic parameters in the Toronto UFP number concentration LUR. The average daily traffic NO_x emissions parameter is the most important variable in this model. Residential area may have also contributed to the observed clustering. LUR = land use regression; NO_x = nitrogen oxides; UFP = ultrafine particles.

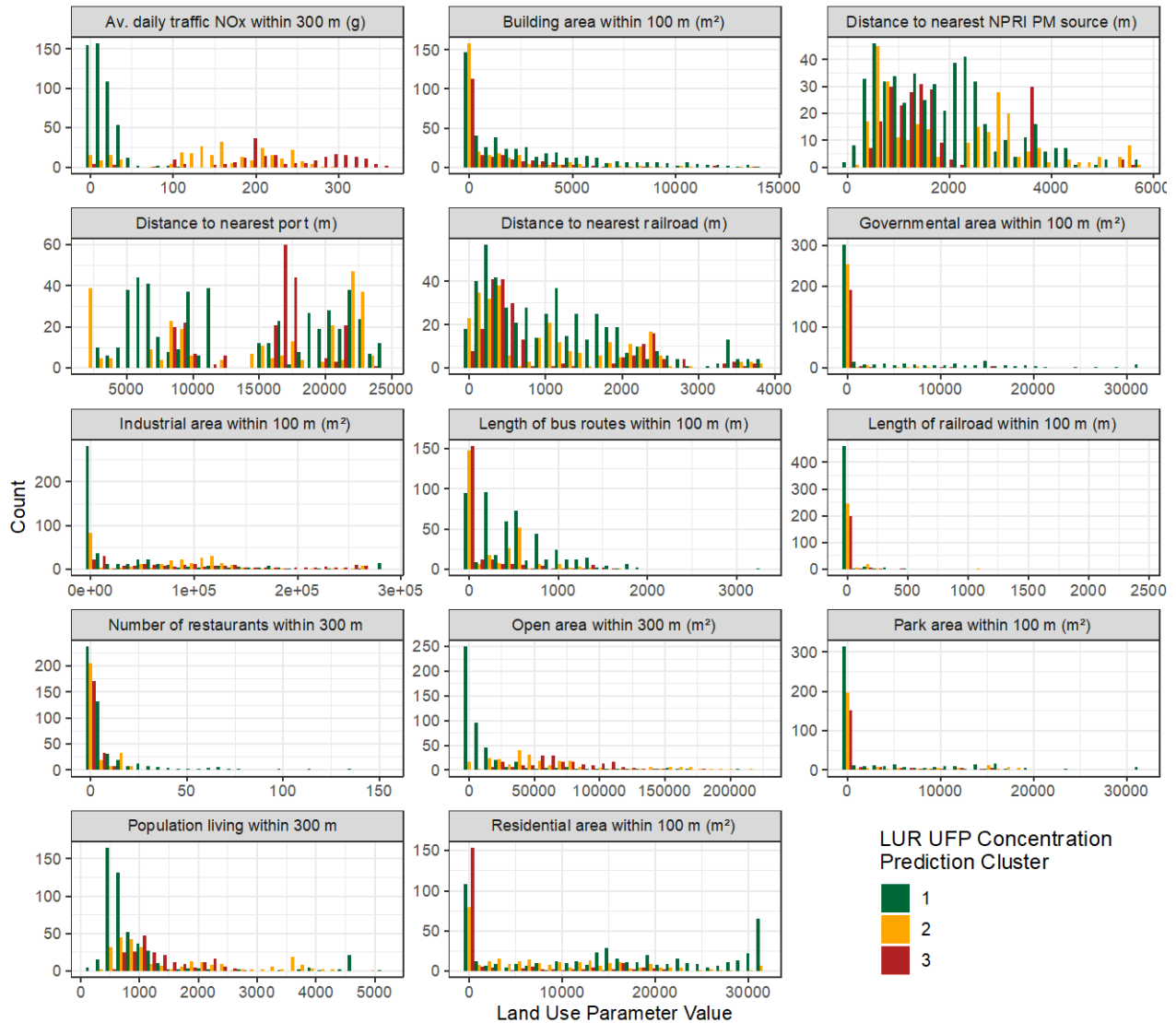


Figure A.29. Average daily traffic NO_x response curves in the Toronto BC and UFP number concentration LUR models.

The BC concentration-response curve flattens at very high levels of average daily traffic NO_x, which is likely why there was less pronounced clustering in the BC concentration prediction scatterplots. The response curve in the UFP number concentration model continues to increase at very elevated levels of average daily traffic NO_x, which was likely on major highways. BC = black carbon; GAM = generalized additive model; LUR = land use regression; NO_x = nitrogen oxides; UFP = ultrafine particles.

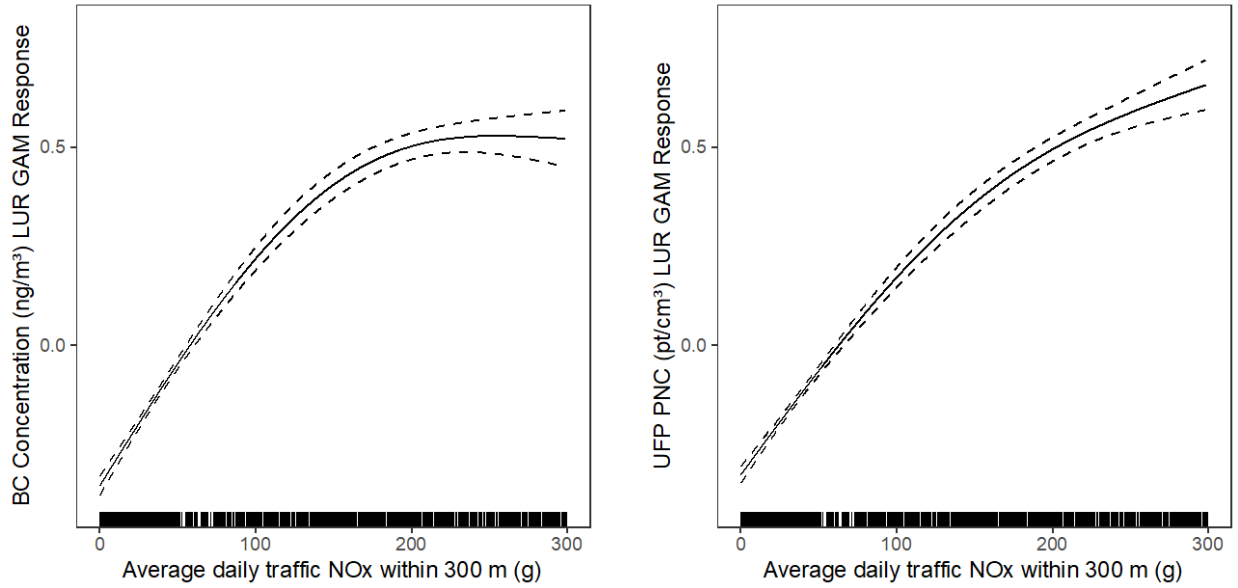


Figure A.30. Spatial distribution of UFP number concentrations model errors (scaled) in all data for the LUR, CNN, and combined models in Toronto and Montreal.

Purple lines are major highways. A small amount of jitter was added to the points to improve visibility of points. CNN = convolutional neural network; LUR = land use regression; UFP = ultrafine particles.

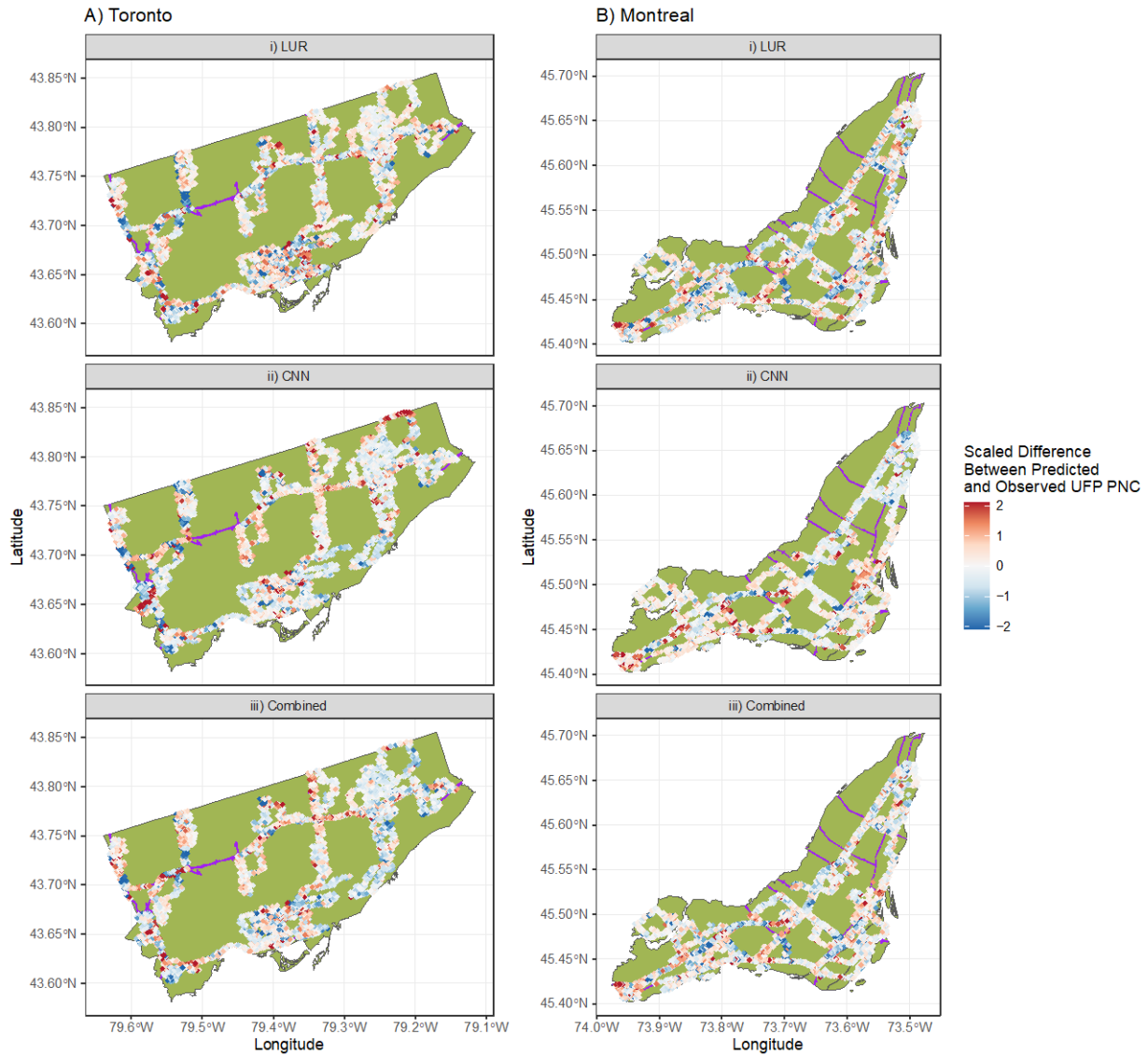


Figure A.31. Spatial distribution of UFP size model errors (scaled) in all data for the LUR, CNN, and combined models in Toronto and Montreal.

Purple lines are major highways. A small amount of jitter was added to the points to improve visibility of points. CNN = convolutional neural network; LUR = land use regression; UFP = ultrafine particles.

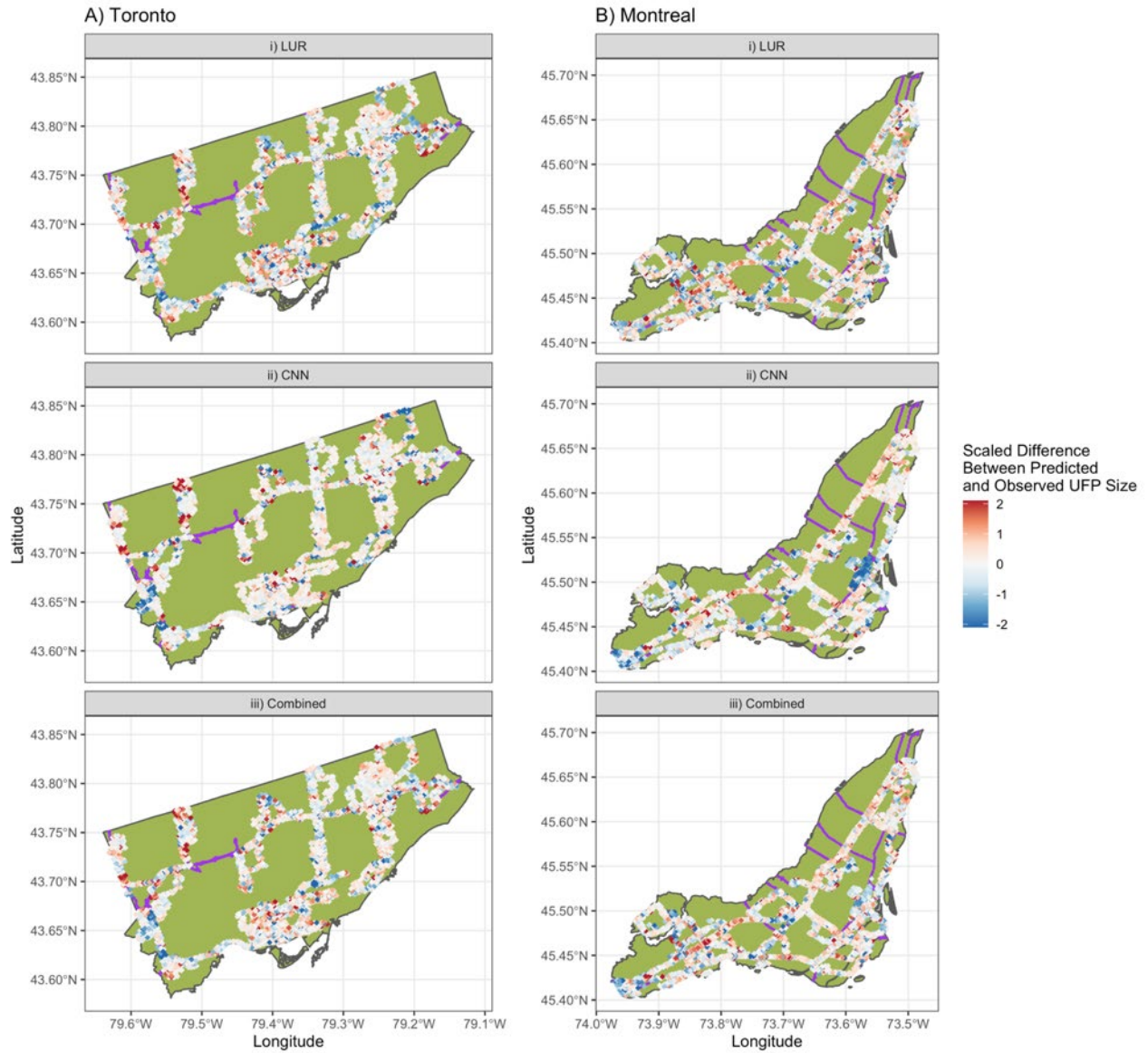


Figure A.32. Spatial distribution of BC model errors (scaled) in all data for the LUR, CNN, and combined models in Toronto and Montreal.

Purple lines are major highways. A small amount of jitter was added to the points to improve visibility of points. BC = black carbon; CNN = convolutional neural network.

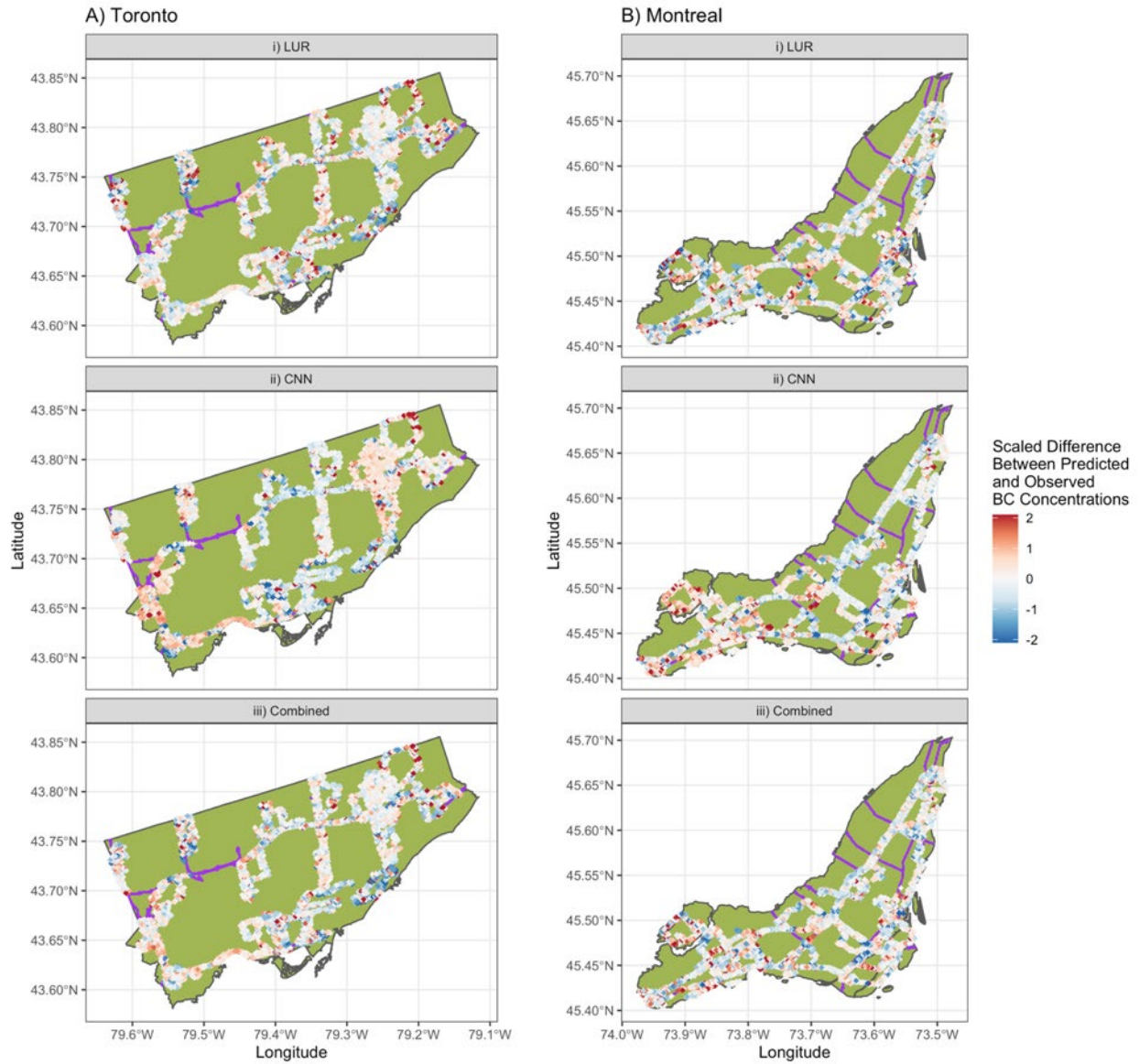


Figure A.33. Surfaces of scaled differences between predicted UFP number concentrations from LUR and CNN models in Toronto and Montreal.

Red indicates areas where the LUR predicted higher than the CNN, and blue indicates areas where the CNN predicted higher than the LUR. The color along major highways differs between the two cities, with the LUR predicting higher in Montreal and the CNN predicting higher in Toronto. CNN = convolutional neural network; LUR = land use regression; UFP = ultrafine particles.

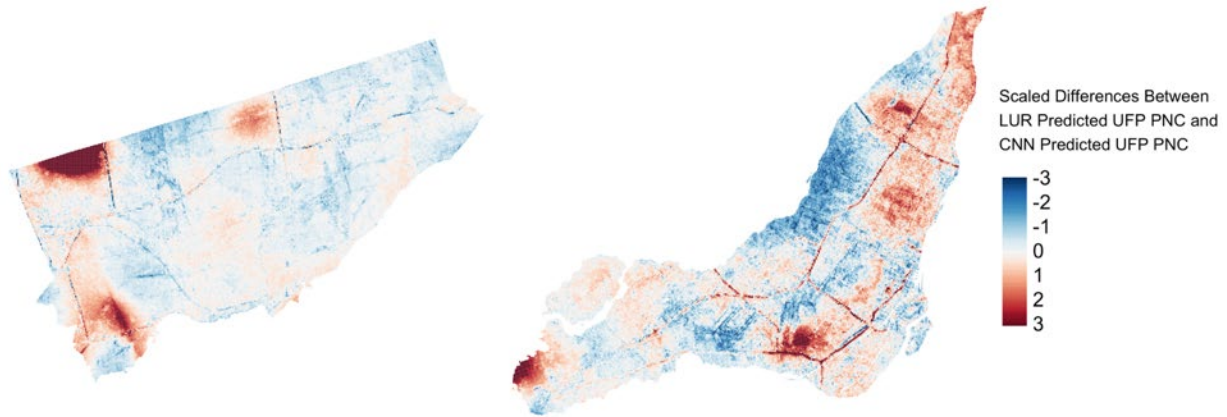


Figure A.34. Surfaces of scaled differences between predicted UFP size from LUR and CNN models in Toronto and Montreal.

Red indicates areas where the LUR predicted higher than the CNN, and blue indicates areas where the CNN predicted higher than the LUR. CNN = convolutional neural network; LUR = land use regression; UFP = ultrafine particles.

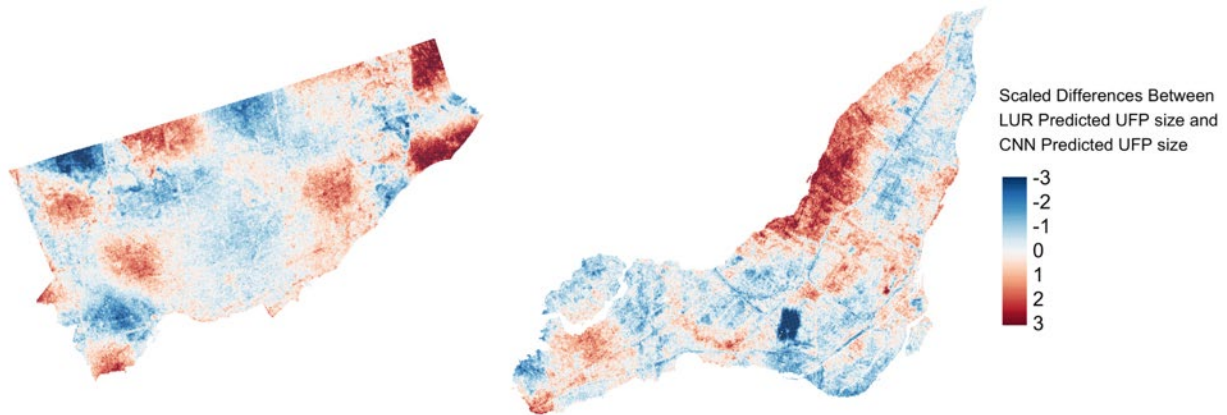


Figure A.35. Surfaces of scaled differences between predicted BC concentrations from LUR and CNN models in Toronto and Montreal.

Red indicates areas where the LUR predicted higher than the CNN, and blue indicates areas when the CNN predicted higher than the LUR. BC = black carbon; CNN = convolutional neural network; LUR = land use regression.

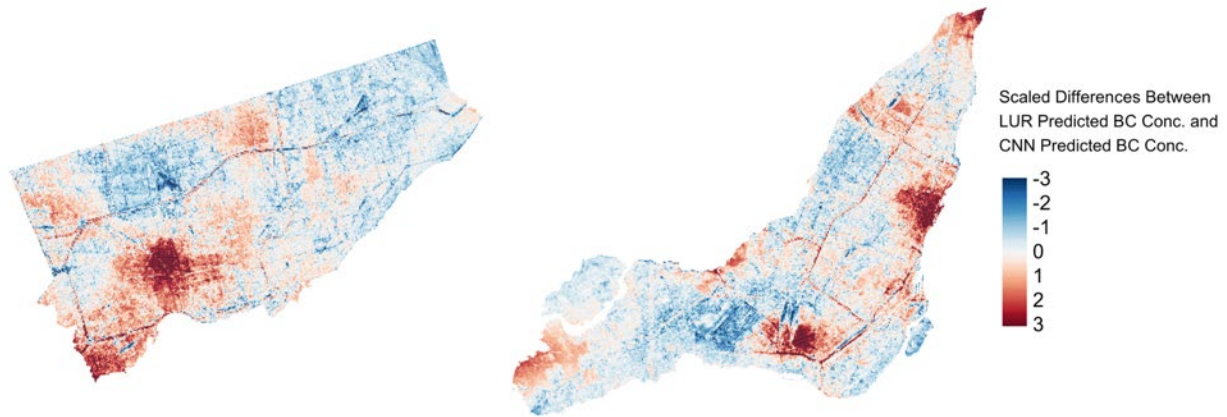


Figure A.36. Sensitivity analysis for UFP number concentrations prediction surfaces from LUR models trained without latitude and longitude for Toronto and Montreal.

LUR = land use regression; UFP = ultrafine particles.

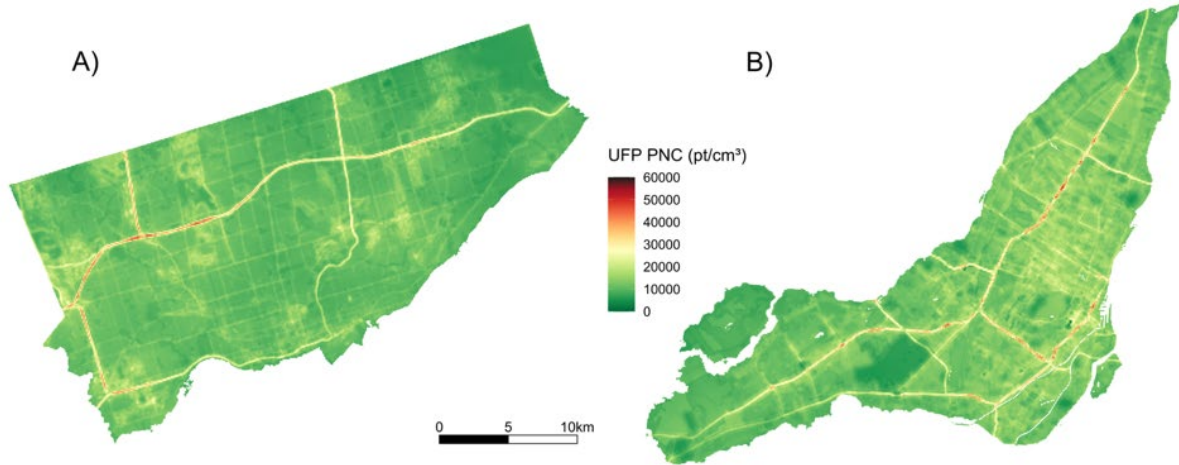


Figure A.37. Sensitivity analysis for UFP size prediction surfaces from LUR models trained without latitude and longitude for Toronto and Montreal.
LUR = land use regression; UFP = ultrafine particles.

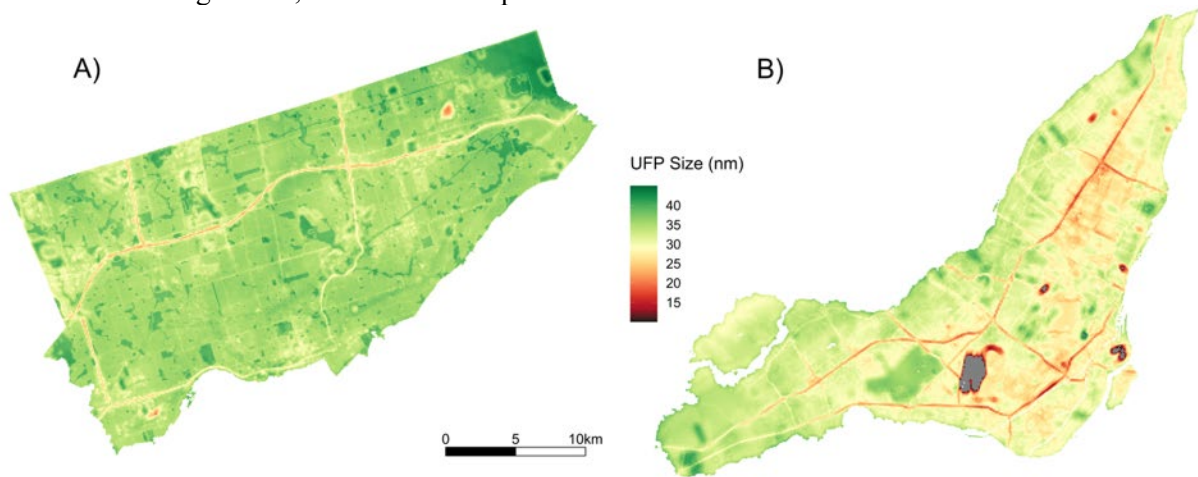


Figure A.38. Sensitivity analysis for BC prediction surfaces from LUR models trained without latitude and longitude for Toronto and Montreal.
BC = black carbon; LUR = land use regression.

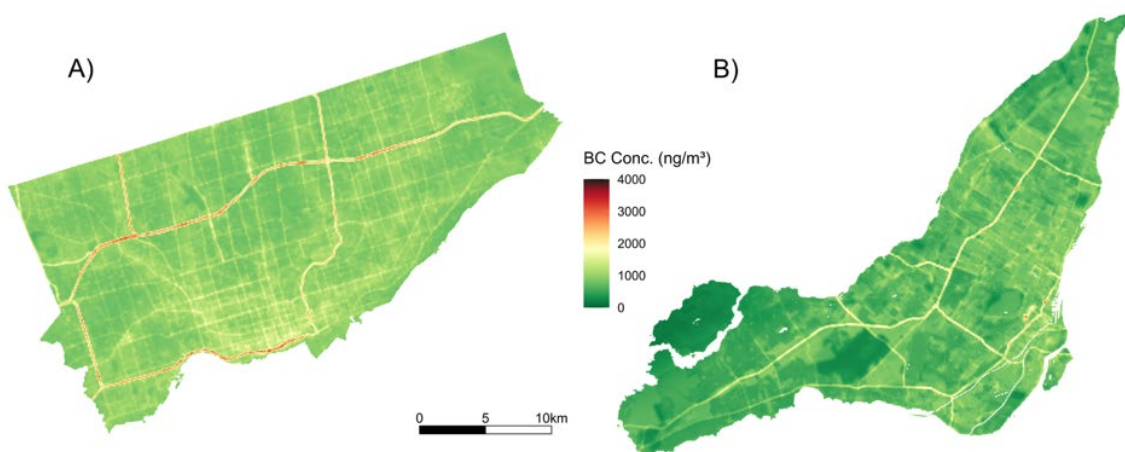





































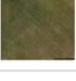



Figure A.39. CNN predictions for UFP number concentrations in Montreal for original and modified images.

Original images (A) have parts of images added (B) to produce modified images (C) with the expectation that the CNN prediction from the original image will become more similar to that of the added image after modification. CNN = convolutional neural network; LUR = land use regression; UFP = ultrafine particles.









| Example Number | A) Original Image | | | | B) Image to Add | | | | C) Modified Image | | |
|-------------------------------------------------------------|-------------------|----------|--------------------------------------|---------------------------------|-------------------------------------------------------------------------------------|---------------------------------|-------------------------------------------------------------------------------------|---------------------------------|--------------------------------------------------------------------------------------|---------------------------------|----------------------------|
| | Longitude | Latitude | Combined UFP Prediction ¹ | LUR UFP Prediction ¹ | Image | CNN UFP Prediction ¹ | Image | CNN UFP Prediction ¹ | Image | CNN UFP Prediction ¹ | CNN Behaviour ² |
| <i>Golf Course Near Railroad and Major Highway</i> | | | | | | | | | | | |
| 1 | -73.55828 | 45.62537 | 13269 | 21349 |  | 8214 |  | 34008 |  | 8710 | as expected |
| 2 | -73.55828 | 45.62537 | 13269 | 21349 |  | 8214 |  | 34008 |  | 28165 | as expected |
| 3 | -73.55828 | 45.62537 | 13269 | 21349 |  | 8214 |  | 35882 |  | 8107 | unexpected |
| 4 | -73.55828 | 45.62537 | 13269 | 21349 |  | 8214 |  | 35882 |  | 27701 | as expected |
| <i>Residential Area Near Main Rail Yard</i> | | | | | | | | | | | |
| 5 | -73.67662 | 45.46140 | 16032 | 23126 |  | 12674 |  | 19539 |  | 13066 | as expected |
| 6 | -73.67662 | 45.46140 | 16032 | 23126 |  | 12674 |  | 19539 |  | 15915 | as expected |
| 7 | -73.67662 | 45.46140 | 16032 | 23126 |  | 12674 |  | 19539 |  | 15258 | as expected |
| 8 | -73.67662 | 45.46140 | 16032 | 23126 |  | 12674 |  | 22234 |  | 14676 | as expected |
| <i>Residential and Agricultural Area Near Major Highway</i> | | | | | | | | | | | |
| 9 | -73.93498 | 45.42213 | 8829 | 9679 |  | 7935 |  | 25259 |  | 20647 | as expected |
| 10 | -73.93498 | 45.42213 | 8829 | 9679 |  | 7935 |  | 25259 |  | 10806 | unexpected |
| 11 | -73.93498 | 45.42213 | 8829 | 9679 |  | 7935 |  | 11410 |  | 7490 | as expected |
| 12 | -73.93309 | 45.42833 | 8730 | 8383 |  | 11410 |  | 25259 |  | 26485 | as expected |
| <i>Open Area Near Airport</i> | | | | | | | | | | | |
| 13 | -73.76786 | 45.46963 | 8898 | 8843 |  | 10590 |  | 16845 |  | 14079 | as expected |
| 14 | -73.76041 | 45.46745 | 7027 | 7281 |  | 6631 |  | 16845 |  | 14270 | as expected |

¹ (pt/cm³)

² Adding highways, industrial buildings, or railroads to images of residential or undeveloped areas was expected to increase the predicted concentrations. Adding undeveloped areas to residential areas was expected to reduce predicted concentrations.

Figure A.40. CNN predictions for BC in Montreal for original and modified images.

Original images (A) have parts of images added (B) to produce modified images (C) with the expectation that the CNN prediction from the original image will become more similar to that of the added image after modification. BC = black carbon; CNN = convolutional neural network; LUR = land use regression.

| Example Number | A) Original Image | | | | | B) Image to Add | | | C) Modified Image | | |
|-------------------------------------------------------------|-------------------|----------|-------------------------------------|--------------------------------|-------------------------------------------------------------------------------------|--------------------------------|---------------------------------------------------------------------------------------|--------------------------------|---------------------------------------------------------------------------------------|--------------------------------|----------------------------|
| | Longitude | Latitude | Combined BC Prediction ¹ | LUR BC Prediction ¹ | Image | CNN BC Prediction ¹ | Image | CNN BC Prediction ¹ | Image | CNN BC Prediction ¹ | CNN Behaviour ² |
| <i>Golf Course Near Railroad and Major Highway</i> | | | | | | | | | | | |
| 1 | -73.55828 | 45.62537 | 635 | 948 |  | 414 |  | 3324 |  | 446 | as expected |
| 2 | -73.55828 | 45.62537 | 635 | 948 |  | 414 |  | 3324 |  | 2190 | as expected |
| 3 | -73.55828 | 45.62537 | 635 | 948 |  | 414 |  | 1907 |  | 278 | unexpected |
| 4 | -73.55828 | 45.62537 | 635 | 948 |  | 414 |  | 1907 |  | 1109 | as expected |
| <i>Residential Area Near Main Rail Yard</i> | | | | | | | | | | | |
| 5 | -73.67662 | 45.46140 | 1202 | 1609 |  | 694 |  | 1700 |  | 678 | unexpected |
| 6 | -73.67662 | 45.46140 | 1202 | 1609 |  | 694 |  | 1700 |  | 1407 | as expected |
| 7 | -73.67662 | 45.46140 | 1202 | 1609 |  | 694 |  | 1700 |  | 1872 | as expected |
| 8 | -73.67662 | 45.46140 | 1202 | 1609 |  | 694 |  | 1838 |  | 1175 | as expected |
| <i>Residential and Agricultural Area Near Major Highway</i> | | | | | | | | | | | |
| 9 | -73.93498 | 45.42213 | 445 | 430 |  | 378 |  | 947 |  | 862 | as expected |
| 10 | -73.93498 | 45.42213 | 445 | 430 |  | 378 |  | 947 |  | 477 | unexpected |
| 11 | -73.93498 | 45.42213 | 445 | 430 |  | 378 |  | 437 |  | 614 | unexpected |
| 12 | -73.93309 | 45.42833 | 383 | 347 |  | 437 |  | 947 |  | 744 | as expected |
| <i>Open Area Near Airport</i> | | | | | | | | | | | |
| 13 | -73.76786 | 45.46963 | 365 | 354 |  | 425 |  | 783 |  | 706 | as expected |
| 14 | -73.76041 | 45.46745 | 314 | 256 |  | 365 |  | 783 |  | 708 | as expected |
















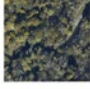





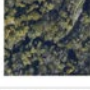


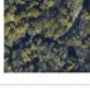








¹ (ng/m³)

² Adding highways, industrial buildings, or railroads to images of residential or undeveloped areas was expected to increase the predicted concentrations. Adding undeveloped areas to residential areas was expected to reduce predicted concentrations.

Figure A.41. CNN predictions for UFP number concentrations in Toronto for original and modified images.

Original images (A) have parts of images added (B) to produce modified images (C) with the expectation that the CNN prediction from the original image will become more similar to that of the added image after modification.

CNN = convolutional neural network; LUR = land use regression; UFP = ultrafine particles.



















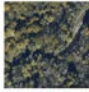


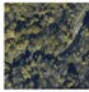


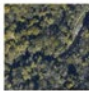


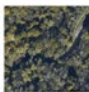





| Example Number | Original Image | | | Image to Add | | | Modified Image | | | | |
|------------------------------------------------------------------------|----------------|----------|--------------------------------------|---------------------------------|-------------------------------------------------------------------------------------|---------------------------------|--------------------------------------------------------------------------------------|---------------------------------|---------------------------------------------------------------------------------------|---------------------------------|----------------------------|
| | Longitude | Latitude | Combined UFP Prediction ¹ | LUR UFP Prediction ¹ | Image | CNN UFP Prediction ¹ | Image | CNN UFP Prediction ¹ | Image | CNN UFP Prediction ¹ | CNN Behaviour ² |
| <i>Residential Area Near Major Highway</i> | | | | | | | | | | | |
| 1 | -79.57036 | 43.66969 | 15221 | 17663 |  | 10703 |  | 34595 |  | 27470 | as expected |
| 2 | -79.57036 | 43.66969 | 15221 | 17663 |  | 10703 |  | 34595 |  | 17167 | as expected |
| <i>Residential Area Near Rail Yard and Forest</i> | | | | | | | | | | | |
| 3 | -79.26103 | 43.80808 | 7223 | 9585 |  | 6799 |  | 17711 |  | 10270 | as expected |
| 4 | -79.26103 | 43.80808 | 7223 | 9585 |  | 6799 |  | 17711 |  | 14910 | as expected |
| 5 | -79.26103 | 43.80808 | 7223 | 9585 |  | 6799 |  | 8318 |  | 6552 | as expected |
| <i>Riparian Park Near Major Road, Railroad, and School Parking Lot</i> | | | | | | | | | | | |
| 6 | -79.20411 | 43.75754 | 6419 | 9425 |  | 6140 |  | 18231 |  | 16107 | as expected |
| 7 | -79.20411 | 43.75754 | 6419 | 9425 |  | 6140 |  | 18231 |  | 9788 | as expected |
| 8 | -79.20411 | 43.75754 | 6419 | 9425 |  | 6140 |  | 18231 |  | 9576 | as expected |
| 9 | -79.20411 | 43.75754 | 6419 | 9425 |  | 6140 |  | 18231 |  | 14946 | as expected |
| 10 | -79.20411 | 43.75754 | 6419 | 9425 |  | 6140 |  | 18855 |  | 11004 | as expected |
| <i>Park with Dry Grass</i> | | | | | | | | | | | |
| 11 | -79.36191 | 43.72184 | 10495 | 10708 |  | 11032 |  | 12514 |  | 13391 | unexpected |

¹ (pt/cm³)

² Adding highways, industrial buildings, or railroads to images of residential or undeveloped areas was expected to increase the predicted concentrations. Adding undeveloped areas to residential areas was expected to reduce predicted concentrations. Combining two parks was not expected to change the prediction.

Figure A.42. CNN predictions for BC in Toronto for original and modified images.

Original images (A) have parts of images added (B) to produce modified images (C) with the expectation that the CNN prediction from the original image will become more similar to that of the added image after modification. BC = black carbon; CNN = convolutional neural network; LUR = land use regression.

| Example Number | Original Image | | Image to Add | | Modified Image | | | | | | |
|------------------------------------------------------------------------|----------------|----------|-------------------------------------|--------------------------------|-------------------------------------------------------------------------------------|--------------------------------|-------------------------------------------------------------------------------------|--------------------------------|---------------------------------------------------------------------------------------|--------------------------------|----------------------------|
| | Longitude | Latitude | Combined BC Prediction ¹ | LUR BC Prediction ¹ | Image | CNN BC Prediction ¹ | Image | CNN BC Prediction ¹ | Image | CNN BC Prediction ¹ | CNN Behaviour ² |
| <i>Residential Area Near Major Highway</i> | | | | | | | | | | | |
| 1 | -79.57036 | 43.66969 | 1064 | 1046 |  | 781 |  | 2751 |  | 1312 | as expected |
| 2 | -79.57036 | 43.66969 | 1064 | 1046 |  | 781 |  | 2751 |  | 1795 | as expected |
| <i>Residential Area Near Rail Yard and Forest</i> | | | | | | | | | | | |
| 3 | -79.26103 | 43.80808 | 791 | 766 |  | 665 |  | 932 |  | 503 | unexpected |
| 4 | -79.26103 | 43.80808 | 791 | 766 |  | 665 |  | 932 |  | 855 | as expected |
| 5 | -79.26103 | 43.80808 | 791 | 766 |  | 665 |  | 672 |  | 647 | as expected |
| <i>Riparian Park Near Major Road, Railroad, and School Parking Lot</i> | | | | | | | | | | | |
| 6 | -79.20411 | 43.75754 | 805 | 895 |  | 509 |  | 1275 |  | 1218 | as expected |
| 7 | -79.20411 | 43.75754 | 805 | 895 |  | 509 |  | 1275 |  | 778 | as expected |
| 8 | -79.20411 | 43.75754 | 805 | 895 |  | 509 |  | 1275 |  | 727 | as expected |
| 9 | -79.20411 | 43.75754 | 805 | 895 |  | 509 |  | 1275 |  | 1143 | as expected |
| 10 | -79.20411 | 43.75754 | 805 | 895 |  | 509 |  | 948 |  | 803 | as expected |
| <i>Park with Dry Grass</i> | | | | | | | | | | | |
| 11 | -79.36191 | 43.72184 | 1197 | 1084 |  | 986 |  | 1059 |  | 846 | unexpected |

¹ (ng/m³)

² Adding highways, industrial buildings, or railroads to images of residential or undeveloped areas was expected to increase the predicted concentrations. Adding undeveloped areas to residential areas was expected to reduce predicted concentrations. Combining two parks was not expected to change the prediction.

Figure A.43. Changes in CNN predictions for UFP number concentrations when using images of Sunnybrook Park in Toronto downloaded in December 2021 versus July 2022.



Google does not provide information on when a satellite image is captured, but it is clear that the Google Maps images were updated at some point in 2022. The updated images are greener than the images used to develop the CNN models. It appears that the greener images have fewer long and straight edges (i.e., boundaries between green and brown grass), which may explain the generally lower CNN predicted UFP PNC values. The CNN model may have learned to associate long straight edges (e.g., highways and railroads) with higher levels of pollution. CNN = convolutional neural network; LUR = land use regression; UFP = ultrafine particles.

| Example Number | Longitude | Latitude | Combined UFP Prediction [†] | LUR UFP Prediction [†] | Images Downloaded in 2021 | | Images Downloaded in 2022 | | Prediction Change |
|----------------|-----------|----------|--------------------------------------|---------------------------------|---------------------------|---------------------------------|---------------------------|---------------------------------|-------------------|
| | | | | | Image | CNN UFP Prediction [†] | Image | CNN UFP Prediction [†] | |
| 1 | -79.36191 | 43.72184 | 10495 | 10708 | | 11032 | | 9323 | -1709 |
| 2 | -79.36067 | 43.72184 | 12636 | 10623 | | 19292 | | 11980 | -7312 |
| 3 | -79.35943 | 43.72183 | 11498 | 10539 | | 12725 | | 12726 | 1 |
| 4 | -79.35819 | 43.72183 | 10844 | 10457 | | 11415 | | 12683 | 1268 |
| 5 | -79.35694 | 43.72183 | 10362 | 10429 | | 11671 | | 10725 | -946 |
| 6 | -79.35570 | 43.72183 | 11036 | 10408 | | 12176 | | 10618 | -1558 |
| 7 | -79.36439 | 43.72274 | 10551 | 10792 | | 11582 | | 10411 | -1171 |
| 8 | -79.36315 | 43.72274 | 11755 | 10941 | | 11527 | | 11026 | -501 |
| 9 | -79.36191 | 43.72274 | 10314 | 10847 | | 9786 | | 9427 | -359 |
| 10 | -79.36067 | 43.72274 | 11336 | 10519 | | 13873 | | 12438 | -1435 |
| 11 | -79.35942 | 43.72274 | 13262 | 10433 | | 12514 | | 11012 | -1502 |

[†] (pt/cm³)

Figure A.44. Changes in CNN predictions for BC when using images of Sunnybrook Park in Toronto downloaded in December 2021 versus July 2022.

BC = black carbon; CNN = convolutional neural network; LUR = land use regression.

| Example Number | Longitude | Latitude | Combined BC Prediction [†] | LUR BC Prediction [†] | Images Downloaded in 2021 | | Images Downloaded in 2022 | | CNN Difference |
|----------------|-----------|----------|-------------------------------------|--------------------------------|-------------------------------------------------------------------------------------|--------------------------------|---------------------------------------------------------------------------------------|--------------------------------|----------------|
| | | | | | Image | CNN BC Prediction [†] | Image | CNN BC Prediction [†] | |
| 1 | -79.36191 | 43.72184 | 1197 | 1084 |  | 986 |  | 888 | -98 |
| 2 | -79.36067 | 43.72184 | 1158 | 1071 |  | 959 |  | 631 | -328 |
| 3 | -79.35943 | 43.72183 | 1150 | 1063 |  | 890 |  | 695 | -195 |
| 4 | -79.35819 | 43.72183 | 1109 | 1043 |  | 768 |  | 743 | -25 |
| 5 | -79.35694 | 43.72183 | 1124 | 1033 |  | 974 |  | 719 | -255 |
| 6 | -79.35570 | 43.72183 | 1035 | 1016 |  | 764 |  | 1001 | 237 |
| 7 | -79.36439 | 43.72274 | 1006 | 1088 |  | 623 |  | 532 | -91 |
| 8 | -79.36315 | 43.72274 | 787 | 1063 |  | 210 |  | 358 | 148 |
| 9 | -79.36191 | 43.72274 | 999 | 1039 |  | 768 |  | 744 | -24 |
| 10 | -79.36067 | 43.72274 | 1123 | 1039 |  | 807 |  | 670 | -137 |
| 11 | -79.35942 | 43.72274 | 1053 | 1026 |  | 1059 |  | 579 | -480 |

[†] (ng/m3)

Figure A.45. Mobility-weighted combined models for UFP number concentrations in Toronto and Montreal using neighborhood-level survey data from various years.
The unweighted surfaces are shown in the last row as a reference. UFP = ultrafine particles.

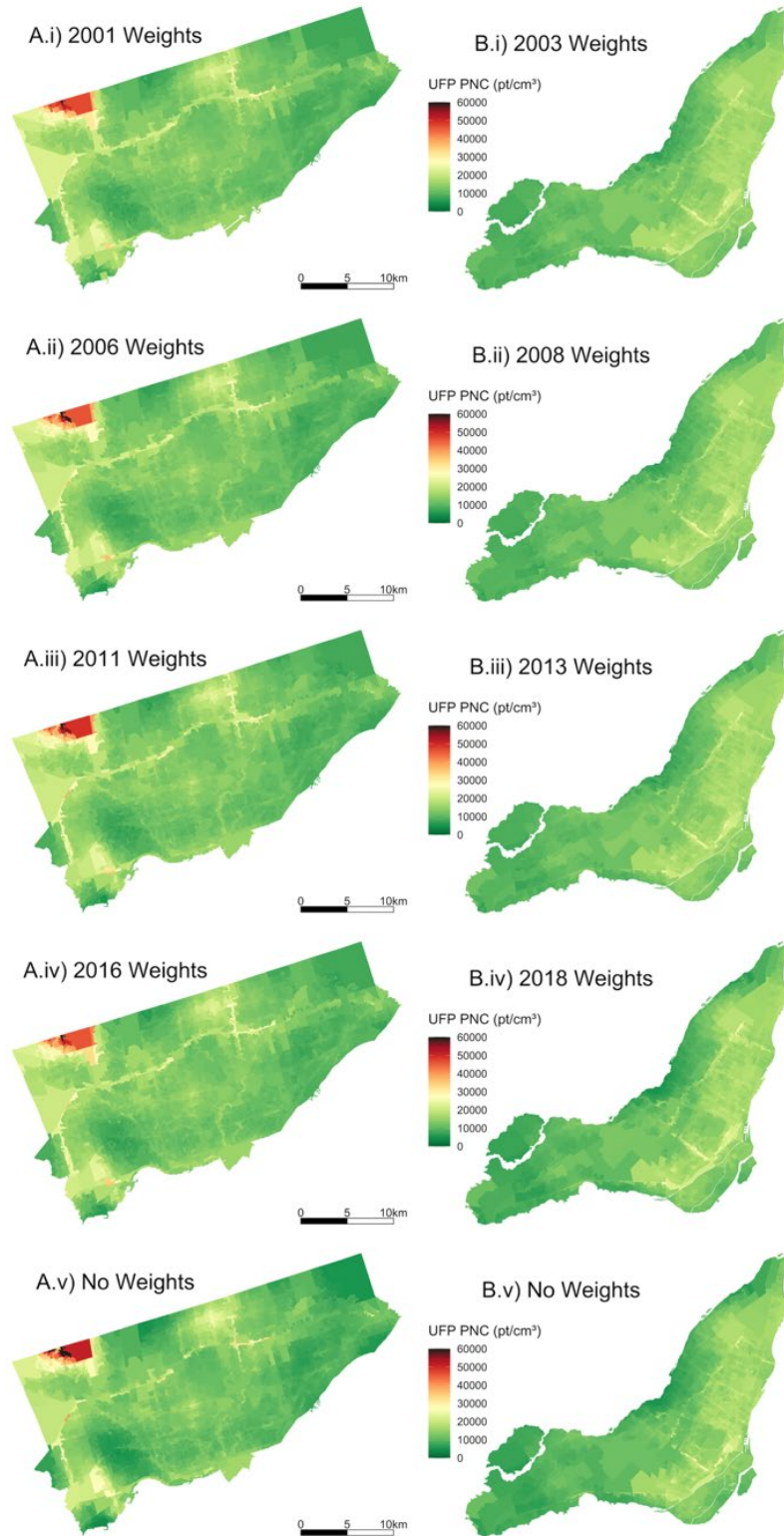


Figure A.46. Mobility-weighted combined models for UFP size in Toronto and Montreal using neighborhood-level survey data from various years.

The unweighted surfaces are shown in the last row as a reference. UFP = ultrafine particles.

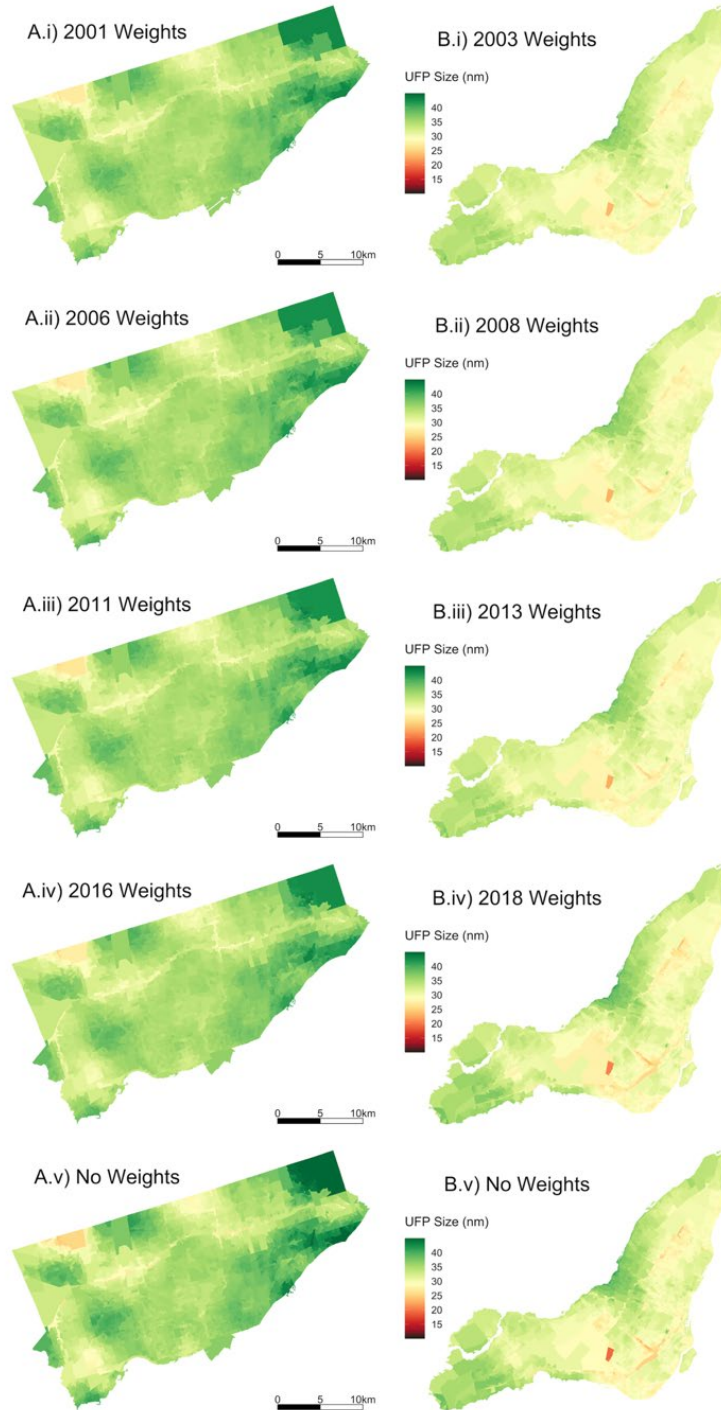


Figure A.47. Mobility-weighted combined models for BC in Toronto and Montreal using neighborhood-level survey data from various years.

The unweighted surfaces are shown in the last row as a reference. BC = black carbon.

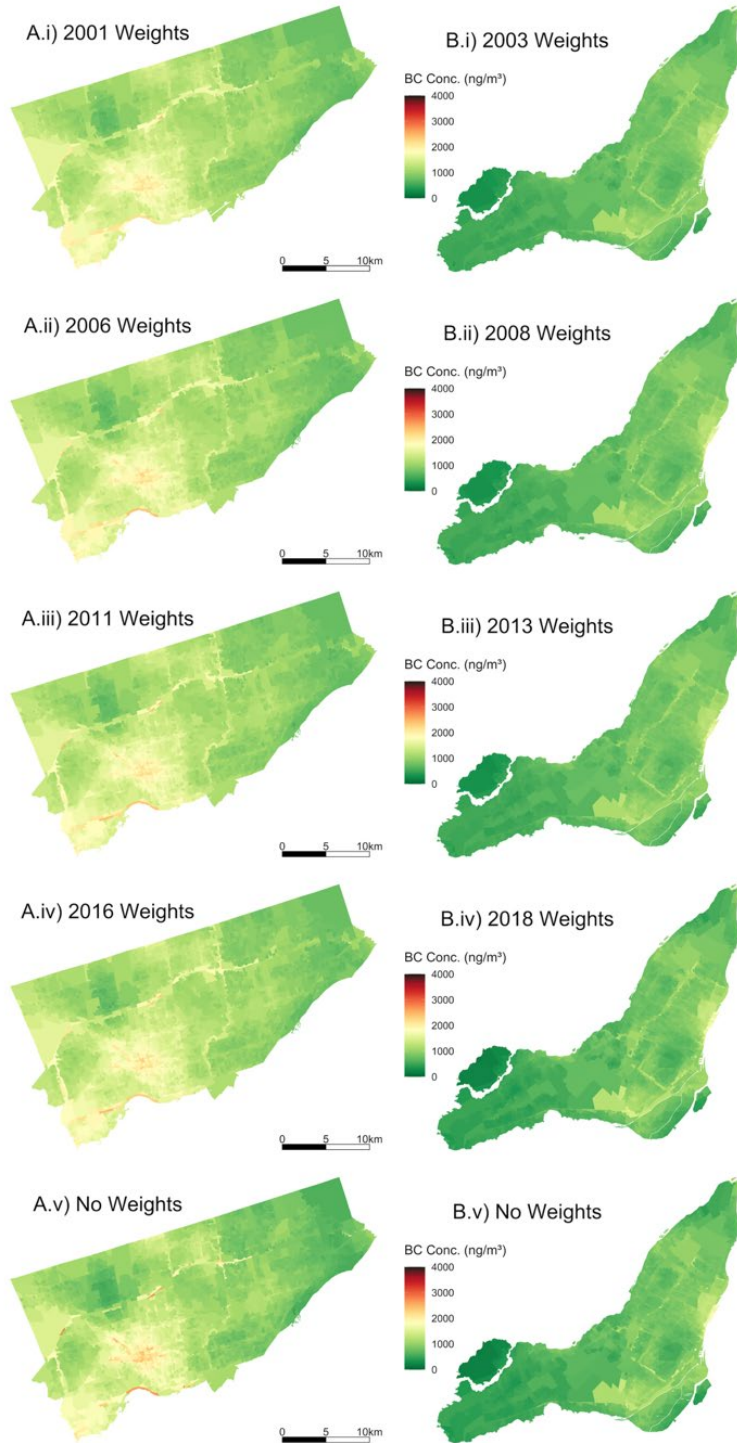


Figure A.48. Change in Toronto combined model UFP number concentrations predictions after applying 2006 and 2016 mobility weights.

Neighborhood border color indicates the neighborhood’s UFP number concentration tertile prior to mobility weighting. Neighborhood area color indicates the change in neighborhood UFP PNC after applying mobility weights. Smoothing can be seen where neighborhoods with green borders and red areas initially had low concentrations that increased after applying mobility weights, and vice versa for neighborhoods with orange borders with green areas. UFP = ultrafine particles.

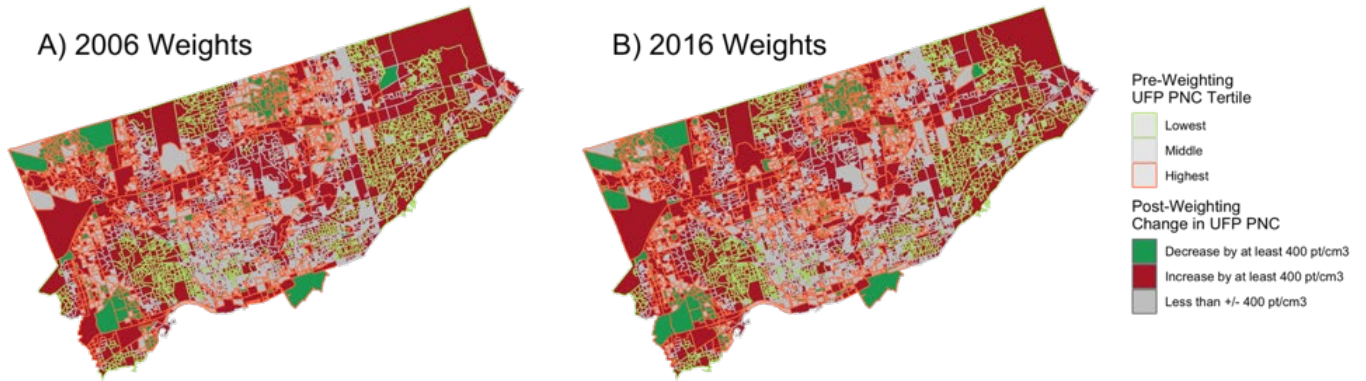


Figure A.49. Change in Toronto combined model BC concentration predictions after applying 2006 and 2016 mobility weights.

Neighborhood border color indicates the neighborhood’s BC concentration tertile prior to mobility weighting. Neighborhood area color indicates the change in neighborhood UFP number concentration after applying mobility weights. Smoothing can be seen where neighborhoods with green borders and red areas initially had low concentrations that increased after applying mobility weights, and vice versa for neighborhoods with orange borders with green areas. BC = black carbon; UFP = ultrafine particles.

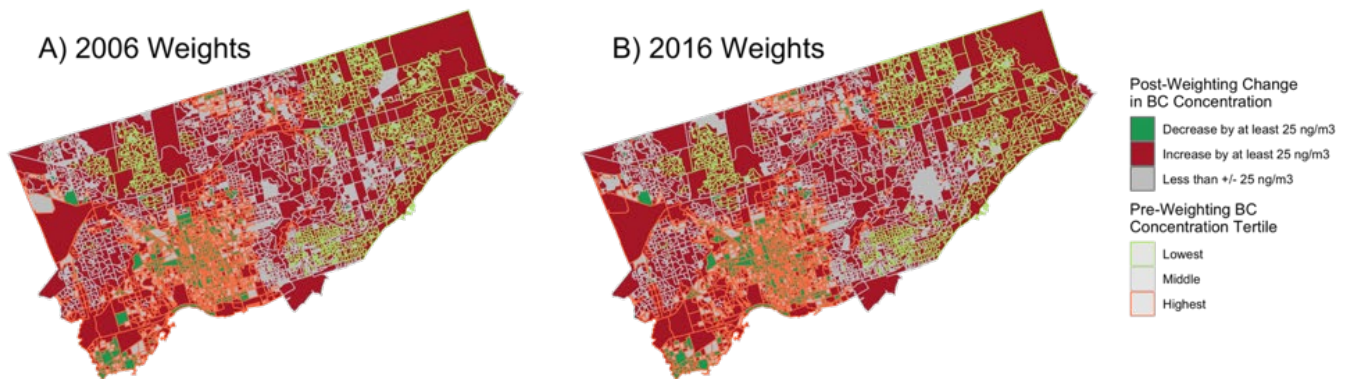


Figure A.50. Change in Montreal combined model UFP number concentration predictions after applying 2003 and 2018 mobility weights.

Neighborhood border color indicates the neighborhood’s UFP number concentrations tertile prior to mobility weighting. Neighborhood area color indicates the change in neighborhood UFP PNC after applying mobility weights. Smoothing can be seen where neighborhoods with green borders and red areas initially had low concentrations that increased after applying mobility weights, and vice versa for neighborhoods with orange borders with green areas. The use of 2003 versus 2018 weights resulted in different degrees of smoothing.

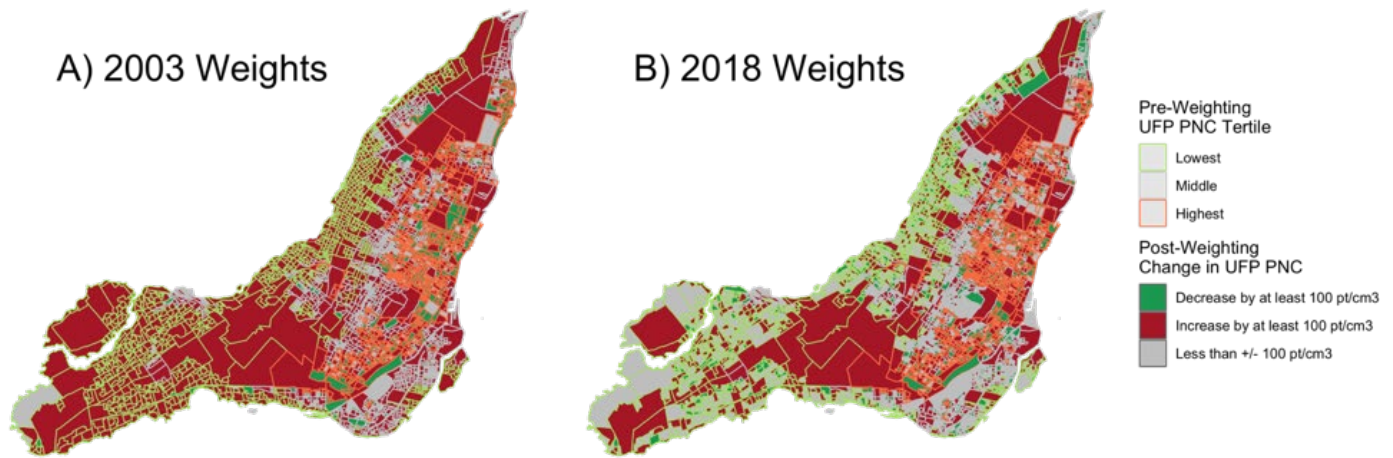


Figure A.51. Change in Montreal combined model BC predictions after applying 2003 and 2018 mobility weights.

Neighborhood border color indicates the neighborhood’s BC concentration tertile prior to mobility weighting. Neighborhood area color indicates the change in neighborhood BC concentration after applying mobility weights. Smoothing can be seen where neighborhoods with green borders and red areas initially had low concentrations that increased after applying mobility weights, and vice versa for neighborhoods with orange borders with green areas. The use of 2003 versus 2018 weights resulted in different degrees of smoothing. BC = black carbon.

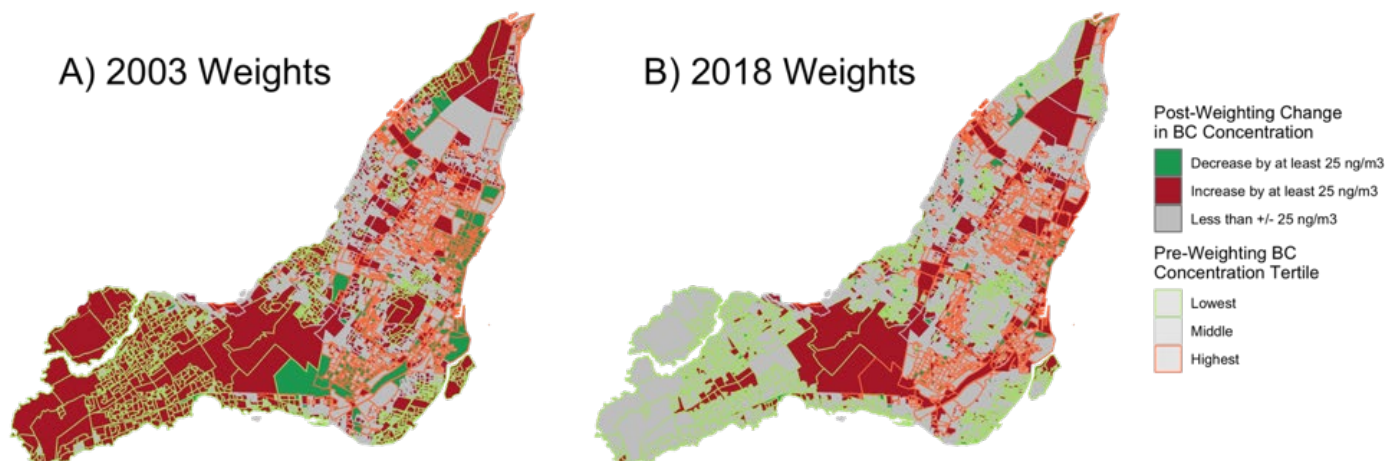


Figure A.52. Toronto combined model UFP number concentrations surfaces backcasted to various years.

LUR predictions using available historical traffic data were incorporated into the combined model. LUR = land use regression; UFP = ultrafine particles.

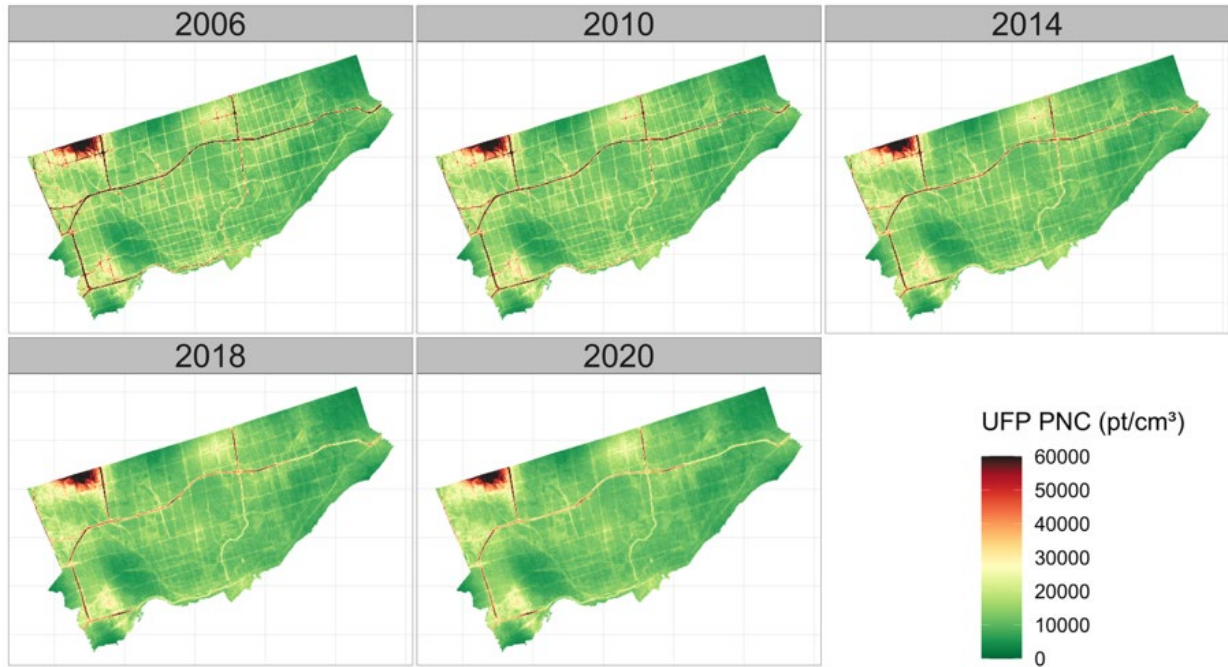


Figure A.53. Toronto combined model UFP size surfaces backcasted to various years.

LUR predictions using available historical traffic data were incorporated into the combined model. The higher historical traffic emissions resulted in smaller predicted UFP size along roads. LUR = land use regression; UFP = ultrafine particles.

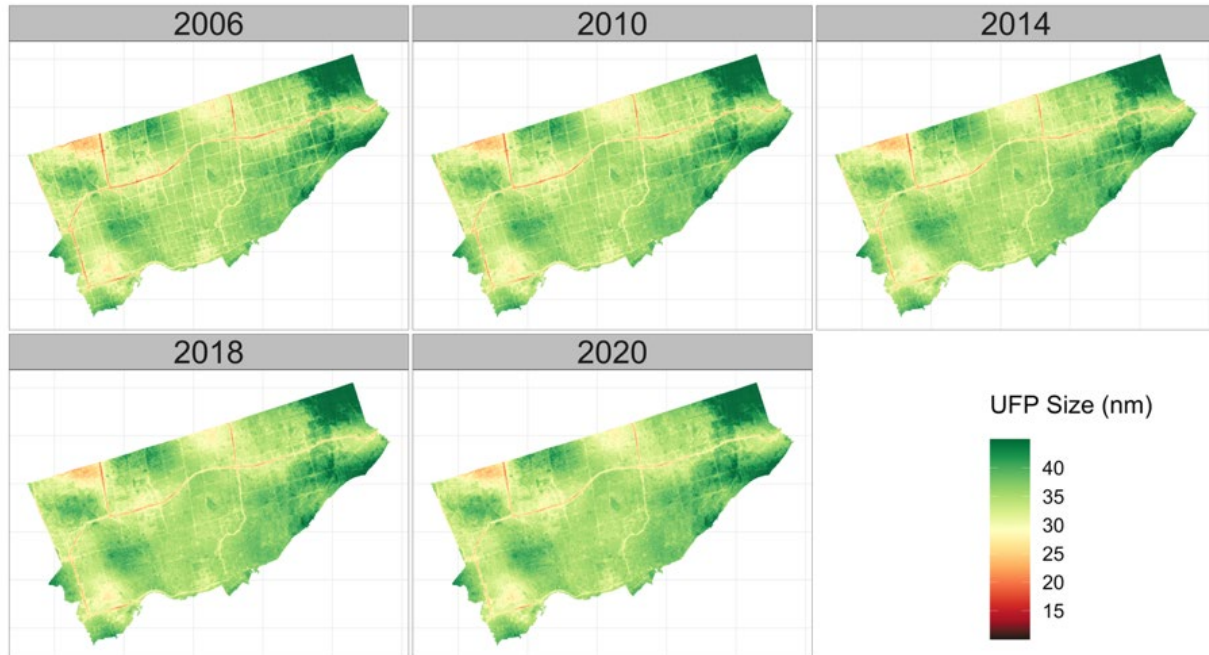


Figure A.54. Toronto combined model BC surfaces backcasted to various years.

LUR predictions using available historical traffic data were incorporated into the combined model. BC = black carbon; LUR = land use regression.

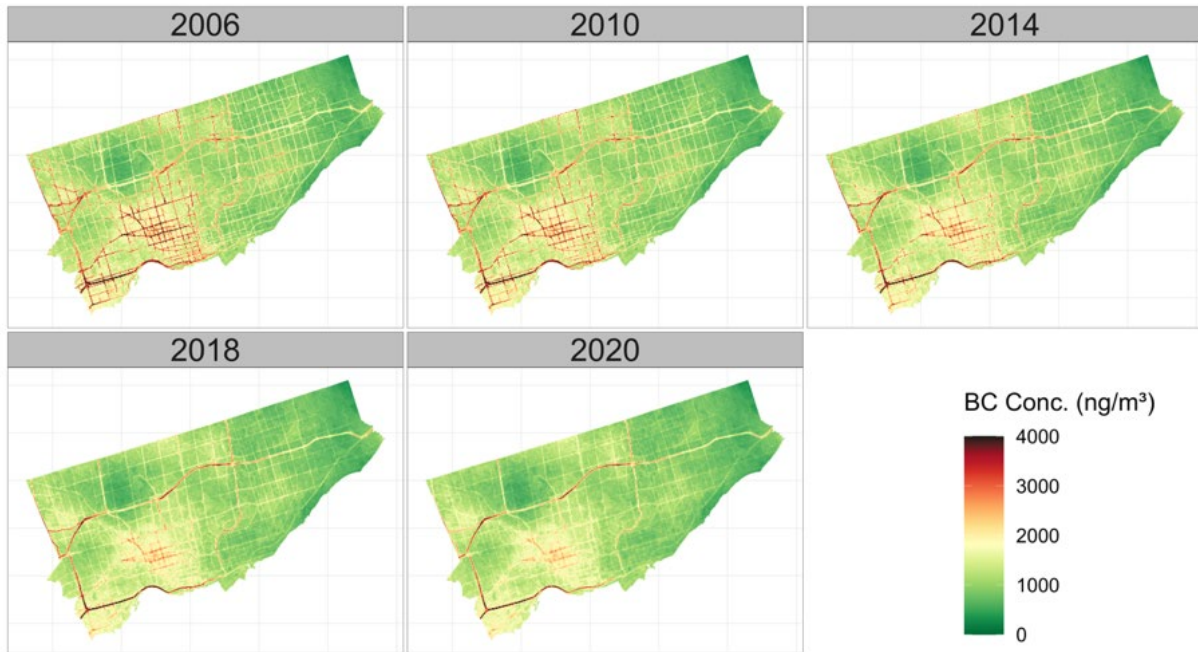


Figure A.55. Montreal combined model UFP number concentration surfaces backcasted to various years.

LUR predictions using available historical traffic data were incorporated into the combined model. LUR = land use regression; UFP = ultrafine particles.

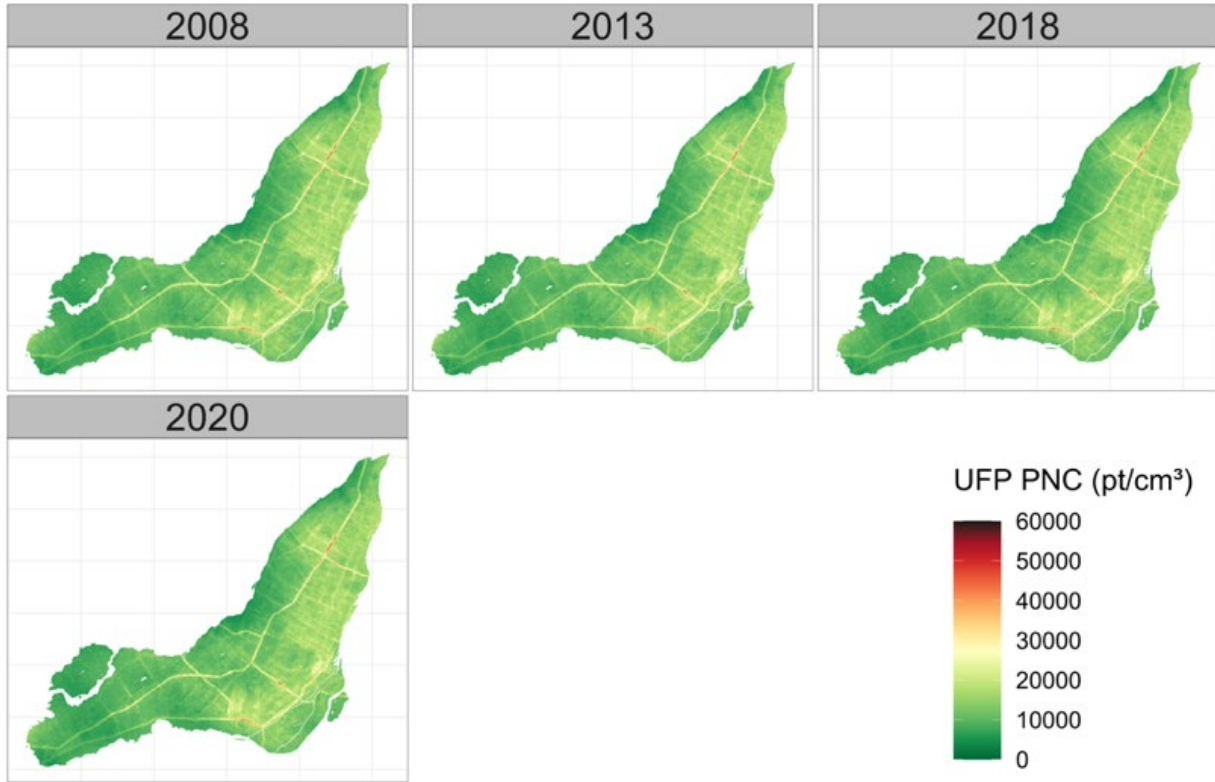


Figure A.56. Montreal combined model UFP size surfaces backcasted to various years.
LUR predictions using available historical traffic data were incorporated into the combined model. LUR = land use regression; UFP = ultrafine particles.

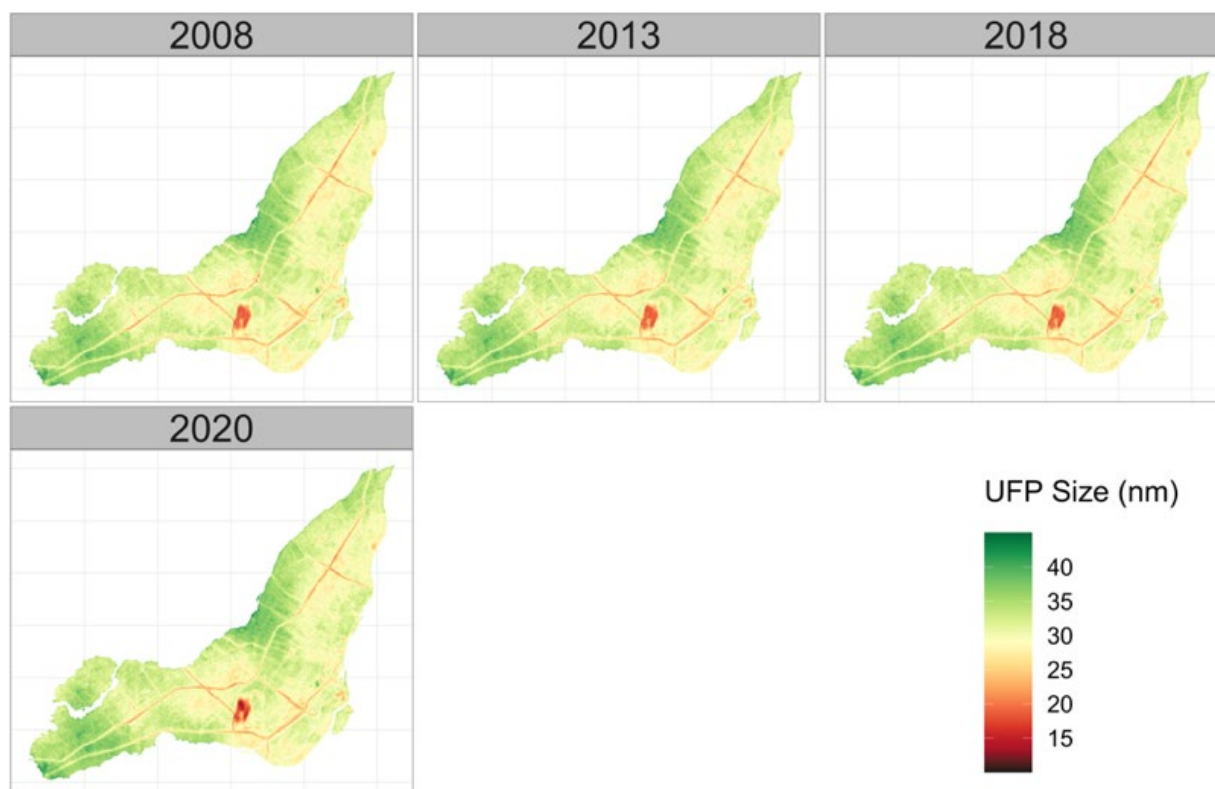


Figure A.57. Montreal combined model BC surfaces backcasted to various years.

LUR predictions using available historical traffic data were incorporated into the combined model. BC = black carbon; LUR = land use regression.

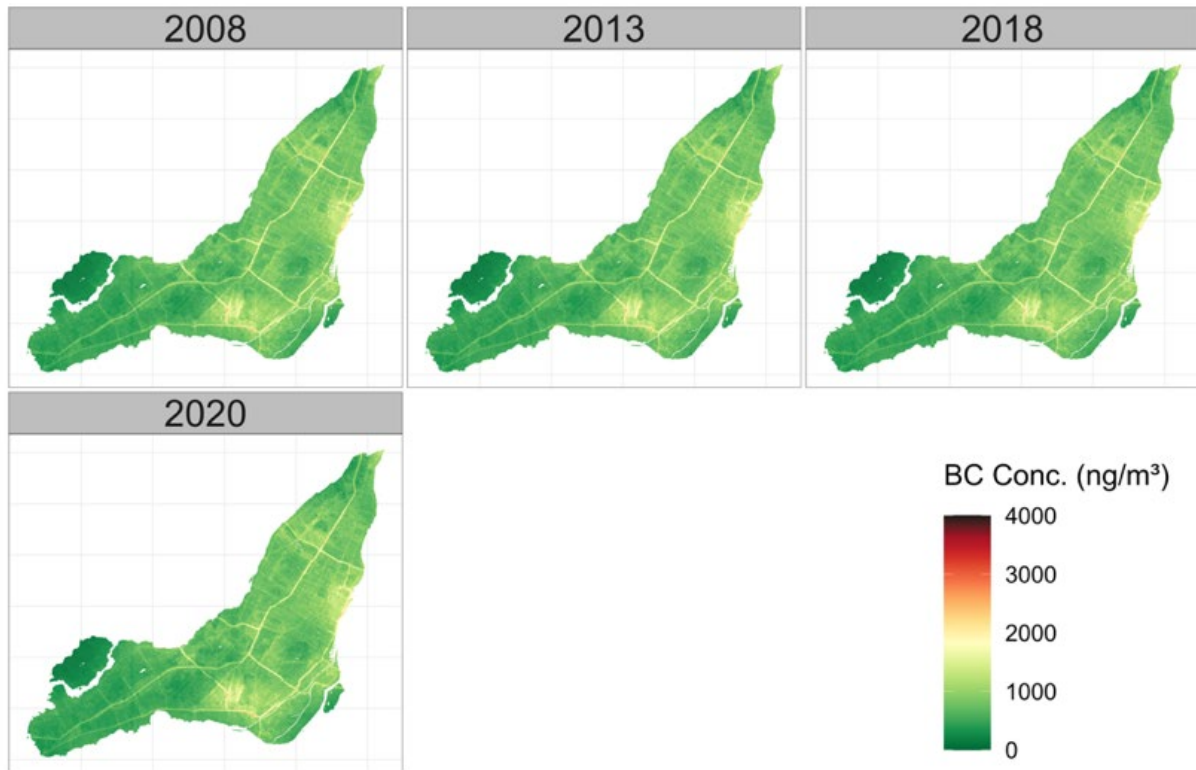


Figure A.58. Concentration-response curves of outdoor BC and mortality outcomes.
BC = black carbon.

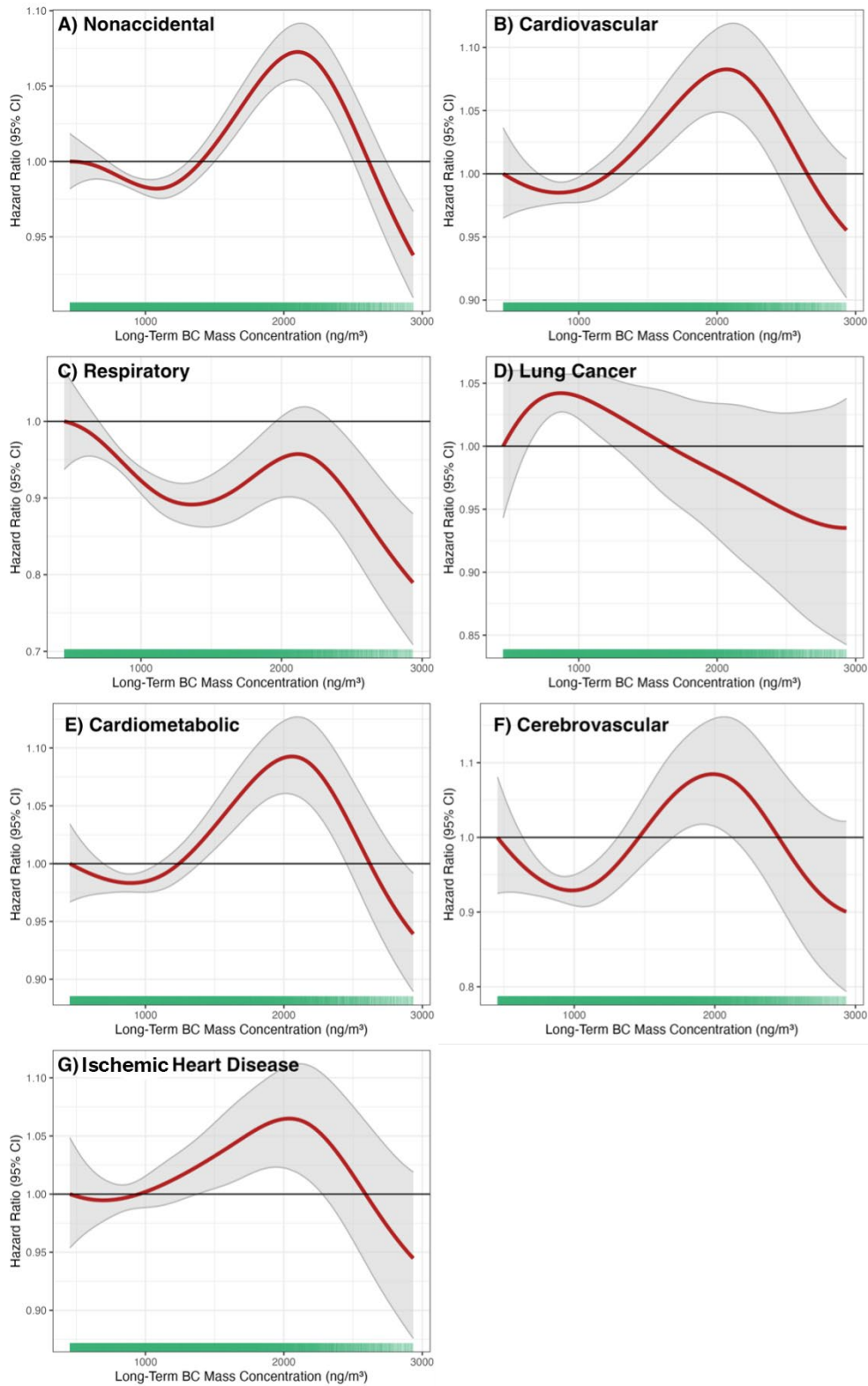
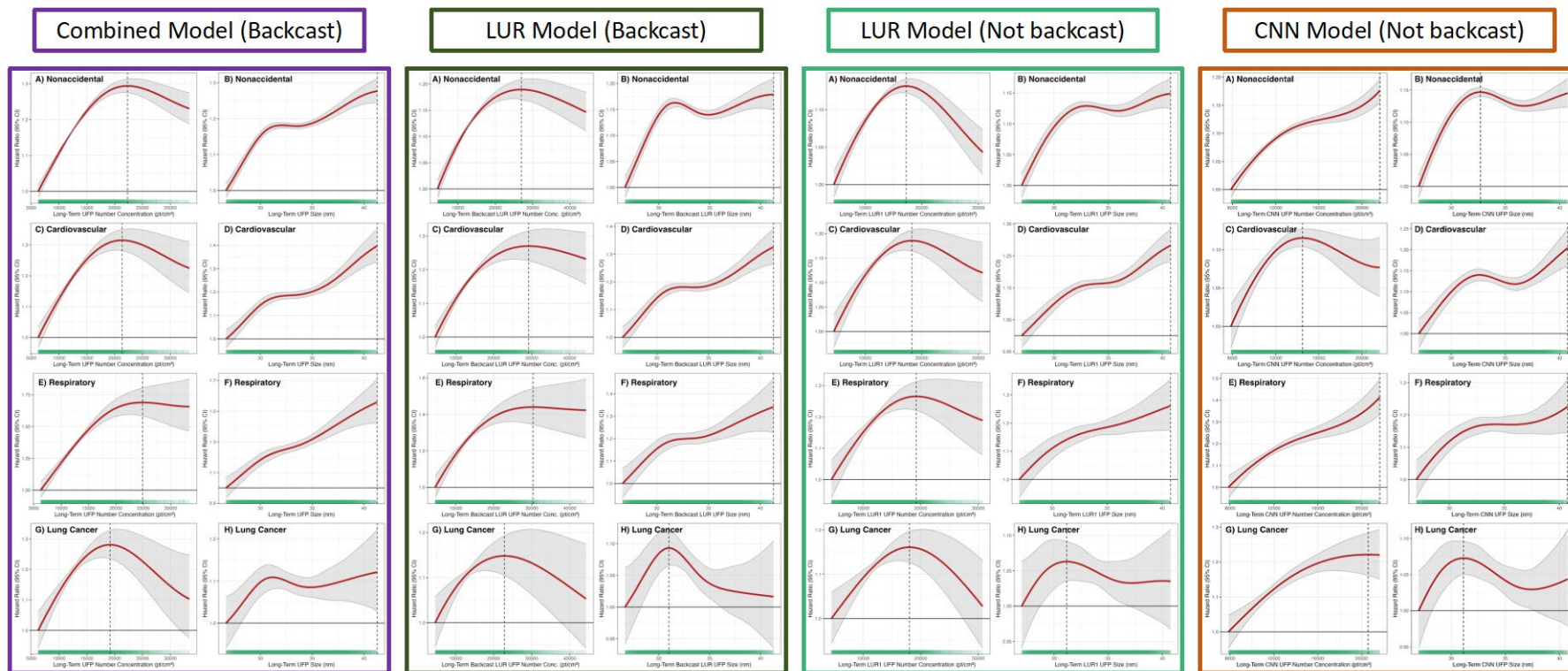


Figure A.59. Concentration-response curves for outdoor UFP number concentrations, UFP size, and mortality outcomes for the LUR and CNN models separately.

CNN = convolutional neural network; LUR = land use regression; UFP = ultrafine particles.



APPENDIX B: MONITORING AND BACKCASTING DETAILS

1. MONITORING LESSONS LEARNED

We completed large-scale mobile and fixed-site monitoring campaigns in Montreal and Toronto. The final models described in this report were developed using UFP and BC data that were collected simultaneously during more than 1,200 hours of mobile monitoring. Unfortunately, we also encountered several challenges that limited the amount of usable data. The challenges, impacts, and lessons learned are listed below.

A. O₃ and NO₂ Mobile Monitoring

1. Challenge: O₃ and NO₂ were monitored during the mobile monitoring campaign using the newly developed Urban Scanner from Scentroid (Stouffville, Ontario, CA). In preparation for the mobile monitoring campaign, a 9-day co-location campaign was conducted in the summer of 2020 next to a US EPA-approved fixed-air quality station in Toronto with additional co-location campaigns planned to take place throughout the mobile monitoring campaign. After the start of the mobile monitoring campaign, it became apparent that the Urban Scanner required much more calibration. This was conducted by Scentroid staff and our team members in Toronto, Canada. We had a second Urban Scanner for Montreal that was sent to Scentroid midway through the mobile monitoring campaign for upgrades and additional calibration, but this second unit never worked properly.
2. Impact: The Montreal O₃ and NO₂ data were not valid, and thus we did not develop new O₃ and NO₂ models for Montreal. The extensive effort to calibrate the Toronto Urban Scanner and the new Toronto O₃ and NO₂ models are described here:
 - a. Ganji A, Youssefi O, Xu J, Mallinen K, Lloyd M, Wang A, et al. Design, calibration, and testing of mobile sensor system for air pollution and build environment data collection: the urban scanner platform. *Environ Pollut* 2023;317:120720.
 - b. Ganji A, Saeedi M, Lloyd M, Xu J, Weichenthal S, Hatzopoulou M. 2023. Air pollution prediction and backcasting through a combination of mobile monitoring and historical on-road traffic emission inventories. Submitted for publication.

For the epidemiological analysis, we applied exposure estimates from these existing models to the cohort rather than mixing our new O₃ and NO₂ model estimates for Toronto with existing O₃ and NO₂ model estimates for Montreal.

3. Lesson learned: Extensive time should be allocated to calibrate and test newly developed monitoring equipment. If that is not feasible, then existing equipment with a proven track record should be used instead of newly developed equipment.

B. Winter Fixed-Site Monitoring

1. Challenge: COVID-19 restrictions prevented our team from meeting in person and conducting winter fixed-site monitoring. Mobile monitoring was still possible because it required only one team member at a time to be in the laboratory or in the monitoring vehicle.
2. Impact: Without winter fixed-site UFP and BC data, we could not develop annual average UFP and BC models based on fixed-site monitoring.
3. Lesson learned: Under certain circumstances, mobile monitoring can be easier to conduct than fixed-site monitoring.

C. Summer UFP Fixed-Site Monitoring

1. Challenge: We used Naneos Partector 2 and Testo DiSCmini handheld UFP monitors for the 2-week-long fixed-site monitoring. Ambient weather conditions during monitoring were unseasonably hot and humid. At times, the ambient temperature exceeded 30°C and relative

humidity exceeded 90%, which are both above the operating conditions of the Partector 2 and the DiscMini.

2. Impact: Within a few days of monitoring, the high ambient temperatures and humidity resulted in errors for most of the UFP monitors. Once there is an error, the data are no longer valid. Consequently, we had valid UFP data for only a handful of fixed sites. Coupled with the lack of fixed-site data during winter due to COVID-19 restrictions, we could not develop annual average UFP models based on fixed-site monitoring.
3. Lesson learned: The Naneos Partector 2 and Testo DiSCmini may not be suitable for continuously monitoring UFP levels over multiple days in high temperature and high relative humidity conditions (i.e., outside of their operating conditions).

D. Summer BC Fixed-Site Monitoring

1. Challenge: The BC 2-week-long fixed-site monitoring was done using Ultrasonic Personal Air Sampler (UPAS) monitors powered by solar panels and external batteries. After we had charged the external batteries, they automatically switched off to prevent unintentional discharge. We failed to recognize this change and did not set the batteries to “always on” mode for the Montreal fixed-site campaign. This meant that each UPAS was being powered only by its internal battery and the solar panel, which led to UPAS monitors shutting down on the second night of monitoring.
2. Impact: We collected only approximately 2 days’ worth of data during Montreal summer BC fixed-site monitoring. Coupled with the lack of fixed-site data during winter due to COVID-19 restrictions, we could not develop annual average BC models based on fixed-site monitoring.
3. Lesson learned: Our UPAS fixed-site monitoring procedure needs to include an external battery power check using a USB-powered LED light for visual confirmation that the external battery is in “always on” mode and providing power to the UPAS as required. This lesson learned was successfully implemented for the Toronto fixed-site campaign.

2. ROUTE SELECTION FOR MOBILE MONITORING

Mobile monitoring routes were selected to include different types of roads and land use characteristics across each city. To do this, we first intersected land use and built environment data (road variables: highway length, major roads, bus routes, traffic emissions; land use: commercial, parks, water; landmarks: airport, port, shoreline; other: elevation, industrial emissions, building height and footprint) with a 100×100 m grid for both Toronto and Montreal. Next, principal component analysis was used to identify components that explained the highest amount of variance in the data. Components that represented the most variance were selected for clustering. Specifically, land use clustering was based on the silhouette (S_i) and Davies-Bouldin methods. The silhouette value for each point is a measure of how similar that point is to other points in its own cluster when compared to points in other clusters. It is calculated as:

$$S_i = (b_i - a_i) / \max(a_i, b_i)$$

where:

- a_i is the average distance (e.g., difference in values for a given land use characteristic) from the i^{th} point to the other points in the same cluster.
- b_i is the minimum average distance from the i^{th} point to points in a different cluster, minimized over clusters.

The silhouette value ranges from -1 to 1 . A high silhouette value indicates that point i is well-matched to its own cluster and poorly matched to other clusters. To find the optimal number of clusters, we used Davies-Bouldin criterion, $DB(C)$, which evaluates how well the clustering has been done. The Davies-Bouldin criterion is based on a ratio of within-cluster to between-cluster distances:

$$DB(C) = \frac{1}{k} \sum_{i=1}^k \max_{j \leq k, j \neq i} D_{ij}, \quad k = |C|,$$

where:

- D_{ij} is the within-to-between cluster distance ratio for the i^{th} and j^{th} clusters (i.e., $D_{ij} = (d_i + d_j) / d_{ij}$).
- d_i is the average distance between every data point in cluster i and its centroid, similar for d_j .
- d_{ij} is the Euclidean distance between the centroids of the two clusters. If two clusters are close together (small d_{ij}) but have a large spread (large $d_i + d_j$), then this ratio will be large, indicating that these clusters are not very distinct.

In Montreal, 14 mobile monitoring routes were identified on the basis of the above procedure, whereas 20 routes were identified in Toronto (Figure A.1). The same sampling protocol was followed for mobile monitoring in both cities with route, day of the week, and start time (7 a.m.–11 p.m.) randomly selected each day. Monitoring was conducted approximately 5 days per week, and approximately four routes were monitored during each sampling period for a total route length of approximately 75 km per monitoring day (~4 hours).

3. QUALITY CONTROL PROCEDURES FOR DATA COLLECTION

3.1. MOBILE MONITORING OF OUTDOOR AIR POLLUTANTS

In each city, mobile monitoring was conducted using a predefined schedule of routes randomized over space, time of day, and day of week (including evenings and weekends). We concurrently used research-grade instruments to measure UFPs (Testo DiSCmini/Naneos Partector 2) and BC (Aethlabs MA350). All air pollution measurements were collected at 1-second resolution. Due to the technical issues with the Montreal O₃ and NO₂ monitors (described earlier under Lessons Learned) and the removal of those gases from the main exposure model development analysis, the QA and QC procedures for mobile O₃ and NO₂ monitoring are not included.

QA AND QC FOR UFP AND BC DATA

All direct-reading UFP and BC monitors were factory-calibrated before use, and all monitors were charged on a daily basis (overnight) to ensure adequate battery life during each mobile monitoring route. Zero checks (i.e., making sure the instrument reads 0 particles/cm³ when a zero filter is placed on the inlet) were performed on the UFP monitors on a monthly basis, and BC monitor sampling tapes were checked weekly to verify that they were not overloaded. The grit pots of the UFP monitors were cleaned weekly using a Kimwipe to remove any accumulating dust. At the start of each monitoring run, the monitors were powered on and time-synced using timeanddate.com. During mobile monitoring, the monitors were periodically checked for error messages, and the run was terminated if there were any errors. At the end of each run, the data were offloaded from the monitors to a hard drive and uploaded to the project's sync.com storage. Any value below the lower limit of detection was imputed with a value of half the lower limit of detection. Any value above the upper limit of detection was imputed with the upper limit of detection. Any monitors that required additional maintenance were sent back to the original equipment manufacturer.

3.2. FIXED-SITE MONITORING OF OUTDOOR AIR POLLUTANTS

Fixed monitoring sites were selected to capture the range of land use and traffic characteristics across Toronto and Montreal while maximizing spatial coverage. Fixed-site monitoring was conducted over 2 weeks in each city (a second 2-week campaign was planned but could not be completed due to COVID-19 restrictions; more details provided under Lessons Learned). In Montreal, fixed-site monitoring took place during June 2021. In Toronto, fixed-site monitoring took place during July 2021. In both cities, fixed-site monitoring of all pollutants (UFPs, BC, NO₂/O₃) took place simultaneously.

QA AND QC FOR FIXED-SITE BC (UPAS)

Integrated 2-week samples of outdoor BC concentrations were collected at approximately 70 locations across Montreal and Toronto using UPAS PM_{2.5} monitors (Access Sensor Technologies) with 37-mm Teflon filters. This setup includes a UPAS monitor running at 75% duty cycle at 1 L/min (i.e., sampling for 45 seconds out of every minute) attached to two external batteries, which are in turn charged by a solar panel. All UPAS monitors used to collect BC samples were flow-checked (using an Alicat mass flow meter) before and after each campaign to verify a sampling flow within 5% of the target flow rate of 1 L/min. In addition, all UPAS monitors were time-synced to ensure simultaneous data collection over each 2-week monitoring period. Field blanks (10%) and duplicate samples (~10%) were collected to evaluate the reliability of field measurements for BC. After the 2-week monitoring campaign, BC concentrations were measured on Teflon filters using a Sootscan Model OT21 Transmissometer (880 nm) (Magee Scientific). All Teflon filters were labeled with a unique barcode and also underwent gravimetric analyses for PM_{2.5}.

mass concentrations at the University of British Columbia to describe ambient air quality conditions during fixed-site monitoring.

QA AND QC FOR FIXED-SITE NO₂ AND O₃ (OGAWA MONITORS)

Integrated samples of outdoor NO₂/O₃ concentrations were measured at the same 70 locations as the BC monitors using Ogawa passive samplers (Ogawa & Co.). All samples were sent for laboratory analyses (ion chromatography, University of Toronto) immediately after each monitoring campaign. Field blanks (10%) and duplicate samples (~10%) were collected to evaluate the reliability of field measurements for NO₂/O₃. Ogawa samplers were stored in sealed containers before and after sample collection and were refrigerated prior to shipping and laboratory analysis.

QA AND QC FOR FIXED-SITE ULTRAFINE PARTICLES

We used 20 to 30 Testo DiSCmini nanoparticle counters (and three Partector 2 nanoparticle dosimeters, which are a newer version of the DiSCmini that operate on the same principle) to collect fixed-site UFP data across Montreal and Toronto. These monitors log real-time measurements of UFP number concentrations (10–300 nm) at 1-second resolution along with mean particle size and lung deposited surface area, which is a function of particle number concentration and particle size. Health Canada has provided in-kind use of approximately 20 of these monitors, and we acquired several more using funding from this application (three instruments). These monitors have been shown to perform well in comparison to laboratory-grade condensation particle counters and are advantageous in that they do not require isopropanol to operate; thus, they can collect data over extended periods of time without continuous oversight.

Data collection for fixed-site UFPs occurred over the same 2-week periods as BC and NO₂/O₃ but at different locations. Different locations were needed for UFP monitors because the instruments are very expensive (~\$11,000–15,000 USD each) and electricity is needed to avoid data loss owing to depleted batteries. Residential locations were targeted for fixed-site UFP monitoring, as residences are generally secure, available across a range of land use and traffic characteristics, and have access to electricity. These sites were recruited through targeted mailing campaigns (including a brief letter outlining the purpose of our study) and door-to-door visits, which have proved effective in past spatial studies. We tried to ensure that sites were near locations where UPAS monitors would be located, but due to the limited number of monitors, there was less coverage. All UFP monitors were factory-calibrated at the start of our study.

4. HISTORIC TRAFFIC DATA

4.1. METHODOLOGY

Traffic and NO_x are two crucial variables for the accurate prediction of traffic-related air pollution¹ and were predicted using the Traffic Emission Prediction scheme (TEPs)^{1,2} from 2006 to 2020 for Toronto and from 2015 to 2020 for Montreal. TEPs uses statistical methods and machine learning techniques (e.g., time series analysis, LUR geostatistical, neural network, and CNN methods) to generate yearly traffic counts and emissions.

For backcasting, we used traffic data and fleet and emission distributions to generate traffic volumes and emission inventories for all roads in Toronto and Montreal. For each road, we computed Sen's slope and Mann-Kendall test to capture trends. Given these trends, traffic and NO_x emission predictors were adjusted and estimated in previous years.

4.2. TEPs

The image processing module extracts the road characteristics, including road width and direction, from images and subsequently detects the number of vehicles on the road. Then, a neural network approach generates hourly and daily traffic volumes for each road based on vehicles extracted from images and road characteristics. Because the traffic fluctuates across hours of the day and weeks, a nearest-neighbor approach was used to generate coefficients of daily to yearly volumes. These coefficients convert the hourly and daily image-based traffic counts to annual average daily traffic (AADT). These coefficients are then used to estimate AADT for roads with aerial images and/or short-term traffic counts.

Pattern recognition uses information from nearby traffic count sites to estimate AADT using daily traffic counts predicted from images. AADT is estimated for each road with short to intermediate-length traffic counts using pattern recognition. This process uses all available historical and predicted counts to estimate a seasonal pattern for both permanent and temporary stations. Then, comparing the normalized seasonal patterns between temporary and permanent stations, a short-term station is assigned to a permanent station to estimate a traffic growth rate and a transformation coefficient for daily, monthly, and yearly volumes. Regression-kriging and regression are used to extend the predicted AADT to roads with no aerial images (poor quality or image showing no traffic) or traffic counts.

4.3. MULTIYEAR TRAFFIC AND EMISSIONS INVENTORIES

The City of Toronto and Montreal manage a traffic data collection program in support of various transportation operations and planning functions. Toronto's traffic count database from 2006 to the present is made of 15-minute traffic counts from different types of stations, including permanent traffic counts (324 stations, ~1%), short-period traffic counts (~95%), and turning movement counts (TMCs) (~4%). The latter are collected manually and are conducted over 10 hours in a single day. Montreal has a network of approximately 950 TMC stations situated at various intersections. The data recorded at these stations typically span less than 8 days. These TMC data, when combined with the information from MTQ permanent stations, play a crucial role in estimating traffic counts for the entire Montreal island.

To spatially and temporally interpolate traffic counts across the entire road network, we used an approach developed by our research group and documented by Ganji and colleagues.^{1,2} The TEPs uses a long record of traffic counts to generate daily traffic. A pattern recognition approach further identifies a coefficient to estimate AADT from daily values. This technique provides a unique basis for using short-term traffic counts (e.g., 1 day) for long-term traffic prediction. TEPs consists of a set of mathematical and statistical approaches. Three modules drive the TEPs framework: image processing, pattern recognition, and interpolation.

TEPs also generates emissions for all roads in Toronto. For this purpose, AADT values on each road segment were multiplied by the length of the road to generate vehicle kilometers traveled (VKT), which

were then multiplied by the corresponding emission factors to obtain emissions. Emission factors for NO_x were derived from the US EPA model MOVES (Motor Vehicle Emission Simulator) calibrated to reflect local conditions.

4.4. TREND ANALYSIS

Using the long-term traffic volumes and emissions derived for each road, we conducted a trend analysis to identify the roads that experienced significant changes from those that did not exhibit significant trends. This is important because traffic varies both spatially and temporally, and while citywide total traffic counts or emissions may exhibit linear trends over time, certain neighborhoods may exhibit sharp changes as a result of changes in population and employment. We employed the Mann-Kendall and Sen's slope estimators, two nonparametric methods to detect trends for every road segment in Toronto.

Mann-Kendall Test

The nonparametric Mann-Kendall^{3,4} is used to quantify the significance of trends in time series^{5,6} with a test statistic Z_S , which is estimated using Equation (1). Positive and negative Z_S indicate increasing and decreasing trends, respectively. For statistical testing of the trend, Z_S is compared with a value obtained from standard normal distribution at the specific α significance level.

$$Z_S = \begin{cases} \frac{S-1}{\sqrt{Var(s)}} & S > 0 \\ 0 & S = 0 \\ \frac{S+1}{\sqrt{Var(s)}} & S < 0 \end{cases} \quad (1)$$

where statistic S is estimated as follows:

$$S = \sum_{i=1}^{n-1} \sum_{j=i+1}^n sgn(x_j - x_i) \quad (2)$$

where $x_j - x_i$ are the difference between data values in time series i and j ($j > i$), n is the number of datasets, and $sgn()$ is the sign function, which is +1, -1, 0 for the case that $x_j - x_i$ is bigger, smaller, and equal to zero, respectively. The variance in Equation (1) is computed as follows:

$$Var(s) = \frac{n(n-1)(2n+5) - \sum_{i=1}^m t_i(t_i-1)(2t_i+5)}{18} \quad (3)$$

where m and t_i are the number of tied groups (set of sample data with the same value) and ties of extent i , respectively. A significance level of $\alpha = 0.05$ was used in this study.

Sen's Slope Estimator

For a given time series of any variable x , Sen's slope,⁷ which is a nonparametric trend analysis, is determined as follows:

$$Q_{med} = \begin{cases} Q_{[(N+1)+2]} & N \text{ is odd} \\ Q_{[\frac{N}{2}]} + Q_{[\frac{N+2}{2}]} & N \text{ is even} \end{cases} \quad (4)$$

where Q_i is determined as follows:

$$Q_i = \frac{x_j - x_k}{j - k} \quad i = 1, \dots, N \quad (5)$$

where j and k represent times j and k ($j > k$), respectively. N is the number of Q_{med} values and is determined using the number of time steps and observations $n(n - 1)/2$. The confidence level of Q_{med} at significance levels of a can be estimated using Equation (6):

$$C_a = Z_{1-\frac{a}{2}} \sqrt{Var(s)} \quad (6)$$

where $Z_{1-\frac{a}{2}}$ can be extracted from a standard normal distribution with significance levels of a and $Var(s)$ was introduced in Equation (3).

5. FIXED-SITE MONITORING

Fixed-site monitoring campaigns were conducted for 2 weeks in each city during summer 2021 (June 2021 for Montreal and July 2021 for Toronto). Fixed-site monitoring locations were selected to overlap with the locations of mobile-monitoring routes, which were designed to capture variations in land use and traffic characteristics across each city, as described previously. In Montreal, 64 sites were successfully monitored for NO₂, 68 for O₃, 0 for BC, and 18 for UFPs. In Toronto, 57 sites were successfully monitored for NO₂, 56 for O₃, 55 for BC, and 21 for UFPs. Data from additional fixed sites were discarded due to monitor errors and failures. Outdoor NO₂/O₃ data were collected using Ogawa passive samplers with subsequent analysis by ion chromatography. Blanks ($n = 31$ for NO₂; $n = 10$ for O₃), and duplicate samples ($n = 12$) were also collected for NO₂/O₃.

Fixed-site BC measurements were collected at the same locations as NO₂/O₃ measurements using UPAS monitors with 37-mm Teflon filters. UPAS monitors were operated at 75% duty cycle at 1 L/min (i.e., sampling for 45 of every 60 seconds); monitors were located in a weather-proof case and were attached to two external batteries, which were in turn charged by a solar panel. After the 2-week monitoring period, BC concentrations were measured using a Sootscan Model OT21 Transmissometer (880 nm). Finally, fixed-site UFP measurements were collected using the same instruments described earlier for mobile monitoring and were located at different locations than those used for BC/NO₂/O₃ because the UFP monitors required access to electricity to operate over the entire 2-week period. Locations for UFP monitors were selected to be as close as possible to locations used for BC/NO₂/O₃. The descriptive data results for fixed-site monitoring are shown in Table A.2.

REFERENCES

1. Ganji A, Shekarrizfard M, Harpalani A, Coleman J, Hatzopoulou M. Methodology for spatio-temporal predictions of traffic counts across an urban road network and generation of an on-road greenhouse gas emission inventory. *Comput-Aided Civ Inf* 2020;35: 1063–1084. <https://doi.org/10.1111/mice.12508>.
2. Ganji A, Zhang M, Hatzopoulou M. Traffic volume prediction using aerial imagery and sparse data from road counts. *Transp Res Part C Emerg Technol* 2022;141. <https://doi.org/10.1016/j.trc.2022.103739>.
3. Bevan JM, Kendall MG. Rank correlation methods. *J R Stat Soc Ser D Stat* 1971;20. <https://doi.org/10.2307/2986801>.
4. Mann HB. Mann nonparametric test against trend. *Econometrica* 1945;13:245–259. <https://doi.org/10.2307/1907187>.
5. Tabari H, Somee BS, Zadeh MR. Testing for long-term trends in climatic variables in Iran. *Atmos Res* 2011;100:132–140. <https://doi.org/10.1016/j.atmosres.2011.01.005>.
6. Tabari H, Marofi S. (2011). Changes of pan evaporation in the west of Iran. *Water Resour Manag* 2011;25:97–111. <https://doi.org/10.1007/s11269-010-9689-6>.
7. Sen Z. (1986). Determination of aquifer parameters by the slope-matching method. *Groundwater* 1986;24:217–223. <https://doi.org/10.1111/j.1745-6584.1986.tb00997.x>.

ABBREVIATIONS AND OTHER TERMS

| | |
|-------|------------------------------------|
| AADT | average annual daily traffic |
| MOVES | Motor Vehicle Emission Simulator |
| TEPs | Traffic Emission Prediction scheme |
| TMC | turning movement counts |
| UPAS | Ultrasonic Personal Air Sampler |